AN ABSTRACT OF THE THESIS OF

Daekwun Ko for the degree of Doctor of Philosophy in

Mechanical Engineering presented on November 12, 1993.

Title: A Numerical Study of Solid Fuel Combustion in a Moving Bed

Abstract approved:

A. Murty Kanury

Coal continues to be burned by direct combustion in packed or moving bed in small size domestic furnaces, medium size industrial furnaces, as well as small power stations. Recent stringent restrictions on exhaust emissions call for a better understanding of the process of combustion of coal in beds.

The present study is a prelude to developing methods of analysis to obtain this improved understanding. A one-dimensional steady-state computational model for combustion of a bed of solid fuel particles with a counterflowing oxidant gas has been developed. Air, with or without preheating, is supplied at the bottom of the bed. Spherical solid fuel particles (composed of carbon and ash) are supplied at the top of the bed. Upon sufficient heating in their downward descent, the carbon in particles reacts with oxygen of the flowing gas.

The governing equations of conservation of mass, energy, and species are integrated numerically to obtain the solid supply rate whose carbon content can be completely consumed by a given gas supply rate. The distributions of solid and gas

temperatures, of concentrations of various gas species, of carbon content in solid, and of velocity and density of gas mixture are also calculated along the bed length. The dependence of these distributions on the solid and gas supply rates, the air supply temperature, the size of solid fuel particle, and the initial carbon content in solid is also investigated.

The calculated distributions are compared with the available measurements from literature to find reasonable agreement. More gas supply is needed for complete combustion at higher solid supply rate. At a given gas supply rate, more solid fuel particles can be consumed at higher gas supply temperature, for larger particle size, and for lower initial carbon content in solid. The temperature of the bed becomes higher for higher solid supply rate, higher gas supply temperature, larger solid particle diameter, or lower initial carbon content in solid. These reasonable results lead one to encourage extension of the model presented here to more complex problems involving combustion of coals in beds including the effects of drying and pyrolysis.

A Numerical Study of Solid Fuel Combustion in a Moving Bed

by

Daekwun Ko

A THESIS

submitted to

Oregon State University

in partial fulfillment of
the requirements for the
degree of

Doctor of Philosophy

Completed November 12, 1993

Commencement June 1994

APPROVED:

Redacted for Privacy

Professor of Mechanical Engineering in charge of major

Redacted for Privacy

Head of Department of Mechanical Engineering

Redacted for Privacy

Dean of Graduate School

Date thesis is presented November 12, 1993

Typed by Daekwun Ko for Daekwun Ko

To Gieun and Jiyoung

ACKNOWLEDGEMENTS

First of all, I would like to express my profound gratitude to my major Professor A. Murty Kanury for his constant encouragement and sincere guidance throughout my graduate study in Oregon State University. With his optimism and energy in pursuing combustion, Professor Kanury inspire my interest in the fascinating "world of combustion."

I wish to thank to Professor Lorin R. Davis, Professor William C. Denison, Professor Richard B. Peterson, Professor James R. Welty, and Professor Robert E. Wilson, for serving as members of my graduate committee as well as their advice. I would also like to thank all the professors who taught me during my study. I would also like to extend my gratitude to the Department of Mechanical Engineering for financial support during my graduate study. Thanks are also due to the fellow students for being so friendly and supportive.

Finally, I would like to thank all the members of my family for all their support and encouragement. I would like to give special thanks to my parents, Youngsun and Bokwoo Ko, and parents-in-law, Joonhee and Bangsil Hong. Without their help, I could not have completed my education so successfully. Lastly, I would like to give my utmost thanks to my wife, Gieun, and my daughter, Jiyoung, for their patience and endless love. Especially, as a student's wife, Gieun has endured hardships so wisely that she made our home warm.

TABLE OF CONTENTS

LIST OF FIGURES

LIST OF TABLES

NOMENCLATURE

A_v Total surface area of solid particles per unit volume of the bed, [1/m]

Ar_n Arrhenius number for the reaction number n, $E_n/(RT_{gin})$

Bi Biot number, $hd(1-\phi)/K_{es}$

C_p Constant pressure specific heat, [J/(kg K)]

$\bar{C}_p$ Molar constant pressure specific heat, [J/(kmol K)]

$\bar{C}_v$ Molar constant volume specific heat, [J/(kmol K)]

D_{ej} Effective diffusion coefficient; diffusion coefficient of gas species j through the ash layer, [m^2/sec]

D_{AB} Diffusion coefficient of binary mixture, [m^2/sec]

D_j Diffusion coefficient of gas species j in gas mixture, [m^2/sec]

Da_n Damköhler number for reaction number n, $k_{0n}Pd^2M_C/D_{O_2in}$ or $k_{0n}P$

d Diameter of solid particles, [m]

E_n Activation energy for reaction number n, [J/kmol]

f_{CO} Mole fraction of carbon monoxide in the products of the reaction of carbon with oxygen to carbon monoxide and carbon dioxide,

G Mass velocity, [kg/(m^2s)]

Ga Galileo number, $\rho_g(\rho_s-\rho_g)gd^3/\mu_g^2$

g Gravitational acceleration, [m/s^2]

Δh_{1A} Enthalpy of reaction of carbon with oxygen to carbon monoxide, [J/kmol]

Δh_{1B} Enthalpy of reaction of carbon with oxygen to carbon dioxide, [J/kmol]

Δh_2 Enthalpy of reaction of carbon with carbon dioxide, [J/kmol]

Δh_3 Enthalpy of reaction of carbon monoxide with oxygen, [J/kmol]

h Convective heat transfer coefficient of gas mixture in packed beds, [W/(m^2 K)]

h_{Dj} Convective mass transfer coefficient of gas species j in packed beds, [kg/(m^2 sec)]

K Thermal conductivity, [W/(m K)]

K_{eg} Effective thermal conductivity of gas mixture in packed bed, [W/(m K)]

K_{es} Effective thermal conductivity of solid in packed bed, [W/(m K)]

K_s Thermal conductivity of solid with the effect of pores, [W/(m K)]

K_{st} Temperature dependent thermal conductivity of solid, [W/(m K)]

k_{0n} Preexponential factor for reaction number n, [kg/(m^2 sec Pa)]

L Bed length, [m]

M Molar mass, [kg/kmol]

Nu_g Nusselt number of gas mixture, hd/K_g

P Pressure in the bed, [Pa]

Pr_g Prandtl number of gas mixture, $\mu_g C_{pg}/K_g$

$\dot{Q}_g'''$ Heat generation by homogeneous chemical reaction, [J/(m^{3}s)]

$\dot{Q}_s'''$ Heat generation by two heterogeneous chemical reactions, [J/(m^{3}s)]

R Universal gas constant, [J/(kmol K)]

Re_g Reynolds number of gas mixture, $\rho_g u_g \phi d/\mu_g$

Re_{mf} Minimum fluidization Reynolds number, $\rho_g u_{mf} \phi d/\mu_g$

Re_s Solid supply Reynolds number; Reynolds number of solid particles at the top of the bed where the solid particles are supplied, $\rho_{gin} u_s d/\mu_{gin}$

Sc_j Schmidt number of gas species j, $\mu_g/(\rho_g D_j)$

Sh_j Sherwood number of gas species j, $h_{Dj} d/(\rho_g D_j)$

T Temperature, [K]

U_g Dimensionless gas velocity through the void in the bed, u_g/u_{gin}

u_g Interstitial velocity of gas in the bed, [m/s]

u_{g0} Superficial velocity of gas, [m/s]

u_{mf} Minimum fluidization interstitial velocity of gas, [m/s]

u_s Velocity of solid in the bed, [m/s]

$\dot{W}_1'''$ Mass generation by the reaction of carbon with oxygen, [kg/(m^{3}s)]

$\dot{W}_2'''$ Mass generation by the reaction of carbon with carbon dioxide, [kg/(m^{3}s)]

$\dot{W}_3'''$ Mass generation by the reaction of carbon monoxide with oxygen, [kg/(m^{3}s)]

$\dot{W}_j'''$ Mass generation of species j by chemical reaction, [kg/(m^{3}s)]

X_j Mole fraction of gas species j in gas mixture

x Axial distance from the bottom of the bed, [m]

Y_j Mass fraction of gas species j in gas mixture

y_j Relative mass fraction of gas species j; mass fraction of gas species j normalized by mass fraction of O_2 at the bottom of the bed, $\mathbf{Y_j / Y_{O_2 in}}$

Greek Symbols

θ Dimensionless temperature, T/T_{gin}

μ Dynamic viscosity, [Pa·s]

ξ Dimensionless axial distance from the bottom of the bed, x/L

$\Delta\xi^i$ Grid interval between i and (i+1)th node for numerical computation

ρ Ratio of core diameter to initial particle diameter

ρ_g Density of gas mixture, [kg/m^3]

$\tilde{\rho}_g$ Dimensionless density of gas mixture, ρ_g/ρ_{gin}

ρ_s Density of solid particles, [kg/m^3]

ϕ Void fraction of the moving bed

ϕ_h Relative humidity

ϕ_p Porosity of ash layer

ε Error criterion for convergence

Ω_j Relative mass fraction of solid species j in solid; mass fraction of solid species j normalized by mass fraction of solid species j at the top of the bed, ω_j/ω_{jin}

ω_j Mass fraction of solid species j in solid, [kg of solid species j/kg of solid]

Subscripts

A	Ash
C	Carbon
CO_2	Carbon dioxide
CO	Carbon monoxide
g	Gas mixture
H_2O	Water
in	At the top of the bed for solid and at the bottom of the bed for gas
j	Kinds of solid and gas species; Ash or Carbon for solid species and O_2, N_2, CO_2, CO, or H_2O for gas species
n	Reaction number; n=2, 21, 22, or 23 for the reaction of carbon with carbon dioxide
N_2	Nitrogen
O_2	Oxygen
s	Solid

Superscripts

i	Node number
N	Number of grid interval

A NUMERICAL STUDY OF SOLID FUEL COMBUSTION IN A MOVING BED

CHAPTER 1

INTRODUCTION

Coal continues to be burned by direct combustion in packed or moving bed in small size domestic furnaces, medium size industrial furnaces, as well as small power stations. Recent stringent restrictions on exhaust emissions call for a better understanding of the process of combustion of coal in beds. The present study is a prelude to developing methods of analysis to obtain this improved understanding.

Recent studies on coal consumption in fixed or moving bed emphasize gasification of coal. Studies on direct combustion of coal are limited. The major differences between direct combustion and gasification of coal can be easily listed. The gas supply for direct combustion is air and that for gasification is a mixture of air (or oxygen) and steam. The product gases for direct combustion are mainly CO, CO_2, and H_2O at high temperature. For gasification, they are mainly H_2, CO_2, CO, CH_4, and H_2O which are fuel-rich. The main reactions in direct combustion are those of carbon with oxygen to produce heat in excess air. In gasification, they are reactions of carbon with oxygen, carbon dioxide, and steam to produce hydrogen and gaseous hydrocarbon in deficient air. The length of the bed is usually longer for gasification than direct combustion because of the slower reaction rate of gasification.

Studies on numerical modeling on coal or char gasification were performed by Winslow,[1] Amundson and Arri,[2] Yoon et al.,[3] and Cho and Joseph.[4] Gibbs and Soo[5] studied the steam gasification of coal by experiment. Caram and Fuentes[6] proposed a simplified model to solve analytically. Both the experimental and modeling studies on char gasification in fixed bed were made by Bhattacharya et al..[7]

The earlier works on combustion in a solid fuel bed were performed by several authors including Nicholls and Eilers[8] and Mayers.[9] Nicholls and Eilers studied the principles of underfeed combustion and the effect of preheated air on overfeed and underfeed fuel beds by experiment. Most earlier works are experimental and mathematical modelling by Mayers[9] is the beginning of the theoretical investigation. Mayers proposed a mathematical model for a solid fuel bed, analytic solutions on temperature and concentration were obtained, and the comparison with experiment showed reasonable agreement. However, knowledge of the coefficients in the governing equations were rather limited at that time. Mayers chose values of the coefficients from literature which gave reasonably good agreement between the temperatures observed by Nicholls and Eilers[8] and those calculated by the analytic calculation. Kuwata et al.[10] developed a theoretical relationship predicting the variation of the relative carbon saturation factor with bed depth and established guidelines for the operational limits during steady operation in a solid fuel bed. Eapen et al.[11] extended a theory of Kuwata et al.[10] that allowed for non-diffusional control assumptions in the kinetic behavior of gasification, together with experimental support for the major elements of the analysis by measurements in a combustion pot. Kuwata et al.[10] and Eapen et al.[11] assumed that the temperature in the bed was

uniform. Barriga and Essenhigh[12] proposed a mathematical model of a combustion pot where carbon reacted with air. Lawson and Norbury[13] proposed a mathematical model and solved numerically for combustion in a porous medium. Neither Barriga and Essenhigh[12] nor Lawson and Norbury[13] show all parameters used in obtaining their results.

Three reactions are involved in the combustion of carbon in a fuel bed: one heterogeneous reaction of carbon with oxygen to produce carbon monoxide and carbon dioxide; one heterogeneous gasification reaction of carbon with carbon dioxide to produce carbon monoxide; and one homogeneous reaction of carbon monoxide with oxygen to produce carbon dioxide. Kuwata et al.[10] and Eapen et al.[11] considered all three reactions but the product by the reaction of carbon with oxygen is assumed to be only carbon monoxide. Mayers[9] and Barriga and Essenhigh[12] considered two reactions; reaction of carbon with oxygen only to carbon dioxide and gasification reaction of carbon with carbon dioxide. Lawson and Norbury[13] considered only one reaction of carbon with oxygen to carbon dioxide. In the above studies, the combustion models were oversimplified or parametric studies were limited.

In the research reported in this dissertation, a one-dimensional steady-state computational model for combustion of a bed of solid fuel particles with a counterflowing oxidant gas has been developed. The schematic diagram of the model is shown in Figure 1. Air, with or without preheating, is supplied at the bottom of the cylindrical bed. Product gases with inert nitrogen are discharged at the top of the bed. Spherical solid fuel particles which are presumed to be composed of carbon and

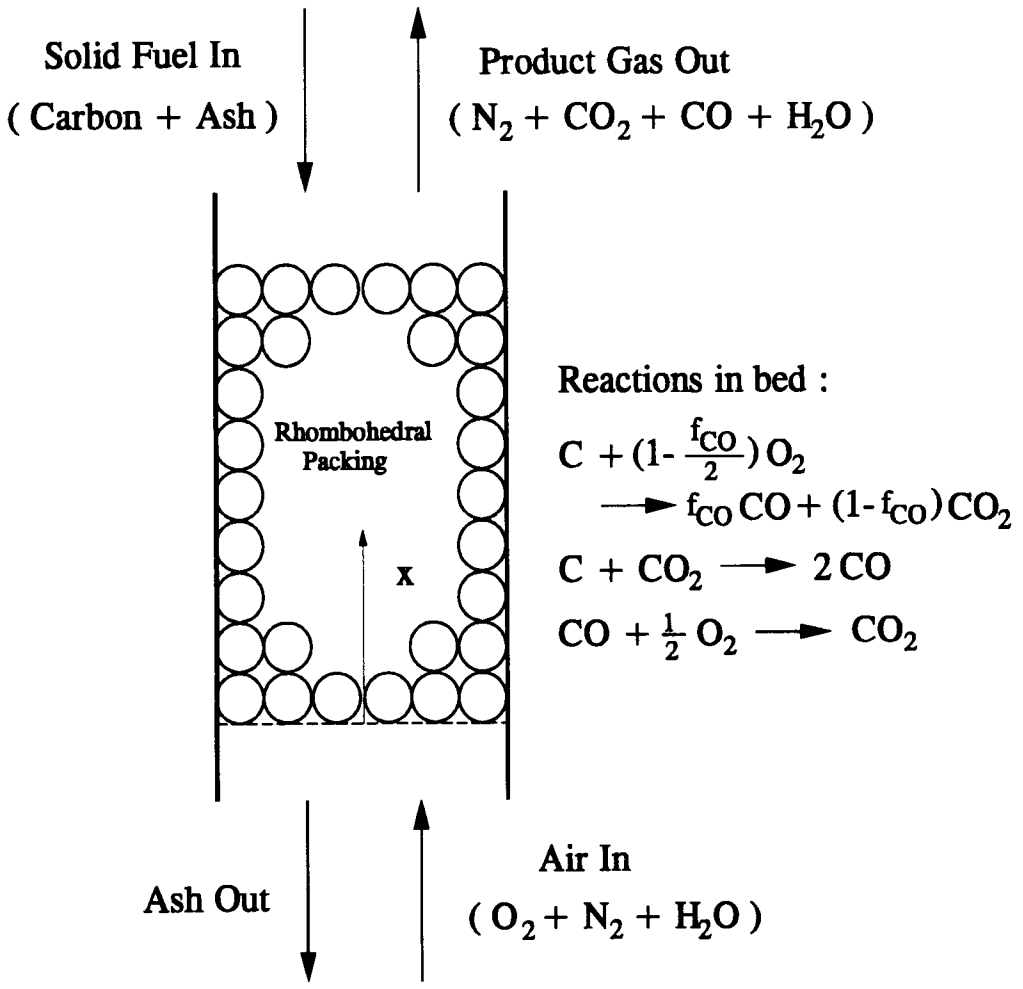

Fig. 1 Schematic diagram of the model.

ash are supplied at the top of the bed, are packed rhombohedrally in the bed to move down slowly to maintain a steady bed depth. Upon sufficient heating by the hot product gases in their downward descent, the carbon in the particles reacts with the oxygen of the flowing gas. Carbon is consumed by two heterogeneous reactions; one reaction of carbon with oxygen to produce carbon monoxide and carbon dioxide; and one reaction of carbon with carbon dioxide to produce carbon monoxide. The carbon monoxide produced by the above two heterogeneous reactions can react with oxygen in the gas-phase to produce carbon dioxide. The residual inert ash is discharged at the bottom of the bed. This type of bed is often referred to as moving, descending, packed, or fixed bed.[14, 15] The solid particles in the bed are slowly moving down so that the bed is referred to as moving bed in the present study.

Several reaction models, from a simple one reaction model to three reaction models, are examined and each reaction model is compared with experiment from available literature in the present study. The particles are considered to be small so that their interior is assumed to be at a uniform temperature. Effective thermal conductivities of solid and gas are used to account for the effect of void fraction, radiation heat transfer, and enhanced heat transfer due to the eddy diffusion by fluid flow around the solid particles. The properties of solid and gas species are taken to be temperature dependent.

The governing equations of mass, energy, and species are nonlinear and coupled so that they can only be integrated numerically. The finite difference method with iterative scheme is used. The rate of solid supply for the complete consumption of carbon content in solid particles at a given rate of gas supply is obtained. The

distributions of solid and gas temperatures, of concentrations of various gas species, of carbon content in solid particles, and of velocity and density of the gas mixture are also calculated along the bed length. The effects of solid and gas supply rate, air supply temperature, size of solid fuel particle, and initial carbon content in solid particles on these distributions and the stoichiometric supply rates are investigated for the parametric study.

This thesis is organized into five chapters in the following order. In this introductory chapter the purpose and description of the present problem, the structure of this thesis, and review of the existing literature on combustion and gasification of solid fuel bed are mentioned. In Chapter 2, the governing equations and boundary conditions are proposed and nondimensionalized. The parameters, such as, the rate of chemical reactions, heat and mass transfer coefficient, effective thermal conductivity, and minimum fluidization velocity, are also explained in detail. Chapter 3 describes the numerical method and temperature dependent properties of solid and gas. Finite difference method with iterative algorithm employed in this study is also described in detail in Chapter 3. In Chapter 4, the results of numerical calculation are compared with the available literature and the effects of the given parameters are extensively discussed. The conclusions and recommendations for the future work on this study are covered in Chapter 5.

CHAPTER 2

MATHEMATICAL FORMULATION

Conservation equations of energy, solid and gas species, and mass, equation of state, and the corresponding boundary conditions describing distributions of solid and gas temperatures, of gas species concentrations, of carbon content in solid particles, and of velocity and density of gas mixture along the bed length are proposed in this chapter. Assumptions for the present mathematical model are also discussed. The coefficients in the governing equations, such as, the rate of chemical reactions, heat and mass transfer coefficients, and effective thermal conductivity are explained in detail. Dimensionless variables and parameters are introduced and the governing equations and boundary conditions are nondimensionalized.

2.1 GOVERNING EQUATIONS AND BOUNDARY CONDITIONS

The terms considered to derive the governing equations and the boundary conditions are discussed below. The energy conservation equations contain (1) conduction heat transfer in solid and gas; (2) convection heat transfer in solid and gas; (3) heat exchange between solid and gas by convection on the contact surface; and (4) heat generation due to chemical reactions. The species conservation equations contain (5) molecular diffusion of each gas species in gas mixture; (6) convection mass transfer of each solid and gas species; and (7) mass loss or generation of carbon, O_2, CO_2, and CO due to chemical reactions. The gas continuity equation contains (8) mass flow of gas mixture; (9) mass loss or generation of O_2, CO_2, and

CO due to chemical reactions. The momentum equation is obviated because the permeability equation is usually used instead of momentum equation in a moving bed and the pressure variation in a moving bed departs very little from the atmospheric pressure for the flow of a low viscosity fluid.[13] One additional governing equation is the equation of state for gas mixture.

The following assumptions are made in this study.

(1) The flow of gas follows a plug flow.

(2) Solid particles are spherical and have uniform initial size and the size of the particles does not change through the bed.

(3) The packing method of the particles is rhombohedral.

(4) The particles are considered to be small so that their interior is at a uniform temperature at any location in the bed.

(5) The temperature and concentration changes in radial direction in the bed are negligible.

(6) Effective thermal conductivity of the bed is used to account for the effects of void fraction, radiation heat transfer, and eddy diffusion in gas phase.

The governing equations and boundary conditions for the present model are shown below. The temperature distributions of the solid (T_s) and gas phase (T_g) in the bed can be obtained by the solid and gas energy equations. These equations indicate balances between conduction, convection, heat exchange between solid and gas, and chemical reaction.

Energy Equations:

$$\frac{d}{dx}\left(K_{eg}\frac{dT_g}{dx}\right) - \frac{d}{dx}(\rho_g u_g \phi C_{pg} T_g) - h A_v(T_g - T_s) + \dot{Q}_g''' = 0 \tag{2.1}$$

$$\frac{d}{dx}\left(K_{es}\frac{dT_s}{dx}\right) + \frac{d}{dx}[\rho_s u_s (1-\phi) C_{ps} T_s] + h A_v(T_g - T_s) + \dot{Q}_s''' = 0 \tag{2.2}$$

where K_{eg} and K_{es} respectively are effective thermal conductivities of solid and gas phase in the bed, ρ_g and ρ_s respectively are the densities of gas mixture and solid, u_g is the velocity of gas mixture through the void in the bed, u_s is the velocity of solid particles, C_{pg} and C_{ps} respectively are the specific heats of gas mixture and solid, ϕ is the void fraction of the bed, h is the convection heat transfer coefficient between solid and gas in the bed, and A_v is the total surface area of solid particles per unit volume of the bed. The heat generations per unit volume of the bed per unit time due to chemical reactions are given by the following equations according to the stoichiometry.

$$\dot{Q}_g''' = \dot{W}_3''' \frac{\Delta h_3}{M_{CO}} \tag{2.3}$$

$$\dot{Q}_s''' = f_{CO} \dot{W}_1''' \frac{\Delta h_{1A}}{M_C} + (1 - f_{CO}) \dot{W}_1''' \frac{\Delta h_{1B}}{M_C} + \dot{W}_2''' \frac{\Delta h_2}{M_C} \tag{2.4}$$

where $\dot{W}_1'''$, $\dot{W}_2'''$, and $\dot{W}_3'''$ respectively are mass generations per unit volume of the bed per unit time due to the reaction of (1) carbon with oxygen, (2) carbon with carbon dioxide, and (3) carbon monoxide with oxygen. Δh_{1A} and Δh_{1B} respectively

are the enthalpies of reaction of carbon with oxygen to produce (A) carbon monoxide and (B) carbon dioxide. Δh_2 and Δh_3 respectively are the enthalpies of reaction of carbon with carbon dioxide and of carbon monoxide with oxygen. M_j is the molar mass of species j and f_{CO} is the fraction of carbon monoxide in product gas by the reaction of carbon with oxygen.

The carbon content in solid particles is consumed by two heterogeneous reactions of carbon with oxygen and with carbon dioxide. The ash in solid particles is inert. The distributions of contents of carbon and ash in solid particles (ω_j) can be obtained by the following solid species equations.

Solid Species Equations:

$$\frac{d\omega_j}{dx} = -\frac{\dot{W}_j'''}{\rho_{sin}(1-\phi)u_s} \tag{2.5}$$

$$\begin{aligned} &\text{For } j = C \quad ; \ \dot{W}_C''' = \dot{W}_1''' + \dot{W}_2''' \\ &\qquad j = Ash \quad ; \ \dot{W}_A''' = 0 \end{aligned} \tag{2.6}$$

where $\dot{W}_j'''$ is the mass loss or generation of solid and gas species j by chemical reactions and ρ_{sin} is the density of solid particles at the top of the bed where solid particles are supplied. The distributions of the mass fraction of gas species Y_j in the bed can be obtained by the gas species equations. The gas species equations indicate balances between molecular diffusion, convection, and chemical reaction.

Gas Species Equations:

$$\frac{d}{dx}\left(\rho_g D_j \phi \frac{dY_j}{dx}\right) - \frac{d}{dx}(\rho_g u_g \phi Y_j) + \dot{W}_j''' = 0 \tag{2.7}$$

$$\text{For } j = O_2 \;;\; \dot{W}_{O_2}''' = \left(1 - \frac{f_{CO}}{2}\right)\dot{W}_1''' \frac{M_{O_2}}{M_C} + \frac{1}{2}\dot{W}_3''' \frac{M_{O_2}}{M_{CO}}$$

$$j = N_2 \;;\; \dot{W}_{N_2}''' = 0$$

$$j = CO_2 \;;\; \dot{W}_{CO_2}''' = -(1 - f_{CO})\dot{W}_1''' \frac{M_{CO_2}}{M_C} + \dot{W}_2''' \frac{M_{CO_2}}{M_C} - \dot{W}_3''' \frac{M_{CO_2}}{M_{CO}} \tag{2.8}$$

$$j = CO \;;\; \dot{W}_{CO}''' = -f_{CO}\dot{W}_1''' \frac{M_{CO}}{M_C} - 2\dot{W}_2''' \frac{M_{CO}}{M_C} + \dot{W}_3'''$$

$$j = H_2O \;;\; \dot{W}_{H_2O}''' = 0$$

where D_j is the diffusion coefficient of gas species j in the gas mixture.

The velocity of gas mixture through the void u_g in the bed can be calculated by the gas continuity equation.

Gas Continuity Equation:

$$\frac{d}{dx}(\rho_g u_g \phi) - \left(\dot{W}_{O_2}''' + \dot{W}_{CO_2}''' + \dot{W}_{CO}'''\right) = 0 \tag{2.9}$$

Assuming ideal gas behavior, the distribution of gas mixture density ρ_g can be obtained by the equation of state.

Equation of State:

$$\rho_g = \frac{P M_g}{R T_g} \tag{2.10}$$

where P is the pressure of the bed, M_g is the molar mass of the gas mixture, and R is the universal gas constant.

The rates of chemical reactions are explained in detail in the next section. The convective mass transfer from bulk gas mixture to the solid surface, molecular diffusion through the ash layer, and reaction on the core surface are taken to be in series for the heterogeneous reactions. The reaction of carbon with oxygen on the core surface is so fast that the reaction is controlled by convective mass transfer and ash layer diffusion. The mass loss of carbon per unit volume of the bed per unit time due to the reaction of carbon with oxygen is:

$$\dot{W}_1''' = -\frac{1}{1-\frac{f_{CO}}{2}} \frac{A_v Y_{O_2}}{\frac{1}{h_{DO_2}\frac{M_C}{M_{O_2}}} + \frac{1}{\frac{2\rho_g D_{eO_2}}{d}\frac{\rho}{1-\rho}\frac{M_C}{M_{O_2}}}} \tag{2.11}$$

where h_{Dj} is the convection mass transfer coefficient of gas species j, D_{ej} is the effective diffusion coefficient of gas species j through the ash layer, and ρ is the ratio of core diameter to particle diameter and is given by the following equation.

$$\rho = \left(\frac{\omega_C}{\omega_{Cin}}\right)^{1/3}$$

where ω_{Cin} is initial (or supply) carbon content in solid.

The gasification reaction of carbon with carbon dioxide is so slow that the reaction is controlled generally by the reaction kinetics. However, when the temperature of the bed is high enough, the reaction kinetics are sufficiently fast to make convective mass transfer and ash layer diffusion important. The mass loss of

carbon per unit volume of the bed per unit time due to the reaction of carbon with carbon dioxide is:

$$\dot{W}_2''' = -\frac{A_v Y_{CO_2}}{\frac{1}{h_{DCO_2}\frac{M_C}{M_{CO_2}}} + \frac{1}{\frac{2\rho_g D_{eCO_2}}{d}\frac{\rho}{1-\rho}\frac{M_C}{M_{CO_2}}} + \frac{1}{\rho^2 k P \frac{M_g}{M_{CO_2}}}} \tag{2.12}$$

where k is the kinetic term given by

$$k = \frac{k_{021}\exp\left(-\frac{E_{21}}{RT_s}\right)}{1 + k_{022}\exp\left(-\frac{E_{22}}{RT_s}\right)Y_{CO}\frac{PM_g}{M_{CO}} + k_{023}\exp\left(-\frac{E_{23}}{RT_s}\right)Y_{CO_2}\frac{PM_g}{M_{CO_2}}}\frac{M_C\rho_s d}{6}$$

k_{0n} and E_n in the above equation are preexponential factors and activation energies for the gasification reaction of carbon with carbon dioxide.

The homogeneous reaction is mostly controlled by gaseous reaction kinetics. However, the intrinsic reaction is so fast that the carbon monoxide (due to the reaction of carbon with oxygen) is consumed as soon as it is produced. Thus, the reaction of carbon monoxide with oxygen is controlled by the reaction of carbon with oxygen. The mass loss of carbon monoxide per unit volume of the bed per unit time due to the reaction of carbon monoxide with oxygen is:

$$\dot{W}_3''' = f_{CO}\dot{W}_1'''\frac{M_{CO}}{M_C} \tag{2.13}$$

The boundary conditions for the above governing equations are shown below.

Boundary Conditions for Energy Equations:

$$x = 0 \quad : \quad T_g = T_{gin} \quad \text{and} \quad K_{es}\frac{dT_s}{dx} - h(1-\phi)(T_s - T_{gin}) = 0 \tag{2.14}$$

$$x = L \quad : \quad \frac{dT_g}{dx} = 0 \quad \text{and} \quad K_{es}\frac{dT_s}{dx} + h(1-\phi)(T_s - T_{sin}) = 0 \tag{2.15}$$

where T_{gin} and T_{sin} are the temperature of gas mixture at the bottom of the bed and of solid at the top of the bed where those are supplied.

Boundary Conditions for Solid Species Equations:

$$x = L \quad : \quad \omega_C = \omega_{Cin} \quad \text{and} \quad \omega_A = \omega_{Ain} \tag{2.16}$$

where ω_{Cin} and ω_{Ain} respectively are the mass fractions of carbon and ash at the top of the bed where solid particles are supplied.

Boundary Conditions for Gas Species Equations:

$$x = 0 \quad : \quad Y_{O_2} = Y_{O_2 in} \quad , \quad Y_{N_2} = Y_{N_2 in} \quad , \quad Y_{CO_2} = 0 \quad , \quad Y_{CO} = 0 \quad , \text{ and } \quad Y_{H_2O} = Y_{H_2Oin} \tag{2.17}$$

$$x = L \quad : \quad \frac{dY_{O_2}}{dx} = 0 \quad , \quad \frac{dY_{N_2}}{dx} = 0 \quad , \quad \frac{dY_{CO_2}}{dx} = 0 \quad , \quad \frac{dY_{CO}}{dx} = 0 \quad , \text{ and } \quad \frac{dY_{H_2O}}{dx} = 0 \tag{2.18}$$

where Y_{jin} is the mass fraction of gas species j at the bottom of the bed where gas is supplied.

Boundary Condition for Gas Continuity Equation:

$$x = 0 \quad : \quad u_g = u_{gin} \tag{2.19}$$

where u_{gin} is the interstitial gas velocity at the bottom of the bed.

The boundary condition for the solid energy equation at the top of the bed in the above energy equation is derived by the balances between conduction and radiation heat transfer through the solid and the convection heat loss to above the bed. Several authors[3, 4, 6] neglected the conduction and radiation heat transfer through the solid in the solid energy equation and used the constant temperature boundary condition at the top of the bed. This constant temperature boundary condition is reasonable when the supply rate of solid particles is very high. When the supply rate of solid particles is low, however, this boundary condition leads to an underestimation of the temperatures of both the solid and the gas at the top of the bed.

2.2 RATES OF CHEMICAL REACTIONS

The following three global reactions are to be considered in the combustion of carbon with oxygen.[10, 12, 16]

(1) Heterogeneous reaction of carbon with O_2 to mainly CO and some CO_2 on the carbon surface,

(2) Heterogeneous reaction of carbon with CO_2 to CO on the carbon surface,

(3) Homogeneous reaction of CO with O_2 to CO_2 in the gas phase.

The above reactions are expressed in the following forms.

$$(1)\quad C + \left(1 - \frac{f_{co}}{2}\right) O_2 \quad \text{-----} \rightarrow \quad f_{co}\, CO + (1 - f_{co})\, CO_2$$

$$(2)\quad C + CO_2 \quad \text{-----} \rightarrow \quad 2\, CO$$

$$(3)\quad CO + \frac{1}{2} O_2 \quad \text{-----} \rightarrow \quad CO_2$$

where f_{co} is the fraction of carbon monoxide produced by reaction (1). Arthur[17] developed a correlation to evaluate f_{co} as a function of solid temperature.

$$\frac{f_{co}}{1 - f_{co}} = 2512 \exp\left(-\frac{6240}{T_s}\right) \tag{2.20}$$

where T_s is in K. The basis of this equation is as follows. Two separate reactions occur between C and O_2, one to produce CO and one to produce CO_2. The ratio of CO to CO_2 production can be obtained by the relative rates of production of CO and CO_2. Arthur combined the two Arrhenius type reaction rate equations to obtain equation (2.20) and the constants in the equation were calculated from experimental data by the method of least squares.

In the present study, several reaction models are examined and each reaction model is compared with the experiment of Nicholls and Eilers.[8] When f_{co} is zero, only carbon dioxide is produced by reaction (1). When f_{co} is 1, only carbon monoxide is produced by reaction (1). When f_{co} is given by the above equation, both carbon monoxide and carbon dioxide are produced by reaction (1). Table 1 shows the list of reaction models investigated in this study. The two reaction model and the three reaction model A are same because carbon monoxide is not produced by reaction (1) and the gaseous reaction of carbon monoxide with oxygen will not occur.

Table 1 Reaction models examined in this study.

Reactions	Single Reaction Model	Two Reaction Model	Three Reaction Model		
			A	B	C
(1) with $f_{CO}=0$	*	*	*		
(1) with $f_{CO}=f(T_s)$				*	
(1) with $f_{CO}=1$					*
(2)		*	*	*	*
(3)			*	*	*

The rate of heterogeneous reaction between solid and gas is usually controlled by three mechanisms: convection mass transfer of gas species from bulk gas mixture to solid surface, molecular diffusion of gas species through the ash layer, and combustion or gasification reaction kinetics on the core surface. Two basic models generally used for heterogeneous reactions are a shrinking core model and a shrinking particle model. Many heterogeneous reactions between solid and gas follow either one or a combination of these two limiting models. The shrinking particle model is a typical model for the combustion of pure carbon containing no ash. The shrinking core model is a model for the combustion of carbon containing some ash content when the ash layer is not removed from solid particles until the particles reach the bottom of the bed. The mechanism of coal combustion is mostly between these two models and it depends on the type of coal. The shrinking core model is employed in this study because the solid particles are composed of both carbon and ash and the shrinking core model is the best simple representation for majority of reacting gas-solid systems.[18]

The reaction of carbon with oxygen is highly exothermic, the temperature in the combustion zone of the bed is very high, and the intrinsic rate of carbon reaction with oxygen is very fast. Since the transport resistances are much larger than the intrinsic chemical kinetic resistance, the precise chemical mechanism involved in reaction (1) is not important. In the present study, the overall reaction of carbon with oxygen is assumed to be controlled by the convection mass transfer of oxygen from the bulk gas mixture to particle surfaces and the molecular diffusion of oxygen through the ash layer.

The mass transfer rate of oxygen from the bulk gas mixture to particle surfaces by convection is:

$$r_{O1} = h_{DO_2}\left(Y_{O_2} - Y_{O_2}^*\right)$$

where Y_{O_2} and $Y_{O_2}^*$ respectively are the mass fraction of oxygen in the bulk gas mixture and on the solid surface. The rate of carbon consumption only by convective mass transfer can be obtained by stoichiometry to the following equation.

$$r_{C1} = h_{DO_2}\left(Y_{O_2} - Y_{O_2}^*\right)\frac{M_C}{\left(1 - \frac{f_{CO}}{2}\right)M_{O_2}} \qquad (2.21)$$

The mass transfer rate of oxygen through the ash layer by molecular diffusion is:

$$r_{O1} = \frac{2\rho_g D_{eO_2}}{d}\frac{\rho}{1-\rho}Y_{O_2}^*$$

The rate of carbon consumption only by molecular diffusion through the ash layer can be obtained by stoichiometry to the following equation.

$$r_{C1} = \frac{2\rho_g D_{eO_2}}{d}\frac{\rho}{1-\rho}Y^*_{O_2}\frac{M_C}{\left(1-\frac{f_{CO}}{2}\right)M_{O_2}} \tag{2.22}$$

The mass fraction of oxygen on the solid surface $Y^*_{O_2}$ can be canceled by combining equation (2.21) and (2.22) and the overall reaction rate of carbon consumption by the reaction of carbon with oxygen becomes:

$$r_{C1} = \frac{1}{\left(1-\frac{f_{CO}}{2}\right)}\frac{Y_{O_2}}{\frac{1}{h_{DO_2}\frac{M_C}{M_{O_2}}} + \frac{1}{\frac{2\rho_g D_{eO_2}}{d}\frac{\rho}{1-\rho}\frac{M_C}{M_{O_2}}}} \tag{2.23}$$

The mass generation term in the governing equation is defined by the mass generation per unit time per unit volume of bed. It can be obtained by multiplying the negative of carbon mass removal per unit time per unit area of solid particle ($-r_{C1}$) by the total surface area of solid particles per unit volume of bed (A_v) for the heterogeneous reaction. The mass generation of carbon by the reaction of carbon with oxygen can be written as:

$$\dot{W}'''_1 = -\frac{1}{\left(1-\frac{f_{CO}}{2}\right)}\frac{A_v Y_{O_2}}{\frac{1}{h_{DO_2}\frac{M_C}{M_{O_2}}} + \frac{1}{\frac{2\rho_g D_{eO_2}}{d}\frac{\rho}{1-\rho}\frac{M_C}{M_{O_2}}}}$$

The effective diffusion coefficient D_{ej} which is proposed by Walker et al.[20] is the diffusion coefficient of gas species j through the ash layer.

$$D_{ej} = D_j \phi_p^2$$

The porosity of the ash layer ϕ_p is regarded to be the same as the initial carbon content in solid ω_{Cin} because carbon is consumed by reaction and the space is void. The ratio of core diameter to particle diameter ρ is given by the following equation.

$$\rho = \left(\frac{\omega_C}{\omega_{Cin}} \right)^{1/3}$$

The ratio of local carbon content to initial carbon content in a solid particle is same as the ratio of volume occupied by unreacted core to volume of the original particle when the densities of carbon and ash are assumed to be same.

The rate of heterogeneous reaction of carbon with carbon dioxide to carbon monoxide is mostly controlled by combustion kinetics because the intrinsic reaction rate of carbon with carbon dioxide is much slower than that of carbon with oxygen. However, the rate is controlled by convective mass transfer and by ash layer diffusion when the temperature of the bed is high enough for the intrinsic reaction rate to be much higher than the rate by convective mass transfer and ash layer diffusion. The overall reaction rate of carbon with carbon dioxide can be derived by combining convective mass transfer, ash layer diffusion, and gasification kinetics.

$$r_{C2} = -\frac{Y_{CO_2}}{\frac{1}{h_{DCO_2}\frac{M_C}{M_{CO_2}}} + \frac{1}{\frac{2\rho_g D_{eCO_2}}{d}\frac{\rho}{1-\rho}\frac{M_C}{M_{CO_2}}} + \frac{1}{\rho^2 k P \frac{M_g}{M_{CO_2}}}} \qquad (2.24)$$

The kinetic rate equation of the gasification reaction by Gadsby et al.[19] is employed.

The mass generation term defined by the mass of carbon generation per unit time per unit volume of bed for the reaction of carbon with carbon dioxide can be written as:

$$\dot{W}_2''' = -\frac{A_v Y_{CO_2}}{\frac{1}{h_{DCO_2}\frac{M_C}{M_{CO_2}}} + \frac{1}{\frac{2\rho_g D_{eCO_2}}{d}\frac{\rho}{1-\rho}\frac{M_C}{M_{CO_2}}} + \frac{1}{\rho^2 k P \frac{M_g}{M_{CO_2}}}}$$

where

$$k = \frac{k_{021}\exp\left(-\frac{E_{21}}{RT_s}\right)}{1 + k_{022}\exp\left(-\frac{E_{22}}{RT_s}\right)Y_{CO}\frac{PM_g}{M_{CO}} + k_{023}\exp\left(-\frac{E_{23}}{RT_s}\right)Y_{CO_2}\frac{PM_g}{M_{CO_2}}}\frac{M_C\rho_s d}{6}$$

The preexponential factors and the activation energies for the gasification reaction of carbon with carbon dioxide are given by Gadsby et al.[19] and are listed in Table 2. The temperature in their experiment ranged from 973 K to 1,103 K. On the other hand, the temperature of the bed in this study ranges from 300 K even to 1,900 K so that it may cause error to be estimated the rate when the temperature of the bed is out of the range given above. When those reaction constants are used, the concentration of carbon dioxide at the top portion of the bed by numerical calculation is much lower than the experimental result[8] so that those values are modified in this study to obtain reasonable agreement with the experiment. The modified constants are also listed in Table 2.

Table 2 Rate constants for gasification reaction of carbon with carbon dioxide.

		Constants by Gadsby at al.[19]	Modified Constants
k_{021}	kmol CO/(sec Pa kg solid)	103.81	3.4×10^{7}
k_{022}	1/Pa	1.2428×10^{-13}	6.229×10^{-13}
k_{023}	1/Pa	31.217	156.5
E_{21}	J/kmol	2.461×10^{8}	4.5×10^{8}
E_{22}	J/kmol	-1.904×10^{8}	-2.051×10^{8}
E_{23}	J/kmol	1.260×10^{8}	1.109×10^{8}

Even though the shrinking core model is the best simple representation for majority of reacting gas-solid systems,[18] some of the ash is segregated from the solid particles, the shrinking core model overestimates diffusion resistance through the ash layer, and it makes the rate of carbon reaction lower than the rate of experiment by Nicholls and Eilers.[8] To reduce the diffusion resistance and to obtain solutions which agree well with experimental results, the ratio of core diameter to initial particle diameter ρ is assumed to be 0.6382 (This is the diameter ratio when local carbon content in solid is about 0.26 times initial carbon content in solid.) when it is less than or equal to 0.6382. In other words, the diffusion resistance through the ash layer is the same when the ash layer thickness is greater than or equal to 0.3618 times initial particle diameter.

The rate of homogeneous reaction of carbon monoxide with oxygen is usually represented by the following equation.

$$r_{CO} = - k_{03} C_{CO}^{a} C_{O_2}^{b} C_{H_2O}^{c} \exp\left(- \frac{E_3}{RT_g}\right)$$

where k_{03} and E_3 respectively are preexponential factor and activation energy, a, b, and c are reaction orders, and C_j is molar concentration of gas species j. The mass generation of carbon monoxide per unit time per unit volume of the bed in terms of mass fraction can be expressed in the following equation by converting molar concentration to mass fraction and by multiplying r_{CO} by molar mass of carbon monoxide and void fraction of the bed.

$$\dot{W}_3''' = r_{CO} M_{CO} \phi$$

$$= - k_{03} Y_{CO}^{a} Y_{O_2}^{b} Y_{H_2O}^{c} \exp\left(- \frac{E_3}{RT_g}\right) \frac{\phi \rho_g^{a+b+c}}{M_{CO}^{a-1} M_{O_2}^{b} M_{H_2O}^{c}}$$

The reaction constants in the above equation are proposed by several authors and are listed in Table 3. The rate of this homogeneous reaction is mostly controlled by only the gaseous reaction kinetics. This reaction is negligibly small in the absence of moisture.[21, 22] However, when oxidant gas contains some moisture, the reaction is so fast that the carbon monoxide produced by the reaction of carbon with oxygen is

Table 3 Rate constants for the reaction of carbon monoxide with oxygen.

Author	k_{03} (1/s $(m^3/kmol)^{a+b+c-1}$)	a	b	c	E_3 (MJ/kmol)
Howard et al.[23]	1.3×10^{11}	1	0.5	0.5	125.6
Dryer and Glassman[24]	2.19×10^{12}	1	0.25	0.5	167.4
Hottel et al.[25]	4.78×10^{8}	1	0.30	0.5	66.97

consumed as soon as it is produced and the reaction of carbon monoxide with oxygen is assumed to be controlled by the reaction of carbon with oxygen. The mass generation of carbon monoxide per unit volume of the bed per unit time due to the reaction of carbon monoxide with oxygen can be written as:

$$\dot{W}_3''' = f_{CO}\,\dot{W}_1'''\,\frac{M_{CO}}{M_C}$$

The rate of carbon monoxide reaction with oxygen which is controlled by the reaction rate of carbon with oxygen and by intrinsic reaction kinetics suggested by several authors[23, 24, 25] are compared in Fig. 7. This figure shows that the assumption is appropriate. The reaction constants of the authors are listed in Table 3.

The enthalpies of reaction for various chemical reactions as a function of temperature are given by Wicks and Block.[26] Those are modified to the following equations which are the enthalpies of reaction for the reaction of carbon with oxygen to carbon monoxide (Δh_{1A}) and to carbon dioxide (Δh_{1B}), for the reaction of carbon with carbon dioxide (Δh_2), and for the reaction of carbon monoxide with oxygen (Δh_3).

$$\Delta h_{1A} = -1.06240\times10^{8} - 3.73\times10^{3}T_s - 1.13T_s^2 - 9.17\times10^{8}/T_s \quad \text{J/kmol of C} \qquad (2.25a)$$

$$\Delta h_{1B} = -3.92000\times10^{8} - 2.97\times10^{3}T_s + 0.293T_s^2 - 1.93\times10^{8}/T_s \quad \text{J/kmol of C} \qquad (2.25b)$$

$$\Delta h_{2} = -1.7952\times10^{8} - 4.49\times10^{3}T_s - 2.553T_s^2 - 1.641\times10^{9}/T_s \quad \text{J/kmol of C} \qquad (2.25c)$$

$$\Delta h_{3} = -2.8576\times10^{8} + 0.76\times10^{3}T_g + 1.423T_g^2 + 7.24\times10^{8}/T_g \quad \text{J/kmol of CO} \qquad (2.25d)$$

Above equations are valid over the range 298 K $\leq$ T $\leq$ 2,000 K and T is in K.

2.3 HEAT AND MASS TRANSFER COEFFICIENTS

In the study of Cho and Joseph[4] for the heterogeneous model for moving-bed coal gasification reactor, the heat transfer coefficient between solid and gas for reactive systems was taken to be proportional to the heat transfer coefficient for nonreactive systems estimated by Gupta and Thodos[27] because no correlations are available for the reactive systems and the result of the calculation gives most close agreement with the experimental data when the proportional constant is 0.3. On the other hand, in the study of Malling and Thodos[28] for the analogy between mass and heat transfer in beds of sphere, they mentioned that the heat and mass transfer data of Gupta and Thodos[27] gave relatively higher values.

In the present study, the correlation of Malling and Thodos[28] is employed to estimate the convection heat and mass transfer coefficient. The convection heat transfer coefficient between solid and gas becomes higher for lower void fraction of the bed, for higher gas velocity, and for higher Prandtl number fluid.

$$Nu_g = \frac{h\,d}{K_g} = \frac{0.539}{\phi^{1.19}} Re_g^{0.563}\, Pr_g^{1/3} \tag{2.26}$$

where

$$Re_g = \frac{\rho_g \phi u_g d}{\mu_g} = \frac{\rho_g u_{g0} d}{\mu_g} \quad \text{and} \quad Pr_g = \frac{\mu_g C_{pg}}{K_g}$$

The convection mass transfer coefficient of gas species j from bulk gas mixture to solid surface becomes higher for lower void fraction of the bed, for higher gas velocity, and for higher Schmidt number.

$$Sh_j = \frac{h_{Dj}\, d}{\rho_g D_j} = \frac{0.539}{\phi^{1.19}} Re_g^{0.563} Sc_j^{1/3} \qquad (2.27)$$

where

$$Sc_j = \frac{\mu_g}{\rho_g D_j}$$

Above heat and mass transfer coefficient equations are valid for the range $185 < Re_g < 8{,}500$. The range of validity of the correlation of Malling and Thodos[28] is limited especially at low gas Reynolds number. Some of the gas Reynolds numbers used in this study as parameters are lower than 185 and it may cause some errors.

2.4 EFFECTIVE THERMAL CONDUCTIVITY

The thermal conductivities of solid and gas phase in a particle bed are different from the thermal conductivities of the solid and gas themselves. In addition to the thermal conductivities of the solid and gas themselves, the effects of void fraction, radiation heat transfer, and enhanced heat transfer due to the eddy diffusion by fluid flow around solid particles are accounted in the conduction heat transfer term. The thermal conductivity which includes above several effects has been defined as the effective thermal conductivity.

Kunii and Smith[29] proposed that the heat transfer in particle bed with stagnant fluid is assumed to occur by the following mechanisms.

(1) Heat transfer through the solid phase.

(a) Conduction through the contact surface of the solid particles.

(b) Conduction through the stagnant fluid near the contact surface.

(c) Radiation between surfaces of solid.

(d) Conduction through the solid phase.

(2) Heat transfer through the fluid in the void space by conduction and radiation between adjacent voids.

The effective thermal conductivity of a bed with stagnant fluid by above mechanisms is:

$$\frac{K_e^{\circ}}{K_g} = \frac{\beta(1-\phi)}{\dfrac{1}{\dfrac{1}{\psi}+\dfrac{d}{K_g}(h_p+h_{rs})} + \gamma\dfrac{K_g}{K_s}} + \phi\left(1+\beta\frac{h_{rv}d}{K_g}\right)$$

The axial effective thermal conductivity due to the eddy diffusion by fluid flow around solid particles was studied by Yagi et al.[30].

$$\frac{K_{ed}}{K_g} = \delta\, Re_g\, Pr_g$$

The effective thermal conductivity in packed bed with fluid flow is the sum of each effective thermal conductivity by the mechanism of heat transfer in packed bed with stagnant fluid and the mechanism of eddy diffusion by fluid flow.

$$\frac{K_e}{K_g} = \frac{K_e^0}{K_g} + \frac{K_{ed}}{K_g} = \frac{\beta(1-\phi)}{\frac{1}{\frac{1}{\psi}+\frac{d}{K_g}(h_p+h_{rs})} + \gamma\frac{K_g}{K_s}} + \phi\left(1+\beta\frac{h_{rv}d}{K_g}\right) + \delta\, Re_g\, Pr_g$$

Above equation can be simplified by the following reasons. The term due to the heat transfer through the contact surface of the solid particles h_p is negligible except at very low pressures.[29] The term due to the radiation heat transfer between adjacent voids h_{rv} is usually insignificant because the gas emissivities are low.[32] Then, the effective thermal conductivity is simplified to the following equation.

$$\frac{K_e}{K_g} = \frac{\beta(1-\phi)}{\frac{1}{\frac{1}{\psi}+\frac{h_{rs}d}{K_g}} + \gamma\frac{K_g}{K_s}} + \phi + \delta\, Re_g\, Pr_g$$

The effective thermal conductivity in packed bed need to be divided into two parts as shown below because the two energy equations, one for the solid phase and one for the gas phase, are set up separately in the present study.

$$\frac{K_{es}}{K_g} = \frac{\beta(1-\phi)}{\frac{1}{\frac{1}{\psi}+\frac{h_{rs}d}{K_g}} + \gamma\frac{K_g}{K_s}} \tag{2.28}$$

$$\frac{K_{eg}}{K_g} = \phi + \delta\, Re_g\, Pr_g \tag{2.29}$$

The constants in the above equations are explained below. The values of these constants may change according to the method of packing, the void fraction, and the solid particle diameter. The value of δ found experimentally by Yagi et al.[30] ranges

from 0.7 to 0.8. It was modified by Wakao and Kaguei[32] and the value of δ is 0.5 in a wide range of Reynolds number. β is the ratio of the average length between the center of two neighboring solids in the direction of heat flow to the particle diameter. The value of β for rhombohedral packing of sphere is 0.894.[29] γ is the ratio of the length of a cylinder having the same volume and diameter as the spherical particle to the diameter of the spherical particle. The value of γ is 2/3.[29] ψ is the ratio of effective thickness of the fluid film adjacent to the surface of two solid particles to the diameter of the solid particle. The value of ψ is represented by the following equation for rhombohedral packing of sphere.[29]

$$\psi = \frac{0.072\left(1-\frac{1}{\kappa}\right)^2}{\ln(\kappa-0.925(\kappa-1))-0.075\left(1-\frac{1}{\kappa}\right)} - \frac{2}{3\kappa} \tag{2.30}$$

where

$$\kappa = \frac{K_s}{K_g}$$

The radiation heat transfer coefficient due to the radiation between surfaces of solid h_{rs} was proposed by several authors. Among them, the relation by Wakao and Kato[31] seems to be the most reasonable formula which includes an overall view factor.

$$h_{rs} = \frac{8\sigma T_s^3}{\frac{2}{\epsilon} - 0.264} \tag{2.31}$$

where σ is the Stefan-Boltzman constant in W/m^2K^4 and ϵ is the emissivity of solid particle surface.

The effective thermal conductivity is a function of temperature so that the conduction terms in the energy equations are nonlinear. The effective thermal conductivity of solid in the bed is usually lower than the thermal conductivity of solid at lower temperature due to the effect of void fraction. On the other hand, the effective thermal conductivity of solid in the bed is higher than the thermal conductivity of solid at higher temperature due to the higher rate of radiation heat transfer.

2.5 MINIMUM FLUIDIZATION

It is necessary to confine the maximum gas velocity in a moving bed to ensure that the bed is not fluidized. The maximum gas velocity in the moving bed should be less than the minimum fluidization velocity u_{mf} which is defined as the velocity of the gas to make the bed in the most loosely packed state but in stable bed configuration.

Wen and Yu[33, 34] proposed the following correlation to obtain the minimum fluidization Reynolds number by considering the pressure drop in the bed.

$$Re_{mf} = \sqrt{(33.7)^2 + 0.0408\,Ga} - 33.7 \qquad (2.32)$$

where Ga is the Galileo number and is defined as:

$$Ga = \frac{\rho_g(\rho_s - \rho_g)g\,d^3}{\mu_g^2}$$

The advantages of the above correlation are it is simple and it does not need information pertaining to the minimum fluidization voidage and the shape factor which are usually unavailable. Saxena and Vogel[35] reported that the computed values

of minimum fluidization Reynolds number from above equation are consistently smaller than the values obtained from their experiment performed at high temperature and they modified to the following correlation.

$$Re_{mf} = \sqrt{(25.28)^2 + 0.0571\,Ga} - 25.28 \tag{2.33}$$

Botterill et al.[36] studied the effect of operating temperature on the minimum fluidization velocity, bed voidage, and general behavior but they did not suggest any correlation.

2.6 VARIABLES AND PARAMETERS OF THE PROBLEM

The independent variable x is normalized by the bed length and the dependent variables are normalized by the proper constant supply parameters as shown below.

Independent Variable:

$$\xi = \frac{x}{L} \tag{2.34}$$

Primary Dependent Variables :

$$\theta_g = \frac{T_g}{T_{gin}} \quad , \quad \theta_s = \frac{T_s}{T_{gin}} \quad , \quad y_j = \frac{Y_j}{Y_{O_2 in}}$$
$$\Omega_j = \frac{\omega_j}{\omega_{jin}} \quad , \quad U_g = \frac{u_g}{u_{gin}} \quad , \quad \tilde{\rho}_g = \frac{\rho_g}{\rho_{gin}} \tag{2.35}$$

The following dimensionless parameters are used in the dimensionless governing equations and boundary conditions.

Given Constant Parameters:

(1) Geometric Parameters:

$$\phi \ , \ \phi_p \ , \ \frac{d}{L} \ , \ A_v d$$

(2) Flow-related Parameters:

$$Re_{gin} = \frac{\rho_{gin} u_{gin} \phi d}{\mu_{gin}} \ , \ Re_s = \frac{\rho_{gin} u_s d}{\mu_{gin}} \ , \ \tilde{\rho}_{in} = \frac{\rho_{sin}}{\rho_{gin}}$$

(3) Energy Parameters:

$$Pr_{gin} = \frac{\mu_{gin} C_{pgin}}{K_{gin}} \ , \ R_T = \frac{T_{sin}}{T_{gin}}$$

(4) Gas Species Parameters:

$$Sc_{O_2 in} = \frac{\mu_{gin}}{\rho_{gin} D_{O_2 in}} \ , \ \tilde{M}_j = \frac{M_j}{M_{gin}} \ , \ Y_{O_2 in} \ , \ Y_{N_2 in} \ , \ \phi_h$$

(5) Solid Species Parameters:

$$\omega_{jin}$$

(6) Chemical Parameters:

$$Da_{21} = \frac{k_{021} P d^2 M_C}{D_{O_2 in}} \ , \ Da_{22} = k_{022} P \ , \ Da_{23} = k_{023} P \ ,$$

$$Ar_{21} = \frac{E_{21}}{R T_{gin}} \ , \ Ar_{22} = \frac{E_{22}}{R T_{gin}} \ , \ Ar_{23} = \frac{E_{23}}{R T_{gin}}$$

Changing Parameters:

(1) Energy Parameters:

$$\tilde{K}_{eg} = \frac{K_{eg}}{K_{gin}} \quad , \quad \tilde{K}_{es} = \frac{K_{es}}{K_{gin}} \quad , \quad \tilde{K}_{g} = \frac{K_{g}}{K_{gin}} \quad , \quad \tilde{C}_{pg} = \frac{C_{pg}}{C_{pgin}} \quad , \quad \tilde{C}_{ps} = \frac{C_{ps}}{C_{pgin}}$$

(2) Species Parameters:

$$\tilde{\mu}_{g} = \frac{\mu_{g}}{\mu_{gin}} \quad , \quad \tilde{D}_{j} = \frac{D_{j}}{D_{O_2 in}} \quad , \quad \tilde{M}_{g} = \frac{M_{g}}{M_{gin}} \quad , \quad \tilde{\rho}_{s} = \frac{\rho_{s}}{\rho_{sin}}$$

(3) Chemical Parameters:

$$f_{CO} \quad , \quad H_{1A} = \frac{-\Delta h_{1A}}{C_{pgin} T_{gin} M_{C}} \quad , \quad H_{1B} = \frac{-\Delta h_{1B}}{C_{pgin} T_{gin} M_{C}} \quad ,$$

$$H_{2} = \frac{-\Delta h_{2}}{C_{pgin} T_{gin} M_{C}} \quad , \quad H_{3} = \frac{-\Delta h_{3}}{C_{pgin} T_{gin} M_{CO}}$$

Auxiliary Changing Parameters:

$$Nu_{g} = \frac{hd}{K_{g}} \quad , \quad Re_{g} = Re_{gin} \frac{\tilde{\rho}_{g} U_{g}}{\tilde{\mu}_{g}} \quad , \quad Pr_{g} = Pr_{gin} \frac{\tilde{\mu}_{g} \tilde{C}_{pg}}{\tilde{K}_{g}} \quad ,$$

$$Sh_{j} = \frac{h_{Dj} d}{\rho_{g} D_{j}} \quad , \quad Sc_{j} = Sc_{O_2 in} \frac{\tilde{\mu}_{g}}{\tilde{\rho}_{g} \tilde{D}_{j}} \quad , \quad Bi = \frac{h\, d(1-\phi)}{K_{es}}$$

where j = Carbon or Ash for solid species and j=O_2, N_2, CO_2, CO, or H_2O for gas species.

2.7 DIMENSIONLESS GOVERNING EQUATIONS AND BOUNDARY CONDITIONS

The dimensionless governing equations and boundary conditions are derived by introducing dimensionless variables and parameters summarized in section 2.6 and are shown below.

Energy Equations:

$$\frac{d}{d\xi}\left(\tilde{K}_{eg}\frac{d\theta_g}{d\xi}\right) - \frac{d}{d\xi}\left(\frac{Re_{gin}Pr_{gin}}{d/L}\tilde{\rho}_g U_g \tilde{C}_{pg}\theta_g\right) - \frac{A_v d}{(d/L)^2}\tilde{K}_g Nu_g(\theta_g-\theta_s) + \dot{q}_g''' = 0 \tag{2.36}$$

$$\frac{d}{d\xi}\left(\tilde{K}_{es}\frac{d\theta_s}{d\xi}\right) + \frac{d}{d\xi}\left(\frac{1-\phi}{d/L}Re_s\, Pr_{gin}\tilde{\rho}_{in}\,\tilde{\rho}_s\tilde{C}_{ps}\theta_s\right) + \frac{A_v d}{(d/L)^2}\tilde{K}_g Nu_g(\theta_g-\theta_s) + \dot{q}_s''' = 0 \tag{2.37}$$

where

$$\dot{q}_g''' = -\frac{Pr_{gin}}{Sc_{O_2in}}Y_{O_2in}H_3\dot{w}_3''' \tag{2.38}$$

$$\dot{q}_s''' = -\frac{Pr_{gin}}{Sc_{O_2in}}Y_{O_2in}\left[f_{CO}H_{1A}\dot{w}_1''' + (1-f_{CO})H_{1B}\dot{w}_1''' + H_2\dot{w}_2'''\right] \tag{2.39}$$

Solid Species Equations:

$$\frac{d\Omega_j}{d\xi} = -\frac{d/L}{1-\phi}\frac{Y_{O_2in}}{Re_s Sc_{O_2in}\tilde{\rho}_{in}\omega_{jin}}\dot{w}_j''' \tag{2.40}$$

$$\text{For } j = C \quad ; \quad \dot{w}_C''' = \dot{w}_1''' + \dot{w}_2''' \qquad (2.41)$$

$$j = \text{Ash} \quad ; \quad \dot{w}_A''' = 0$$

Gas Species Equations:

$$\frac{d}{d\xi}\left(\tilde{\rho}_g \tilde{D}_j \phi \frac{dy_j}{d\xi}\right) - \frac{d}{d\xi}\left(\frac{Re_{gin} Sc_{O_2 in}}{d/L} \tilde{\rho}_g U_g y_j\right) + \dot{w}_j''' = 0 \qquad (2.42)$$

$$\text{For } j = O_2 \quad ; \quad \dot{w}_{O_2}''' = \left(1 - \frac{f_{CO}}{2}\right)\dot{w}_1''' \frac{\tilde{M}_{O_2}}{\tilde{M}_C} + \frac{1}{2}\dot{w}_3''' \frac{\tilde{M}_{O_2}}{\tilde{M}_{CO}}$$

$$j = N_2 \quad ; \quad \dot{w}_{N_2}''' = 0$$

$$j = CO_2 \quad ; \quad \dot{w}_{CO_2}''' = -(1 - f_{CO})\dot{w}_1''' \frac{\tilde{M}_{CO_2}}{\tilde{M}_C} + \dot{w}_2''' \frac{\tilde{M}_{CO_2}}{\tilde{M}_C} - \dot{w}_3''' \frac{\tilde{M}_{CO_2}}{\tilde{M}_{CO}}$$

$$j = CO \quad ; \quad \dot{w}_{CO}''' = -f_{CO}\dot{w}_1''' \frac{\tilde{M}_{CO}}{\tilde{M}_C} - 2\dot{w}_2''' \frac{\tilde{M}_{CO}}{\tilde{M}_C} + \dot{w}_3'''$$

$$j = H_2O \quad ; \quad \dot{w}_{H_2O}''' = 0 \qquad (2.43)$$

Gas Continuity Equation:

$$\frac{d}{d\xi}(\tilde{\rho}_g U_g) - \frac{(d/L) Y_{O_2 in}}{Re_{gin} Sc_{O_2 in}}\left(\dot{w}_{O_2}''' + \dot{w}_{CO_2}''' + \dot{w}_{CO}'''\right) = 0 \qquad (2.44)$$

Equation of State:

$$\tilde{\rho}_g = \frac{\tilde{M}_g}{\theta_g} \quad \text{and} \quad \rho_{gin} = \frac{P M_{gin}}{R T_{gin}} \qquad (2.45)$$

The dimensionless mass generation terms in the above governing equations for the two heterogenous reactions and one homogeneous reaction are:

$$\dot{w}_1''' = -\frac{A_v d}{(d/L)^2}\frac{1}{1-\frac{f_{CO}}{2}}\frac{y_{O_2}}{\frac{1}{\tilde{\rho}_g \tilde{D}_{O_2} Sh_{O_2}\frac{\tilde{M}_C}{\tilde{M}_{O_2}}} + \frac{1}{2\tilde{\rho}_g \tilde{D}_{eO_2}\frac{\rho}{1-\rho}\frac{\tilde{M}_C}{\tilde{M}_{O_2}}}} \tag{2.46}$$

$$\dot{w}_2''' = -\frac{A_v d}{(d/L)^2}\frac{y_{CO_2}}{\frac{1}{\tilde{\rho}_g \tilde{D}_{CO_2} Sh_{CO_2}\frac{\tilde{M}_C}{\tilde{M}_{CO_2}}} + \frac{1}{2\tilde{\rho}_g \tilde{D}_{eCO_2}\frac{\rho}{1-\rho}\frac{\tilde{M}_C}{\tilde{M}_{CO_2}}} + \frac{1}{\frac{1}{6}\rho^2 \tilde{\rho}_s \tilde{\rho}_{in} \tilde{k}\frac{\tilde{M}_g}{\tilde{M}_{CO_2}}}} \tag{2.47}$$

$$\dot{w}_3''' = f_{CO}\,\dot{w}_1'''\frac{\tilde{M}_{CO}}{\tilde{M}_C} \tag{2.48}$$

where

$$\tilde{k} = \frac{Da_{21}\exp\left(-\frac{Ar_{21}}{\theta_s}\right)}{1 + Da_{22}\exp\left(-\frac{Ar_{22}}{\theta_s}\right) y_{CO}\, Y_{O_2 in}\frac{\tilde{M}_g}{\tilde{M}_{CO}} + Da_{23}\exp\left(-\frac{Ar_{23}}{\theta_s}\right) y_{CO_2}\, Y_{O_2 in}\frac{\tilde{M}_g}{\tilde{M}_{CO_2}}}$$

$$\tilde{D}_{ej} = \tilde{D}_j \phi_p^2$$

$$\rho = \Omega_C^{1/3}$$

Boundary Conditions for Energy Equations:

$$\xi = 0 \; : \quad \theta_g = 1 \quad , \quad \frac{d\theta_s}{d\xi} - \frac{1-\phi}{d/L}\frac{\tilde{K}_g}{\tilde{K}_{es}} Nu_g(\theta_s - 1) = 0 \tag{2.49}$$

$$\xi = 1 \; : \quad \frac{d\theta_g}{d\xi} = 0 \quad , \quad \frac{d\theta_s}{d\xi} + \frac{1-\phi}{d/L}\frac{\tilde{K}_g}{\tilde{K}_{es}} Nu_g(\theta_s - R_T) = 0 \tag{2.50}$$

Boundary Conditions for Solid Species Equations:

$$\xi = 1 \; : \quad \Omega_C = 1 \quad , \quad \Omega_A = 1 \tag{2.51}$$

Boundary Conditions for Gas Species Equations:

$$\xi = 0 \; : \quad y_{O_2} = 1 \quad , \quad y_{N_2} = \frac{Y_{N_2 in}}{Y_{O_2 in}} \quad , \quad y_{CO_2} = 0 \quad , \quad y_{CO} = 0 \quad , \quad y_{H_2O} = \frac{Y_{H_2Oin}}{Y_{O_2 in}} \tag{2.52}$$

$$\xi = 1 \; : \quad \frac{dy_{O_2}}{d\xi} = 0 \quad , \quad \frac{dy_{N_2}}{d\xi} = 0 \quad , \quad \frac{dy_{CO_2}}{d\xi} = 0 \quad , \quad \frac{dy_{CO}}{d\xi} = 0 \quad , \quad \frac{dy_{H_2O}}{d\xi} = 0 \tag{2.53}$$

Boundary Condition for Gas Continuity Equation:

$$\xi = 0 \; : \quad U_g = 1 \tag{2.54}$$

When all the known parameters except gas supply rate are given, the gas supply rate for the complete consumption of carbon in solid particles at the bottom of the bed can be uniquely determined. This unique gas supply rate is defined as the stoichiometric gas supply rate or the eigenvalue of gas supply rate. The stoichiometric gas supply rate or the eigenvalue of gas supply rate is again defined by

the gas supply rate when the carbon in solid particles is completely consumed at the bottom of the bed at the given condition. The stoichiometric or eigenvalue of solid supply rate can also be determined when all other parameters except the solid supply rate are given. When the gas supply rate is higher than the stoichiometric gas supply rate at a given condition, the air supply is excess and the carbon in solid particles is completely consumed before the particles reach the bottom of the bed. On the other hand, when the gas supply rate is lower than the stoichiometric gas supply rate, the air supply is deficient, the carbon content in solid particles never become zero in the bed, and unburned carbon in solid particles will be discharged at the bottom of the bed. The relation between stoichiometric solid and gas supply Reynolds numbers can be estimated by the following equation for single reaction model.

$$\frac{Re_{gin}}{Re_s} = \frac{\omega_{Cin}}{Y_{O_2 in}} \rho_{sin}(1-\phi) \frac{R\,T_{gin}}{P\,M_{gin}} \frac{M_{O_2}}{M_C} \tag{2.55}$$

For the two or three reaction model, the stoichiometric solid and gas supply Reynolds numbers can be estimated by numerical calculation. The stoichiometric solid and gas supply rates or Reynolds numbers will be determined at various given conditions for the parametric study.

A mathematical model for the combustion of solid fuel particles in a moving bed is proposed in this chapter. The governing equations and boundary conditions are also nondimensionalized by introducing dimensionless variables and parameters. In the next chapter, these dimensionless governing equations and boundary conditions are discretized by finite difference approximation and a numerical scheme to solve these equations is proposed.

CHAPTER 3

SOLUTION PROCEDURE

The energy and gas species equations are of second order while the solid species and gas continuity equations are of first order. The coefficients of these equations are functions of temperature and/or concentration making these equations nonlinear and coupled. It is impossible to obtain closed form solutions. Finite difference method is employed here to solve the governing equations by iteration. In this chapter, the equations and boundary conditions are discretized and an iterative solution algorithm is proposed. The temperature-dependent properties of the solid, each gas species, and their mixtures are also calculated. The values of given parameters for the numerical calculations are listed.

3.1 FINITE DIFFERENCE DISCRETIZATION

Finite difference approximation is employed to find numerical solutions for the energy equations, gas species equations, solid species equations, and gas continuity equation. The second order terms are approximated by central difference. Upwind scheme is used to discretize the first order terms in the governing equations. The first order terms in the boundary conditions are discretized by central difference.

Central Difference:

$$\frac{d}{d\xi}\left(c\frac{d\theta}{d\xi}\right) \approx \frac{c^{i}+c^{i+1}}{(\Delta\xi^{i-1}+\Delta\xi^{i})\Delta\xi^{i}}(\theta^{i+1}-\theta^{i}) - \frac{c^{i-1}+c^{i}}{(\Delta\xi^{i-1}+\Delta\xi^{i})\Delta\xi^{i-1}}(\theta^{i}-\theta^{i-1})$$

$$\frac{d\theta}{d\xi} \approx \frac{\theta^{i+1}-\theta^{i-1}}{\Delta\xi^{i-1}+\Delta\xi^{i+1}}$$

Upwind Method:

$$+\frac{d}{d\xi}(c\theta) \approx \frac{1}{\Delta\xi^{i}}(c^{i+1}\theta^{i+1} - c^{i}\theta^{i})$$

$$-\frac{d}{d\xi}(c\theta) \approx -\frac{1}{\Delta\xi^{i-1}}(c^{i}\theta^{i} - c^{i-1}\theta^{i-1})$$

The superscripts of variables in finite difference equations are node numbers.

The finite difference governing equations are then as follows.

Energy Equations:

$$C_{g1}^{i}\theta_{g}^{i-1} - C_{g2}^{i}\theta_{g}^{i} + C_{g3}^{i}\theta_{g}^{i+1} = -C_{g4}^{i}\theta_{s}^{i} - C_{g5}^{i} \qquad (3.1)$$

$$C_{s1}^{i}\theta_{s}^{i-1} - C_{s2}^{i}\theta_{s}^{i} + C_{s3}^{i}\theta_{s}^{i+1} = -C_{s4}^{i}\theta_{g}^{i} - C_{s5}^{i} \qquad (3.2)$$

where

$$C_{g1}^{i} = \tilde{K}_{eg}^{i-1} + \tilde{K}_{eg}^{i} + (\Delta\xi^{i-1} + \Delta\xi^{i})\frac{Re_{gin}\,Pr_{gin}}{d/L}\,\tilde{\rho}_{g}^{i-1}\,U_{g}^{i-1}\,\tilde{C}_{pg}^{i-1}$$

$$C_{g2}^{i} = \frac{\Delta\xi^{i-1}}{\Delta\xi^{i}}\left(\tilde{K}_{eg}^{i} + \tilde{K}_{eg}^{i+1}\right) + \left(\tilde{K}_{eg}^{i-1} + \tilde{K}_{eg}^{i}\right) + (\Delta\xi^{i-1} + \Delta\xi^{i})\frac{Re_{gin}\,Pr_{gin}}{d/L}\,\tilde{\rho}_{g}^{i}\,U_{g}^{i}\,\tilde{C}_{pg}^{i}$$

$$+ (\Delta\xi^{i-1} + \Delta\xi^{i})\Delta\xi^{i-1}\frac{A_v d}{(d/L)^2}\,\tilde{K}_{g}^{i}\,Nu_{g}^{i}$$

$$C_{g3}^{i} = \frac{\Delta\xi^{i-1}}{\Delta\xi^{i}}\left(\tilde{K}_{eg}^{i} + \tilde{K}_{eg}^{i+1}\right)$$

$$C_{g4}^{i} = (\Delta\xi^{i-1} + \Delta\xi^{i})\Delta\xi^{i-1}\frac{A_v d}{(d/L)^2}\tilde{K}_{g}^{i}\,Nu_{g}^{i}$$

$$C_{g5}^{i} = (\Delta\xi^{i-1} + \Delta\xi^{i})\Delta\xi^{i-1}\left(\dot{q}_{g}^{'''}\right)^{i}$$

$$C_{s1}^{i} = \tilde{K}_{es}^{i-1} + \tilde{K}_{es}^{i}$$

$$C_{s2}^{i} = \frac{\Delta\xi^{i-1}}{\Delta\xi^{i}}\left(\tilde{K}_{es}^{i} + \tilde{K}_{es}^{i+1}\right) + \left(\tilde{K}_{es}^{i-1} + \tilde{K}_{es}^{i}\right) + (\Delta\xi^{i-1} + \Delta\xi^{i})\Delta\xi^{i-1}\frac{A_v d}{(d/L)^2}\,\tilde{K}_{g}^{i}\,Nu_{g}^{i}$$

$$+ (\Delta\xi^{i-1} + \Delta\xi^{i})\frac{\Delta\xi^{i-1}}{\Delta\xi^{i}}\frac{1-\phi}{d/L}\,Re_{s}\,Pr_{gin}\,\tilde{\rho}_{in}\,\tilde{\rho}_{s}^{i}\,\tilde{C}_{ps}$$

$$C_{s3}^{i} = \frac{\Delta\xi^{i-1}}{\Delta\xi^{i}}\left(\tilde{K}_{es}^{i} + \tilde{K}_{es}^{i+1}\right) + (\Delta\xi^{i-1} + \Delta\xi^{i})\frac{\Delta\xi^{i-1}}{\Delta\xi^{i}}\frac{1-\phi}{d/L}\,Re_{s}\,Pr_{gin}\,\tilde{\rho}_{in}\,\tilde{\rho}_{s}^{i+1}\,\tilde{C}_{ps}$$

$$C_{s4}^{i} = (\Delta\xi^{i-1} + \Delta\xi^{i})\Delta\xi^{i-1}\frac{A_v d}{(d/L)^2}\tilde{K}_{g}^{i}\,Nu_{g}^{i}$$

$$C_{s5}^{i} = (\Delta\xi^{i-1} + \Delta\xi^{i})\Delta\xi^{i-1}\left(\dot{q}_{s}^{'''}\right)^{i}$$

Gas Species Equations:

$$C_{j1}^{i} y_j^{i-1} - C_{j2}^{i} y_j^{i} + C_{j3}^{i} y_j^{i+1} = -C_{j4}^{i} \tag{3.3}$$

where

$$C_{j1}^{i} = \left(\tilde{\rho}_g^{i-1} \tilde{D}_j^{i-1} + \tilde{\rho}_g^{i} \tilde{D}_j^{i}\right)\phi + \left(\Delta\xi^{i-1} + \Delta\xi^{i}\right)\frac{Re_{gin} Sc_{O_2 in}}{d/L} \tilde{\rho}_g^{i-1} U_g^{i-1}$$

$$C_{j2}^{i} = \frac{\Delta\xi^{i-1}}{\Delta\xi^{i}}\left(\tilde{\rho}_g^{i} \tilde{D}_j^{i} + \tilde{\rho}_g^{i+1} \tilde{D}_j^{i+1}\right)\phi + \left(\tilde{\rho}_g^{i-1} \tilde{D}_j^{i-1} + \tilde{\rho}_g^{i} \tilde{D}_j^{i}\right)\phi$$

$$+ \left(\Delta\xi^{i-1} + \Delta\xi^{i}\right)\frac{Re_{gin} Sc_{O_2 in}}{d/L} \tilde{\rho}_g^{i} U_g^{i}$$

$$C_{j3}^{i} = \frac{\Delta\xi^{i-1}}{\Delta\xi^{i}}\left(\tilde{\rho}_g^{i} \tilde{D}_j^{i} + \tilde{\rho}_g^{i+1} \tilde{D}_j^{i+1}\right)\phi$$

$$C_{j4}^{i} = \left(\Delta\xi^{i-1} + \Delta\xi^{i}\right)\Delta\xi^{i-1}\left(\dot{w}_j'''\right)^{i}$$

Boundary Conditions for Energy Equations:

$$\xi = 0 \;:\; \theta_g^{1} = 1 \;,\; \theta_s^{0} = \theta_s^{2} - C_b^{1}\left(\theta_s^{1} - 1\right) \tag{3.4}$$

$$\xi = 1 \;:\; \theta_g^{N+2} = \theta_g^{N} \;,\; \theta_s^{N+2} = \theta_s^{N} - C_b^{N+1}\left(\theta_s^{N+1} - R_T\right) \tag{3.5}$$

where

$$C_b^{1} = 2\left(\Delta\xi^{1}\right)\frac{1-\phi}{d/L}\frac{\tilde{K}_g^{1}}{\tilde{K}_{es}^{1}} Nu_g^{1}$$

$$C_b^{N+1} = 2\left(\Delta\xi^{N}\right)\frac{1-\phi}{d/L}\frac{\tilde{K}_g^{N+1}}{\tilde{K}_{es}^{N+1}} Nu_g^{N+1}$$

Boundary Conditions for Gas Species Equations:

$$\xi = 0 \;:\; y_{O_2}^1 = 1 \;,\; y_{N_2}^1 = \frac{Y_{N_2 in}}{Y_{O_2 in}} \;,\; y_{CO_2}^1 = 0 \;,\; y_{CO}^1 = 0 \;,\; y_{H_2O}^1 = \frac{Y_{H_2Oin}}{Y_{O_2 in}} \tag{3.6}$$

$$\xi = 1 \;:\; y_{O_2}^{N+2} = y_{O_2}^{N} \;,\; y_{N_2}^{N+2} = y_{N_2}^{N} \;,\; y_{CO_2}^{N+2} = y_{CO_2}^{N} \;,\; y_{CO}^{N+2} = y_{CO}^{N} \;,\; y_{H_2O}^{N+2} = y_{H_2O}^{N} \tag{3.7}$$

The points i=0 and i=N+2 in the above finite difference form of boundary conditions are imaginary and the values at those points are canceled each other by combining governing equations and boundary conditions. θ_s^0 is plugged into the finite difference equation for i=1 and θ_s^{N+2}, θ_g^{N+2}, and y_j^{N+2} are plugged into the finite difference equations for i=N+1. The matrix forms of the finite difference equations are shown below. The matrix forms of finite difference equations are tridiagonal and are solved by Thomas algorithm.

Matrix Form of Energy Equation for Gas:

$$i=2 \;:\; -C_{g2}^2\theta_g^2 + C_{g3}^2\theta_g^3 = -C_{g4}^2\theta_s^2 - C_{g5}^2 - C_{g1}^2$$

$$i=3 \text{ to } N \;:\; C_{g1}{}^i\theta_g^{i-1} - C_{g2}{}^i\theta_g^{i} + C_{g3}{}^i\theta_g^{i+1} = -C_{g4}{}^i\theta_s^{i} - C_{g5}^i \tag{3.8}$$

$$i=N+1 \;:\; \left(C_{g1}^{N+1} + C_{g3}^{N+1}\right)\theta_g^N - C_{g2}^{N+1}\theta_g^{N+1} = -C_{g4}^{N+1}\theta_s^{N+1} - C_{g5}^{N+1}$$

Matrix Form of Energy Equation for Solid:

$$i=1 \;:\; -\left(C_{s1}^{1} C_{b}^{1} + C_{s2}^{1}\right)\theta_{s}^{1} + \left(C_{s1}^{1} + C_{s3}^{1}\right)\theta_{s}^{2} = -C_{s}\,4^{1}\,\theta_{g}^{1} - C_{s5}^{1} - C_{s1}^{1} C_{b}^{1}$$

$$i=2 \text{ to } N \;:\; C_{s1}^{i}\,\theta_{s}^{i-1} - C_{s2}^{i}\,\theta_{s}^{i} + C_{s3}^{i}\,\theta_{s}^{i+1} = -C_{s4}^{i}\,\theta_{g}^{i} - C_{s5}^{i} \qquad (3.9)$$

$$i=N+1 \;:\; \left(C_{s1}^{N+1} + C_{s3}^{N+1}\right)\theta_{s}^{N} - \left(C_{s2}^{N+1} + C_{s3}^{N+1} C_{b}^{N+1}\right)\theta_{s}^{N+1} = -C_{s4}^{N+1}\,\theta_{g}^{N+1} - C_{s5}^{N+1} - C_{s3}^{N+1} C_{b}^{N+1} R_{T}$$

Matrix Form of Species Equations for Gas Species:

$$i=2 \;:\; -C_{j2}^{2}\,y_{j}^{2} + C_{j3}^{2}\,y_{j}^{3} = -C_{j4}^{2} - C_{j1}^{2}\,C_{jb}$$

$$i=3 \text{ to } N \;:\; C_{j1}^{i}\,y_{j}^{i-1} - C_{j2}^{i}\,y_{j}^{i} + C_{j3}^{i}\,y_{j}^{i+1} = -C_{j4}^{i} \qquad (3.10)$$

$$i=N+1 \;:\; \left(C_{j1}^{N+1} + C_{j3}^{N+1}\right)y_{j}^{N} - C_{j2}^{N+1}\,y_{j}^{N+1} = -C_{j4}^{N+1}$$

where

$$C_{O_2 b} = 1 \;;\; C_{N_2 b} = \frac{Y_{N_2 in}}{Y_{O_2 in}} \;;\; C_{CO_2 b} = 0 \;;\; C_{COb} = 0 \;;\; C_{H_2 Ob} = \frac{Y_{H_2 Oin}}{Y_{O_2 in}}$$

The solid species equations and gas continuity equation are first order. The first order finite difference equations and boundary conditions are shown below.

Solid Species Equations:

$$\Omega_{j}^{i} = \Omega_{j}^{i+1} + C_{\Omega j}\,\Delta\xi^{i}\left(\frac{\dot{w}_{j}^{'''\,i+1} + \dot{w}_{j}^{'''\,i}}{2}\right) \qquad (3.11)$$

where

$$C_{\Omega j} = \frac{d/L}{1-\phi} \frac{Y_{O_2 in}}{Re_s Sc_{O_2 in} \tilde{\rho}_{in} \omega_{jin}}$$

Boundary Conditions for Solid Species Equations:

$$i = N+1 \; : \; \Omega_C^{N+1} = 1 \; , \; \Omega_A^{N+1} = 1 \tag{3.12}$$

Gas Continuity Equation:

$$U_g^i = \frac{1}{\tilde{\rho}_g^i} \left[\tilde{\rho}_g^{i-1} U_g^{i-1} + \frac{C_U}{2} \Delta \xi^i \left(\sum_{j=gas} \dot{w}_j^{'''\, i-1} + \sum_{j=gas} \dot{w}_j^{'''\, i} \right) \right] \tag{3.13}$$

where

$$C_U = \frac{d/L \; Y_{O_2 in}}{Re_{gin} Sc_{O_2 in}}$$

Boundary Condition for Gas Continuity Equation:

$$i = 1 \; : \; U_g^1 = 1 \tag{3.14}$$

The right hand sides of the finite difference equations for solid species and gas continuity are all known, such as, boundary conditions, the values at the last calculation step in an iteration step, or the values at the last iteration step.

3.2 ITERATION ALGORITHM

An iterative solution algorithm is used to obtain numerical solutions because all the governing equations are coupled with each other. The iteration steps are explained below and are also shown in flow chart Figure 2.

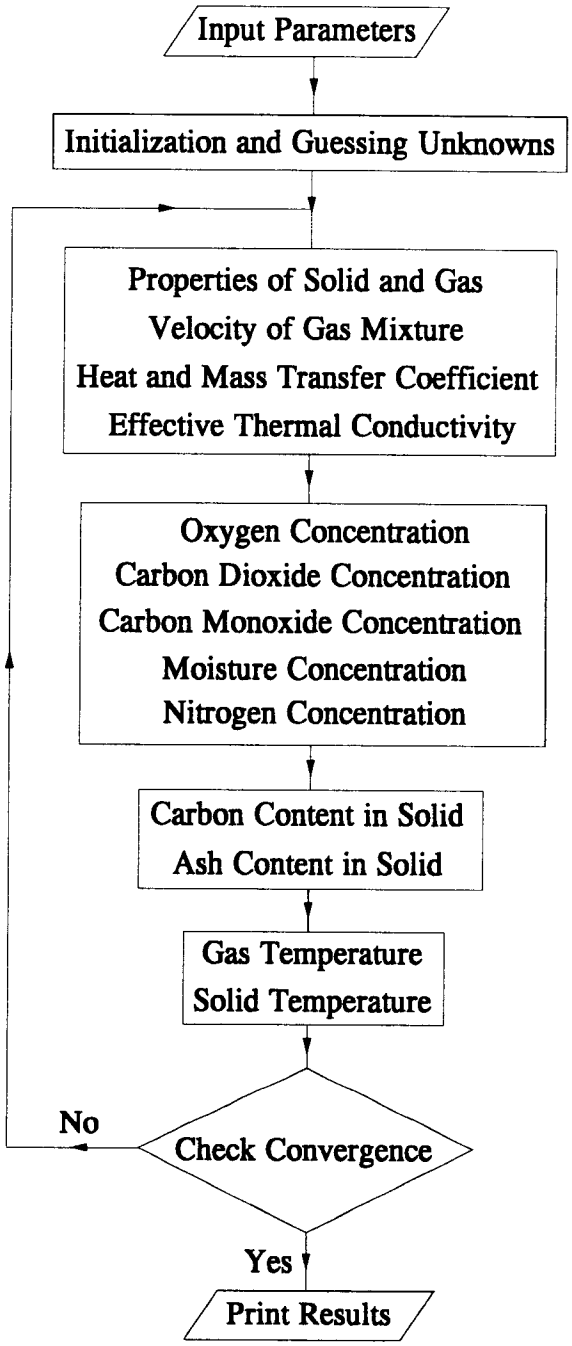

Fig.2 Flow chart of iterative solution algorithm.

STEP 1. Read input parameters.

STEP 2. Initialize and guess the values of dependent variables.

STEP 3. Calculate properties of solid and gas and some dimensionless parameters.

STEP 4. Calculate velocity of gas mixture through the bed.

STEP 5. Calculate heat and mass transfer coefficients, effective thermal conductivities of solid and gas, and some additional dimensionless parameters.

STEP 6. Calculate oxygen concentration in gas mixture.

STEP 7. Calculate carbon dioxide concentration in gas mixture.

STEP 8. Calculate carbon monoxide concentration in gas mixture.

STEP 9. Calculate moisture concentration in gas mixture.

STEP 10. Calculate nitrogen concentration in gas mixture.

STEP 11. Calculate carbon content in solid particles.

STEP 12. Calculate ash content in solid particles.

STEP 13. Calculate gas temperature.

STEP 14. Calculate solid temperature.

STEP 15. Repeat from STEP 3 to STEP 14 until the temperatures of solid and gas, concentrations of gas species, and carbon content in solid satisfy the convergence condition.

STEP 16. Print out the results.

The convergence condition for the iteration is that the maximum error in the whole domain is less than the given error criterion.

$$\text{Max} \left| \frac{\text{new value - old value}}{\text{old value}} \right|^{i} < \varepsilon \qquad (3.15)$$

The value of error criterion for convergence ε in the present study is 10^{-7}. The heat and mass generation terms in the energy and species equations are large and dominant and the gradients of the variables are high around the bottom portion of the bed where the combustion reaction occurs. The numerical solution of the present study depends on the mesh sizes. When the mesh size is not small enough, the iteration does not converge. The very small mesh sizes are used. The number of mesh is 500 for most cases and the maximum number of meshes is 1,000 for excess air case when the carbon content in solid particles is completely consumed before the particles reach the bottom of the bed so that the reaction zone is narrower. The CPU time for the standard run with 500 mesh which is one of the case listed in Table 8 is about 6 minutes when the program is executed in VAX 9,000 computer at Oregon State University Computer Center. The CPU time for the excess air case with 1000 mesh is about 11 minutes.

3.3 VALUES OF PROPERTIES AND PARAMETERS

The solid is taken to be particulate carbon with some ash content. The input gas is air with some moisture. The properties of solid and gas species are taken to be temperature dependent. The method can be extended to coals. The properties of mixture can be calculated by combining the properties of each species.

3.3.1 Properties of Solid

The properties of coal are used for the properties of solid. The values of the properties of coal are found in the book of Rose and Cooper[37] and are listed in Table 4. The changes in density and thermal conductivity of solid due to the loss of carbon from solid by reaction can be estimated by the following equation.

$$\rho_s = \rho_{sin}(\omega_C + \omega_A) \tag{3.16}$$

$$K_s = K_{st}(\omega_C + \omega_A) \tag{3.17}$$

3.3.2 Properties of Gas Species

The empirical correlation to predict the properties of each gas species at high temperature in polynomial form is limited and extrapolation to the higher temperature than the specified range sometimes gives high errors. These high errors cause wrong results and sometimes they make the computational run diverge especially when the specific heat is underestimated. Theoretical predictions with empirical correction factors are the best alternative. Reid et al.[38] give abundant information on the theoretical prediction of properties of gas species.

Table 4. Properties of solid.

Properties of Solid		Values (T_s in ° C)
ρ_{sin}	kg/m^3	1.75×10^3
C_{ps}	J/(kg K)	$0.75\times10^3 + 0.293\ T_s$
K_{st}	W/(m K)	$0.130 + 0.54\times10^{-3}\ T_s + 0.63\times10^{-6}\ T_s^2$

The specific heats of gas species as a function of temperature found in the book of Van Wylen and Sonntag[39] give reliable values even at high temperature and are shown in Table 5. The several methods for the prediction of temperature dependent dynamic viscosity of gas species are reviewed in the book of Reid et al.[38] and among them the method of Chung et al.[40, 41] is employed in this study.

$$\mu = 4.0785\times10^{-6} \frac{F_c(MT_g)^{1/2}}{V_c^{2/3}\,\Omega_v} \tag{3.18}$$

where μ is the dynamic viscosity in Pa·s, M is the molar mass in kg/kmol, T_g is the temperature of gas in K, V_c is the critical volume in cm_3/mole. The viscosity collision integral Ω_v and a factor F_c to account for molecular shapes and polarities are:

$$\Omega_v = A\,(T^*)^{-B} + C\exp(-DT^*) + E\exp(-FT^*)$$

where $T^*=1.2593\ T_r$, $T_r=T_g/T_c$, T_c is the critical temperature in K, A=1.16145, B=0.14874, C=0.52487, D=0.77320, E=2.16178, and F=2.43787.

Table 5. Constant-pressure specific heats of gas species.

Gas	$\bar{C}_p$ (kJ/kmol K) (where $\Theta = T_g(K) / 100$)	Range (K)
O_2	$37.432 + 0.020\,102\,\Theta^{1.5} - 178.57\,\Theta^{-1.5} + 236.88\,\Theta^{-2}$	300-3500
N_2	$39.060 - 512.79\,\Theta^{-1.5} + 1072.7\,\Theta^{-2} - 820.40\,\Theta^{-3}$	300-3500
CO_2	$-3.7357 + 30.529\,\Theta^{0.5} - 4.1034\,\Theta + 0.024\,198\,\Theta^{2}$	300-3500
CO	$69.145 - 0.70463\,\Theta^{0.75} - 200.77\,\Theta^{-0.5} + 176.76\,\Theta^{-0.75}$	300-3500
H_2O	$143.05 - 183.54\,\Theta^{0.25} + 82.751\,\Theta^{0.5} - 3.6989\,\Theta$	300-3500

$$F_c = 1 - 0.2756\,\omega + 0.059035\,\eta_r^4$$

where ω is the acentric factor and η_r is a dimensionless dipole moment and is given by the following equation.

$$\eta_r = 131.3\frac{\eta}{(V_c T_c)^{1/2}}$$

where η is the dipole moment in debyes.

The method of Chung et al.[40, 41] is employed to calculate temperature dependent thermal conductivity of gas species.

$$\frac{K M}{\mu \bar{C}_v} = \frac{3.75\,\Psi}{\bar{C}_v/R} \tag{3.19}$$

where K is the thermal conductivity in W/mK, M is the molar mass in kg/kmol, μ is the low pressure gas viscosity in Pa·s, $\bar{C}_v$ ($=\bar{C}_p$-R) is the specific heat at constant volume in J/kmol K, and R is the universal gas constant in J/kmol K. The value of Ψ is calculated with the following equation.

$$\Psi = 1 + \alpha[(0.215 + 0.28288\alpha - 1.061\beta + 0.26665Z)/(0.6366 + \beta Z + 1.016\alpha\beta)]$$

where

$$\alpha = (\bar{C}_v/R) - 3/2$$

$$\beta = 0.7862 - 0.7109\,\omega + 1.3168\,\omega^2$$

$$Z = 2.0 + 10.5T_r^2$$

The values of several parameters to calculate dynamic viscosity and thermal conductivity of gas species are given in Table 6.

Table 6. Values of parameters for the estimation of gas properties.

Gas	M (kg/kmol)	T_c (K)	P_c (bar)	V_c (cm^3/mol)	Z_c	ω (debye)	η
O_2	31.999	154.6	50.4	73.4	0.288	0.025	0.0
N_2	28.013	126.2	33.9	89.8	0.290	0.039	0.0
CO_2	44.010	304.1	73.8	93.9	0.274	0.239	0.0
CO	28.010	132.9	35.0	93.2	0.295	0.066	0.1
H_2O	18.015	647.3	221.2	57.1	0.235	0.344	1.8

The binary diffusion coefficients of each pair of gas species are estimated by the method of Fuller et al.[42]

$$D_{AB} = \frac{1.43 \times 10^{-7} T_g^{1.75}}{P M_{AB}^{1/2} \left[(\Sigma_v)_A^{1/3} + (\Sigma_v)_B^{1/3} \right]} \tag{3.20}$$

where D_{AB} is the binary diffusion coefficient in m^2/sec, T_g is the gas temperature in K, the values of atomic diffusion volume of each species Σ_v are shown in Table 7, and M_{AB} is defined by the following equation.

Table 7. Atomic diffusion volumes.

Gas	Σ_v
O_2	16.3
N_2	18.5
CO_2	26.9
CO	18.0
H_2O	13.1

$$M_{AB} = 2\left(\frac{1}{M_A} + \frac{1}{M_B}\right)$$

where M_A and M_B are the molar masses of A and B gas species in kg/kmol.

3.3.3 Properties of Gas Mixture

The properties of gas mixture are calculated by combining the properties of each gas species with the following relations found in the book of Reid et al..[38]

$$C_{pg} = \sum_{j=1}^{n} Y_j C_{pj} \tag{3.21}$$

$$\mu_g = \sum_{i=1}^{n} \frac{X_i \mu_i}{\sum_{j=1}^{n} X_j A_{ij}} \tag{3.22}$$

$$K_g = \sum_{i=1}^{n} \frac{X_i K_i}{\sum_{j=1}^{n} X_j A_{ij}} \tag{3.23}$$

where

$$A_{ij} = \frac{\left[1 + (\mu_i/\mu_j)^{1/2} (M_j/M_i)^{1/4}\right]^2}{\left[8(1 + M_i/M_j)\right]^{1/2}}$$

Diffusion coefficient of gas species i in gas mixture can be calculated by the following relation.

$$D_i = \frac{1 - X_i}{\sum_{\substack{j=1 \\ j \neq i}}^{n} \frac{X_j}{D_{ij}}} \tag{3.24}$$

where D_{ij} is the binary diffusion coefficient and X_i and X_j respectively are the mole fractions of gas species i and j in gas mixture.

3.3.4 Parameters

For rhombohedral packing of sphere, the value of void fraction ϕ is 0.26, independent of the particle diameter. The total surface area of particles per unit volume of bed A_v is $6(1-\phi)/d$.

The ranges of parameters used in numerical calculation are chosen by the following reasons. The diameter of the solid particles for the moving bed combustion ranges from 1 to 5 cm and the optimum size of the particles is about 1 or 1.5 cm.[43] The minimum fluidization gas Reynolds numbers estimated by Wen and Yu[33,34] and Saxena and Vogel[35] are 2,840 and 3,370 when T_{gin}=300 K and d=0.015 m and 660 and 800 at T_{gin}=1,000 K and d=0.015 m. Essenhigh[43] suggest that the maximum velocity of cold air supply for fixed bed coal combustor is 0.5 m/sec and the corresponding gas supply Reynolds number is 480 when T_{gin}=300 K and d=0.015 m. The highest gas supply Reynolds number as a parameter for the numerical calculation is chosen to be less than both the minimum fluidization gas Reynolds number and the maximum values suggested by Essenhigh.[43] The minimum solid supply Reynolds number is chosen to be about 0.0111 which corresponds the solid supply velocity of 1 m per 24 hours when T_{gin}=300 K and d=0.015 m.

The major parameters in computational runs are solid and gas supply Reynolds numbers (Re_{gin} and Re_s), temperature of the air supply (T_{gin}), diameter of the solid particles (d), and initial carbon content in solid particles (ω_{Cin}). The values of parameters in a standard computer run are $Re_{gin}=173.4$, $Re_s=0.0280465$, $T_{gin}=300$ K, $T_{sin}=300$ K, d=0.015 m, L=0.6096 m, $\omega_{Cin}=0.913$, $\phi=0.26$, and $\phi_h=0.3$ where ϕ_h is relative humidity of air supply. The values of parameters to be investigated are listed in Table 8. Whereas Run No. 0 is standard, Runs 1-3 relate the effect of the amount of air supplied relative to the solid supply. Runs 4-9 describe the effect of preheating the air; Runs 10-15 give the effect of particle diameter; and Runs 16-21 reveal the influence of the ash content on the burning process. The values of parameters not specified in Table 8 except solid supply Reynolds number (Re_s) are the same that of the standard run. The stoichiometric solid supply Reynolds number can be obtained by numerical experiment. As an example, the stoichiometric solid supply Reynolds number for standard run is found to be 0.0280465. The complete consumption of carbon content in solid particles is assumed when the dimensionless carbon content in solid at the bottom of the bed is less than 1.0×10^{-4}.

Governing equations and boundary conditions are discretized by finite difference approximation and iterative solution algorithm is proposed in this chapter. Temperature dependent properties and parameters for the computational run are also mentioned in this chapter. The stoichiometric solid and gas supply rates and distributions of temperature, concentration, gas velocity, and gas density under various conditions are obtained in next chapter. The effects of various parameters are also investigated.

Table 8 Parameters for computer runs.

Run No.	Effect of	G_{gin}	T_{gin} (K)	d (m)	ω_{Cin}	Re_{gin}
0	Standard Run	0.21074	300	0.015	0.913	173.4
1	Re_{gin}	0.10537	300	0.015	0.913	86.70
2		0.21074				173.40
3		0.31611				260.10
4	T_{gin}	0.10537	400	0.015	0.913	69.855
5		0.21074				139.71
6		0.31611				209.57
7		0.10537	500			59.566
8		0.21074				119.13
9		0.31611				178.70
10	d	0.10537	300	0.01	0.913	57.80
11		0.21074				115.6
12		0.31611				173.4
13		0.10537		0.02		115.6
14		0.21074				231.2
15		0.31611				346.8
16	ω_{Cin}	0.10537	300	0.015	0.7	86.70
17		0.21074				173.40
18		0.31611				260.10
19		0.10537			0.5	86.70
20		0.21074				173.40
21		0.31611				260.10

CHAPTER 4

RESULTS AND DISCUSSIONS

The major goal of this study is to find the stoichiometric solid and gas supply rates and to investigate the effects of various parameters. The major input parameters are: gas supply Reynolds number; corresponding solid supply Reynolds number; gas supply temperature; diameter of the solid particles; and initial carbon content in solid particles. The distributions of: solid and gas temperatures; gas species concentrations; carbon content in solid particles; and density and velocity of gas mixture through the bed are the dependent variables determined for various values of the input parameters portrayed in Table 8. In this chapter, the general nature of the predicted temperature and concentration distributions along the bed length is described and the results by five different reaction models listed in Table 1 are compared with the experimental results of Nicholls and Eilers[8] and are discussed. The effects of major input parameters on the stoichiometric solid and gas supply rates and the distributions of dependent variables are also discussed in this chapter.

To briefly summarize the discussion from the previous chapter, the combustion of carbon with oxygen occurs by three reactions; (1) heterogeneous reaction of carbon with oxygen to carbon monoxide and carbon dioxide, (2) heterogeneous reaction of carbon with carbon dioxide, and (3) homogeneous reaction of carbon monoxide with oxygen. The reactions considered for five different reaction models are listed in Table 1. The single reaction model considers only reaction (1) with $f_{CO}=0$. The two reaction model considers reaction (1) with $f_{CO}=0$ and reaction

(2). The three reaction model A considers reaction (1) with $f_{CO}=0$, reaction (2), and reaction (3). The three reaction model B considers reaction (1) with f_{CO} given as a function of temperature, reaction (2), and reaction (3). The three reaction model C considers reaction (1) with $f_{CO}=1$, reaction (2), and reaction (3). The three reaction model denoted by B in Table 1, being the most general, is used for the parametric study.

4.1 GENERAL NATURE OF RESULTS

The distributions of solid and gas temperatures along the bed length are shown in Figure 3 for the three reaction model B with the parameters of standard run. The corresponding distributions of carbon content in solid particles and gas species concentrations are shown in Figure 4 . The supply rates of solid and gas for the standard run are stoichiometric as indicated in Figure 4 the zero carbon content in solid particles at the bottom of the bed. Solid particles are supplied at the top of the bed while gas mixture is supplied at the bottom of the bed. The temperature of the gas mixture increases as it flows upwards through the bed and the temperature of solid particles which move down decreases by heat transfer from hot solid particles to cold gas mixture. The temperatures of solid and gas reach their maxima at a location where heat is released by two exothermic reactions; one heterogeneous reaction of carbon with oxygen and one homogeneous reaction of carbon monoxide with oxygen. Some portion of heat is absorbed by the endothermic gasification reaction of carbon with carbon dioxide. The maximum temperature of gas mixture is higher than that of solid in this region because the specific heat of gas mixture is much lower than that

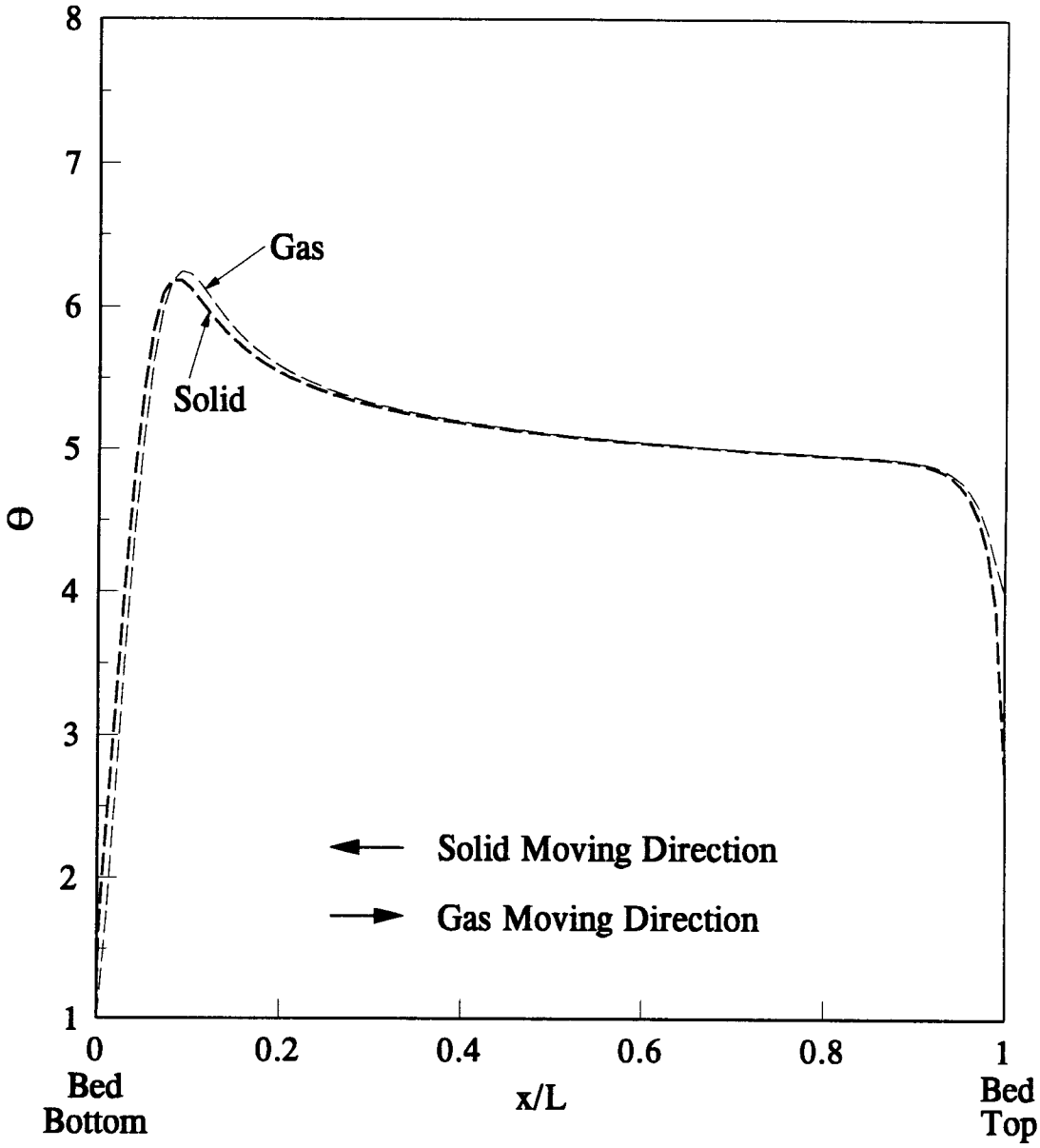

Fig. 3 Temperature distributions of solid and gas along the bed length for the three reaction model B with standard run parameters.

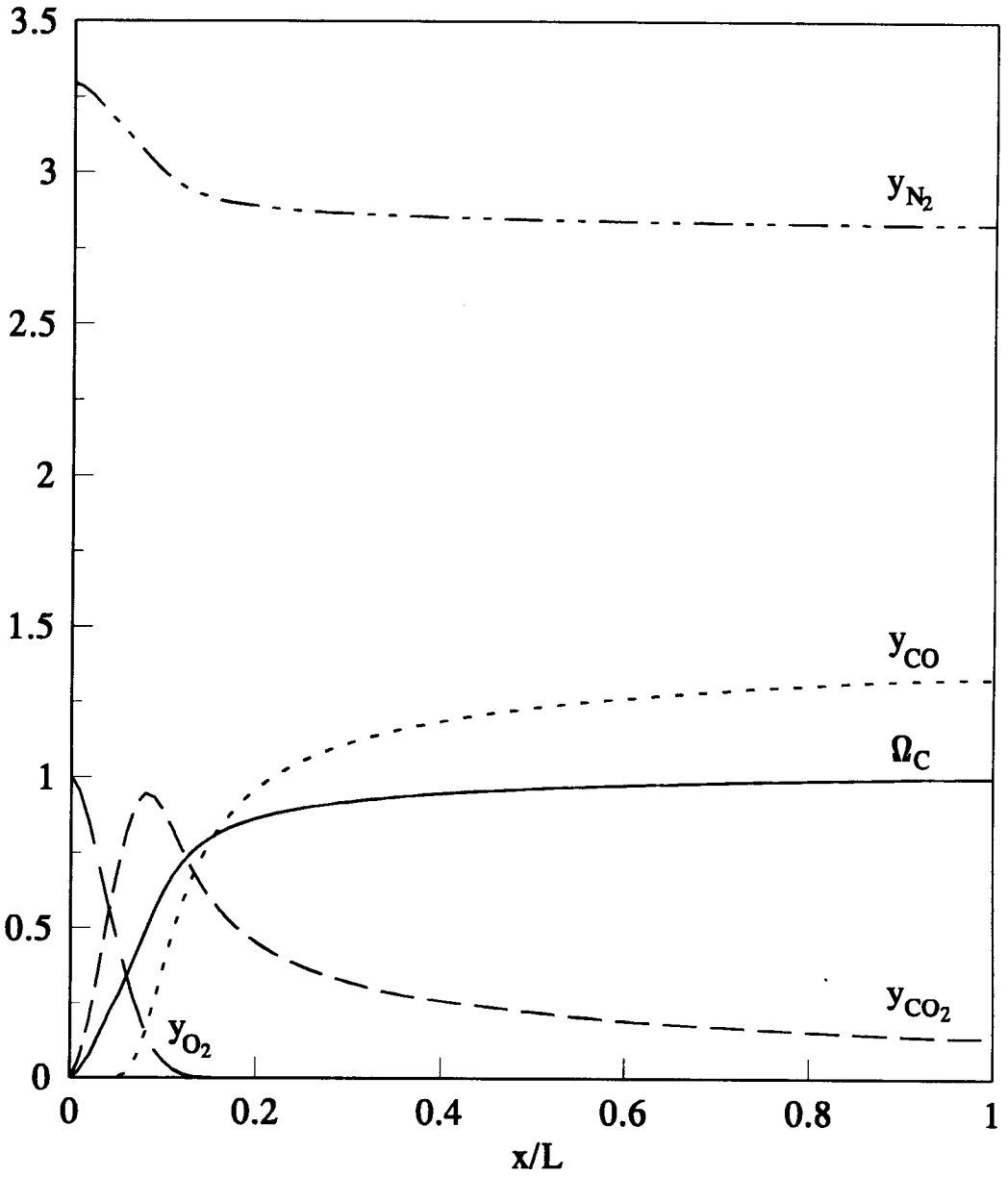

Fig. 4 Distributions of carbon content in solid particles and gas species concentrations along the bed length for the three reaction model B with standard run parameters.

of solid. Evident from Figure 4 is that all the oxygen is consumed at the end of this combustion zone and the reactions of carbon and carbon monoxide with oxygen end. The gasification reaction of carbon with carbon dioxide continues even after the oxygen is exhausted and the temperatures of solid and gas decrease as x increases. At the top portion of the bed, the temperature of gas mixture decreases further due to heat transfer to the solid supply. The solid and gas are almost in thermal equilibrium except near the very top and bottom portion of the bed due to the sufficient heat exchange between solid and gas.[§]

The distributions of carbon content in solid particles and of gas species concentrations along the bed length are shown in Figure 4. After solid particles are supplied at the top of the bed, the carbon content in solid particles begins to gradually, even if slowly, decrease and a small portion of carbon is consumed by gasification reaction of carbon with carbon dioxide outside the combustion zone.

---

§ The mass and energy balances across the top and bottom of the bed are examined for the three reaction model B with the standard run parameters. The total mass in and mass out per unit cross-sectional area of the bed are respectively calculated to be 0.24860 kg/s and 0.24857 kg/s. The error in mass balance thus is about 0.015 %. The total heat produced by the chemical reactions is 0.36743 MW, the total heat used to raise the products temperature is 0.23059 MW, and the total heat lost through the top and bottom of the bed is 0.13642 MW. The error in energy balance thus is about 0.115 %. These small errors indicate that the mass and energy are conserved in this system.

In the combustion zone, the carbon content in solid particles decreases rapidly so as to consume most of the carbon by the two heterogeneous reactions. Finally, the carbon in solid particles is completely consumed by the time the bottom of the bed is reached.

As soon as oxygen is supplied at the bottom of the bed, the concentration of oxygen begins to decrease due to the combustion reactions of carbon and carbon monoxide with oxygen. Soon, all oxygen is consumed. The concentration of carbon dioxide increases at the bottom portion of the bed by the reactions of carbon and carbon monoxide with oxygen to carbon dioxide and then it decreases by the gasification reaction of carbon with carbon dioxide to carbon monoxide even after oxygen is exhausted. The concentration of carbon monoxide begins to increase at some distance from the bottom of the bed and continues to increase by the gasification reaction of carbon with carbon dioxide. The mass fraction of nitrogen mostly decreases in the combustion zone due to the addition of carbon to the gas mixture in the forms of carbon monoxide and carbon dioxide by the heterogeneous reactions. The concentration of water is quite low in the bed and is not shown in this and other figures.

4.2 COMPARISON WITH EXPERIMENTS

The temperature and concentration distributions obtained by the present numerical calculation for various reaction models and by the experiment of Nicholls and Eilers[8] are compared in Figures 5 and 6. The studies by Barriga and Essenhigh[12] and Lawson and Norbury[13] do not state the values of parameters, such as, the rates of

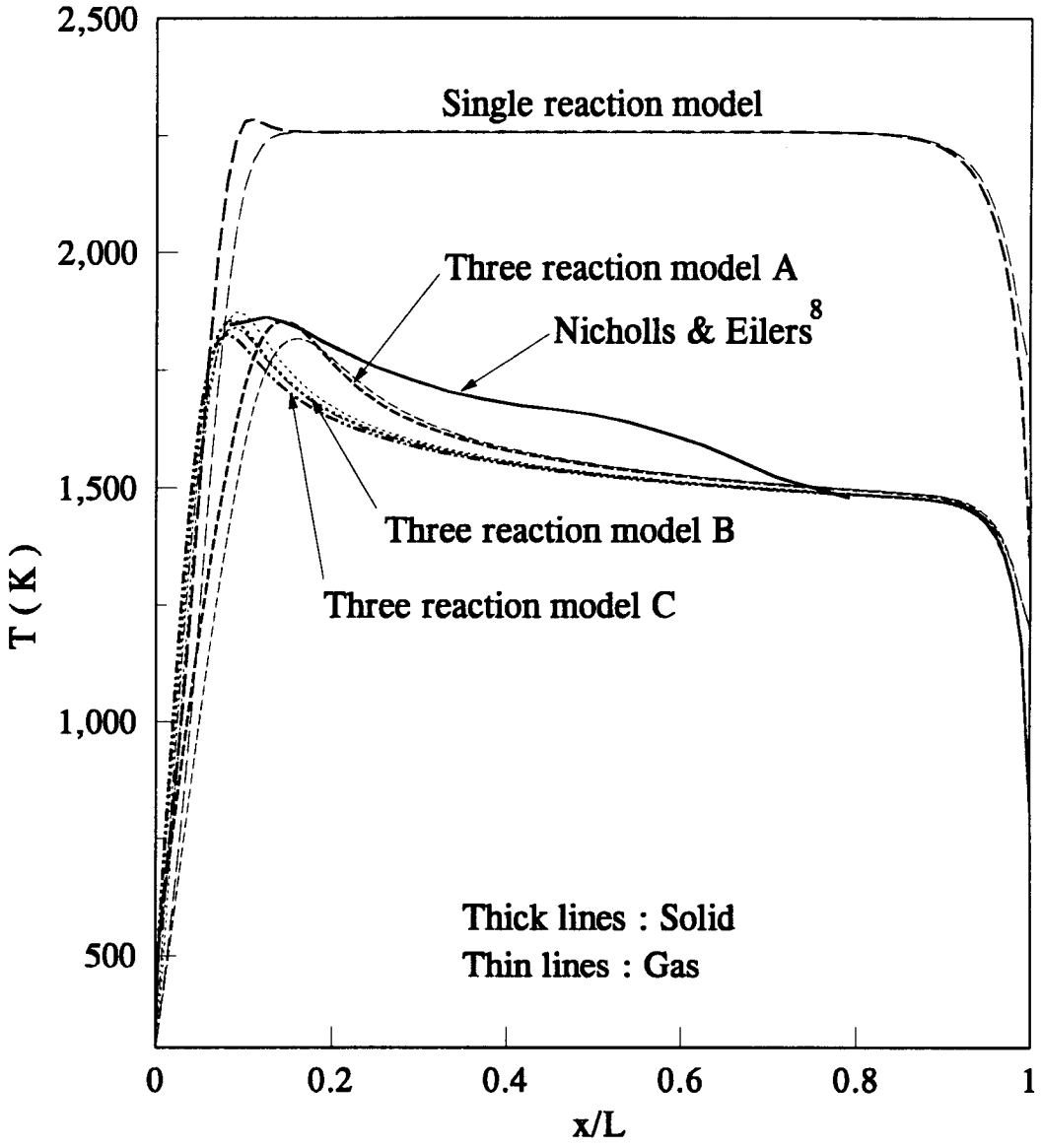

Fig. 5 Temperature distributions of solid and gas for the comparison of the present numerical calculation by various reaction models with experiment of Nicholls and Eilers[8]. (Re_{gin}=173.4, T_{gin}=300 K, T_{sin}=300 K, ϕ=0.26, ϕ_h=0.3, L=0.6096 m, d=0.015 m, ω_{Cin}=0.913)

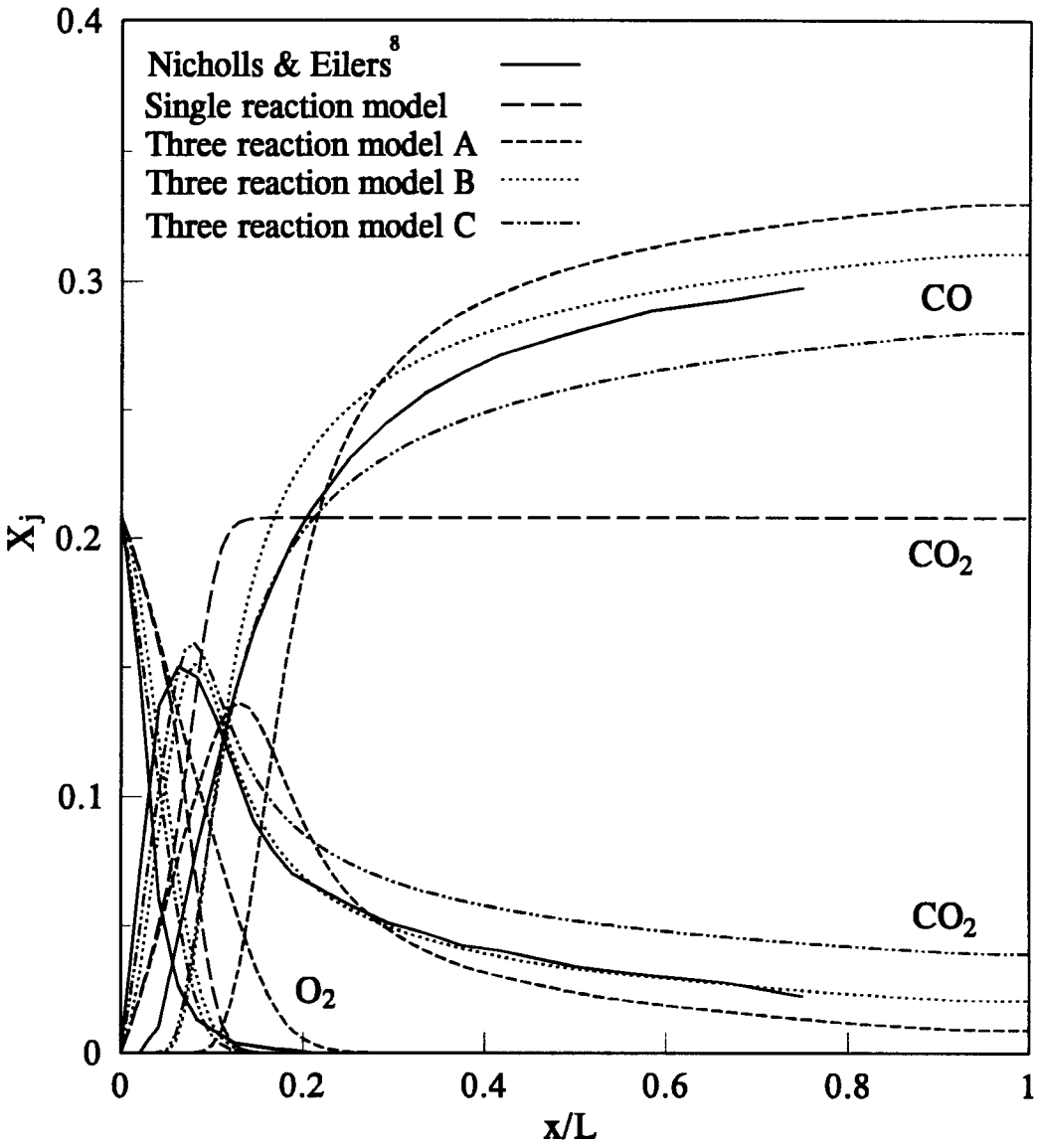

Fig. 6 Concentration distributions of gas species for the comparison of the present numerical calculation by various reaction models with experiment of Nicholls and Eilers[8]. (Re_{gin}=173.4, T_{gin}=300 K, T_{sin}=300 K, ϕ=0.26, ϕ_h=0.3, L=0.6096 m, d=0.015 m, ω_{Cin}=0.913)

solid and gas supply. This incompleteness of all the information prevents us from comparing the results of these studies with the present calculations. The temperature by Nicholls and Eilers[8] shown in Figure 5 is that of the coke surface measured by optical pyrometer. The temperature of the bed calculated by the three reaction models with any f_{CO} value reasonably agrees with the Nicholls and Eilers experimental result. The maximum temperature of gas mixture by the three reaction model B and C is higher than that of solid due to the gaseous reaction and lower specific heat of gas mixture. On the other hand, the maximum temperature of gas mixture by three reaction model A is lower than that of solid because gas phase reaction is not considered. The location of the peak temperature of the bed is shifted to the bottom of the bed when f_{CO} is larger because oxygen is consumed by both the reaction of carbon with oxygen and the reaction of carbon monoxide with oxygen so that oxygen is exhausted at the lower location of the bed as shown in Figure 6. The temperature of the bed by single reaction model is higher than that measured by Nicholls and Eilers[8] because the endothermic gasification reaction of carbon with carbon dioxide is neglected. The reaction of carbon with carbon dioxide should be considered to get a result in reasonable agreement with experiment.

The comparison between the concentration distributions of gas species by present numerical calculation and measured by Nicholls and Eilers[8] is shown in Figure 6. Even though the concentration distribution of oxygen by the single reaction model appears to agree with the experimental result reasonably, the concentration distribution of carbon dioxide is quite different from the experimental result. The reason for this disagreement is that carbon monoxide is not considered in this model.

The locations where oxygen is depleted, where the concentration of carbon dioxide is maximum, and where the concentration of carbon monoxide begins to increase are higher in the bed by three reaction model A than by the experimental results. The concentration distributions by reaction model C show relatively good agreement with experimental result but the concentration of carbon dioxide is higher than that by experiment and the concentration of carbon monoxide is lower than that by experiment because the temperature of the bed is lower than that by experiment and the rate of gasification reaction of carbon with carbon dioxide which is the only reaction mostly controlled by chemical kinetics is underestimated. The distributions of gas species concentrations by reaction model B show best agreement with experiment and this three reaction model B is used for the parametric study in later sections.

At a given gas supply rate (Re_{gin}=173.4), the stoichiometric solid supply rate is higher by which the reaction model gives higher concentration of carbon monoxide or lower concentration of carbon dioxide at the top of the bed in the order of single reaction model (Re_s=0.014915), three reaction model C (Re_s=0.0266), three reaction model B (Re_s=0.0280465), and three reaction model A (Re_s=0.0290185). This is because one mole of oxygen reacts with twice more carbon to produce carbon monoxide than to produce carbon dioxide.

Figure 7 shows the rates of reaction of carbon monoxide with oxygen for the standard run parameters when the rate is controlled by reaction of carbon with oxygen, reaction kinetics of Howard et al.,[22] Dryer and Glassman[24], and Hottel et al..[25] The reaction rates by these detailed reaction kinetics are much higher than the

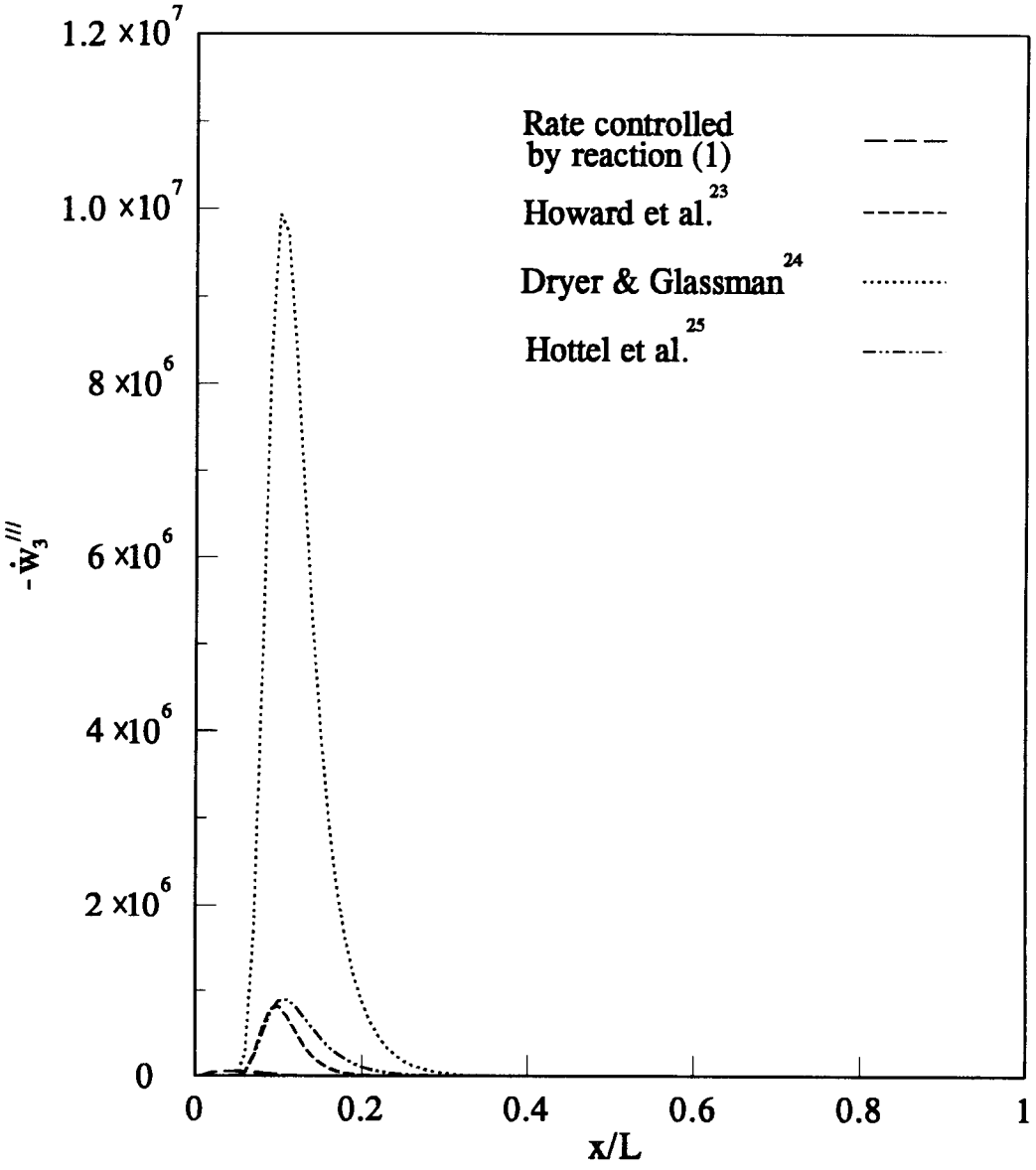

Fig. 7 Comparison of rate of gas phase reaction of carbon monoxide with oxygen by several authors and rate controlled by reaction (1) for standard run.

rate controlled by the reaction of carbon with oxygen and it is reasonable to assume that the rate of gas phase reaction of carbon monoxide with oxygen is so fast that carbon monoxide is consumed as soon as it is produced by reaction (1).

The error caused by the uniform temperature assumption in solid particles is generally less than 5% when Biot number is less than 0.1. The Biot numbers obtained through the numerical calculation in this study range from 0.75 to 2.3 so that the error by the assumption is much more than 5% and the temperature distribution inside solid particle is not uniform. However, this uniform temperature assumption is widely used since it makes the mathematical model simple.

4.3 EFFECT OF SOLID AND GAS SUPPLY RATES

The values of stoichiometric solid supply rate for several given gas supply rates are estimated by numerical calculation to be as shown in Figure 8. The solid line in Fig. 8 shows the stoichiometric relation of solid and gas supply rates. By "stoichiometric solid supply rate", it is meant the rate of solid supply which would be completely consumed by the given gas flow rate leaving behind only the ash residue. If the solid supply rate is higher than this "stoichiometric", there shall be left some carbon unburnt, i.e., Ω_C at the bottom of bed will be not zero. The stoichiometric solid supply rate becomes higher when gas supply rate becomes higher because more oxygen is needed for the more carbon consumption. When the relation of solid and gas supply rates is in the upper left region of Figure 8 (Region 1), that is, the gas supply rate is higher than the stoichiometric supply rate, excess air is supplied and the combustion zone is shifted to the upper portion of the bed. On the other hand,

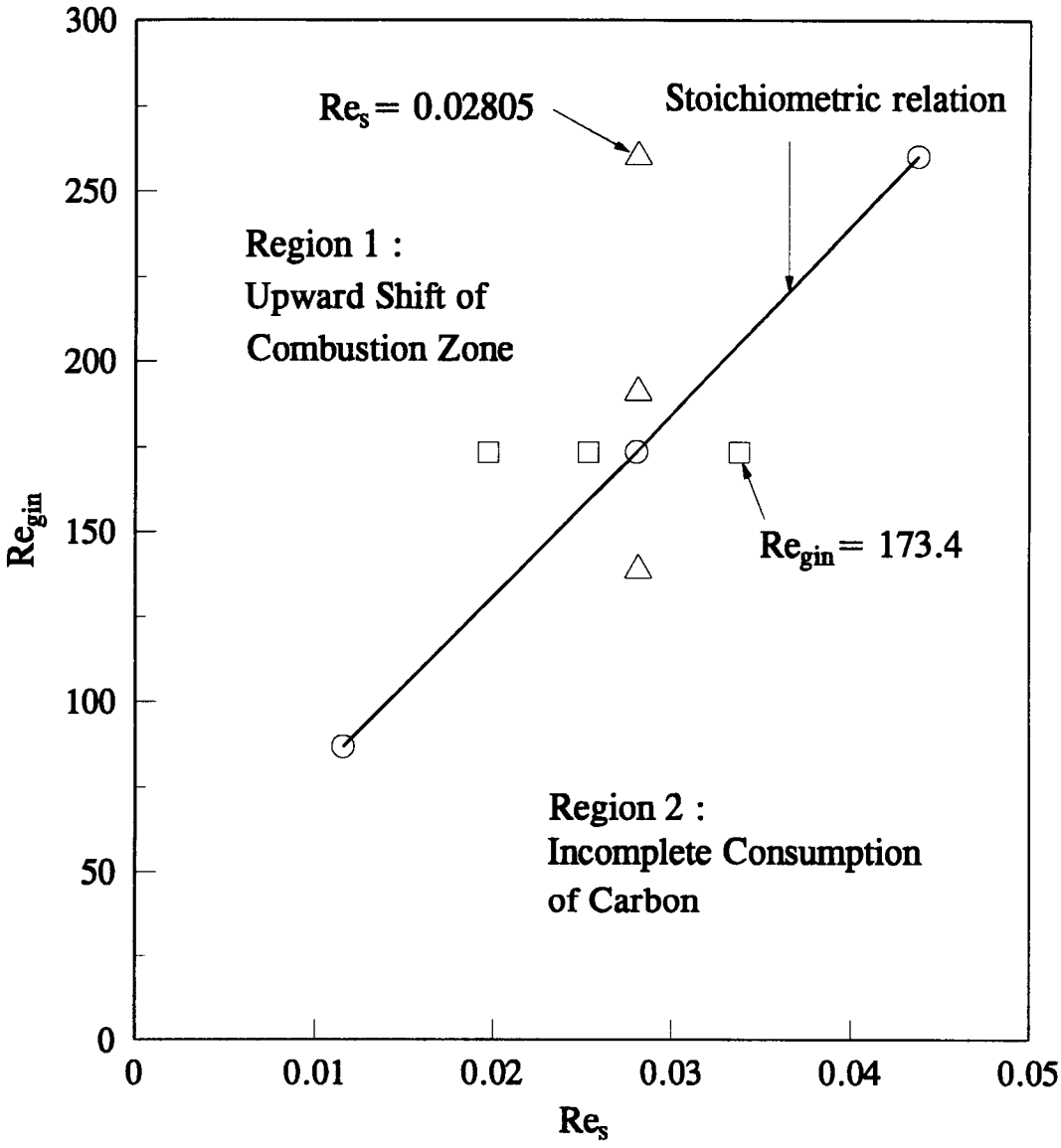

Fig. 8 Relation of stoichiometric solid and gas supply rates. (T_{gin}=300 K, T_{sin}=300 K, ϕ=0.26, ϕ_h=0.3, L=0.6096 m, d=0.015 m, ω_{Cin}=0.913)

when the relation of solid and gas supply rates is in the lower right region of Figure 8 (Region 2), that is, the solid supply rate is higher than the stoichiometric supply rate, excess solid is supplied, carbon is not completely consumed in the bed, and unburnt carbon is discharged at the bottom of the bed.

The square points in Figure 8 are the cases of excess or deficient solid supply rate at a given gas supply rate and the distributions of solid and gas temperatures, of carbon content in solid, and of gas species concentrations are shown in Figures 9 and 10. When the solid supply rate is higher than the stoichiometric solid supply rate, the peak temperature of the bed (or the combustion zone) is shifted downward as shown in Figure 9 and the carbon in solid at the bottom of the bed is not completely consumed as shown in Figure 10(a). The corresponding distributions of gas species concentrations are also shifted downward. Figure 10(b) shows the distributions of carbon content in solid and gas species concentrations for the stoichiometric solid and gas supply rates. When the solid supply rate is less than the stoichiometric solid supply rate, the peak temperature of the bed (or the combustion zone) is shifted upward as shown in Figure 9 and the carbon content in solid particles is depleted to zero in the bed before the solid particles reach the bottom as shown in Figures 10(c) and 10(d). The corresponding distributions of gas species concentrations are also shifted upward.

The triangle points in Figure 8 are the cases of excess or deficient gas supply rate at a given solid supply rate and the distributions of solid and gas temperatures, of carbon content in solid, and of gas species concentrations are shown in Figures 11 and 12. When the gas supply rate is less than the stoichiometric gas supply rate, the

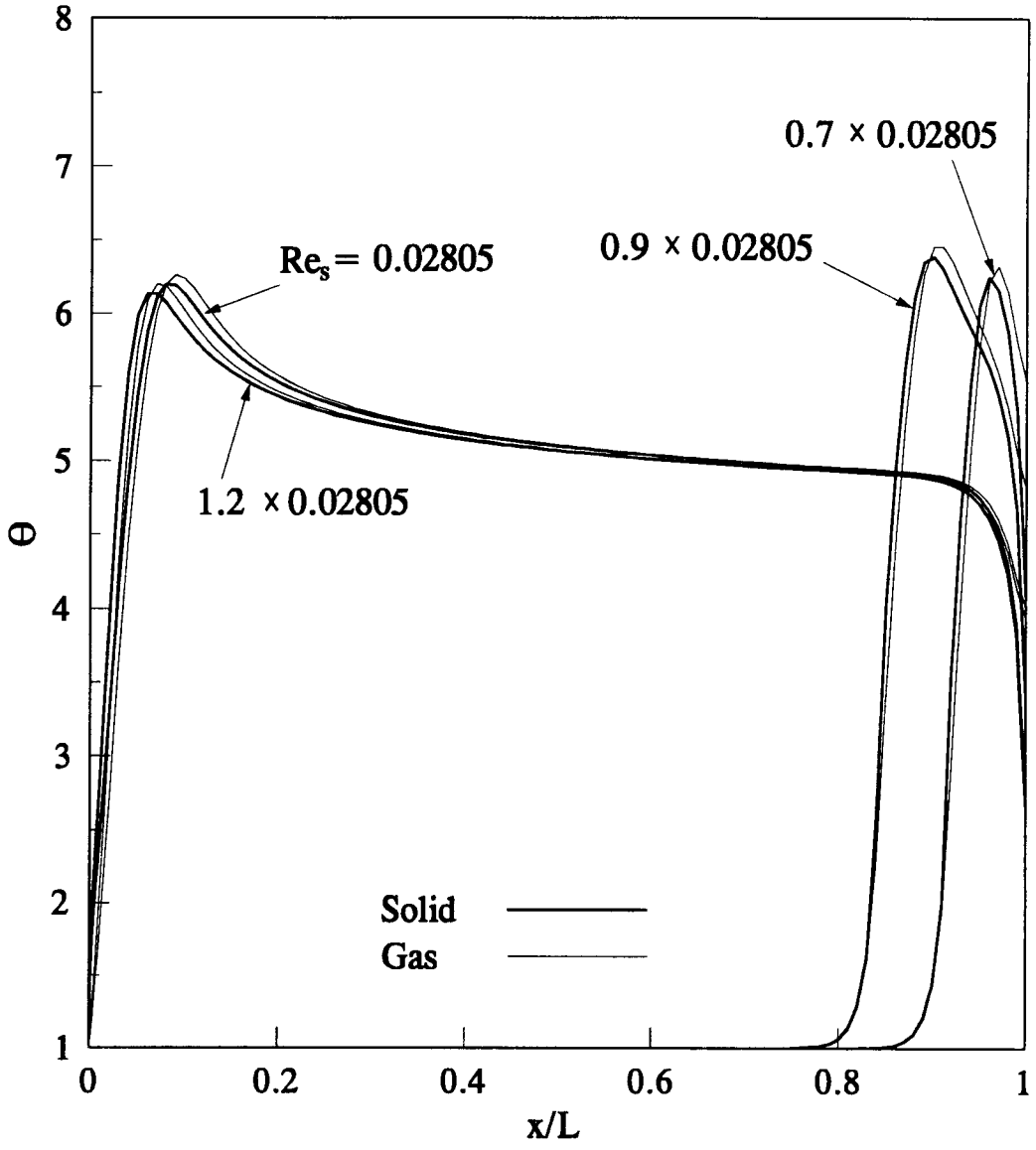

Fig. 9 Effect of solid supply rate on temperature distributions of solid and gas for excess or deficient solid supply rate. (Re_{gin}=173.4)

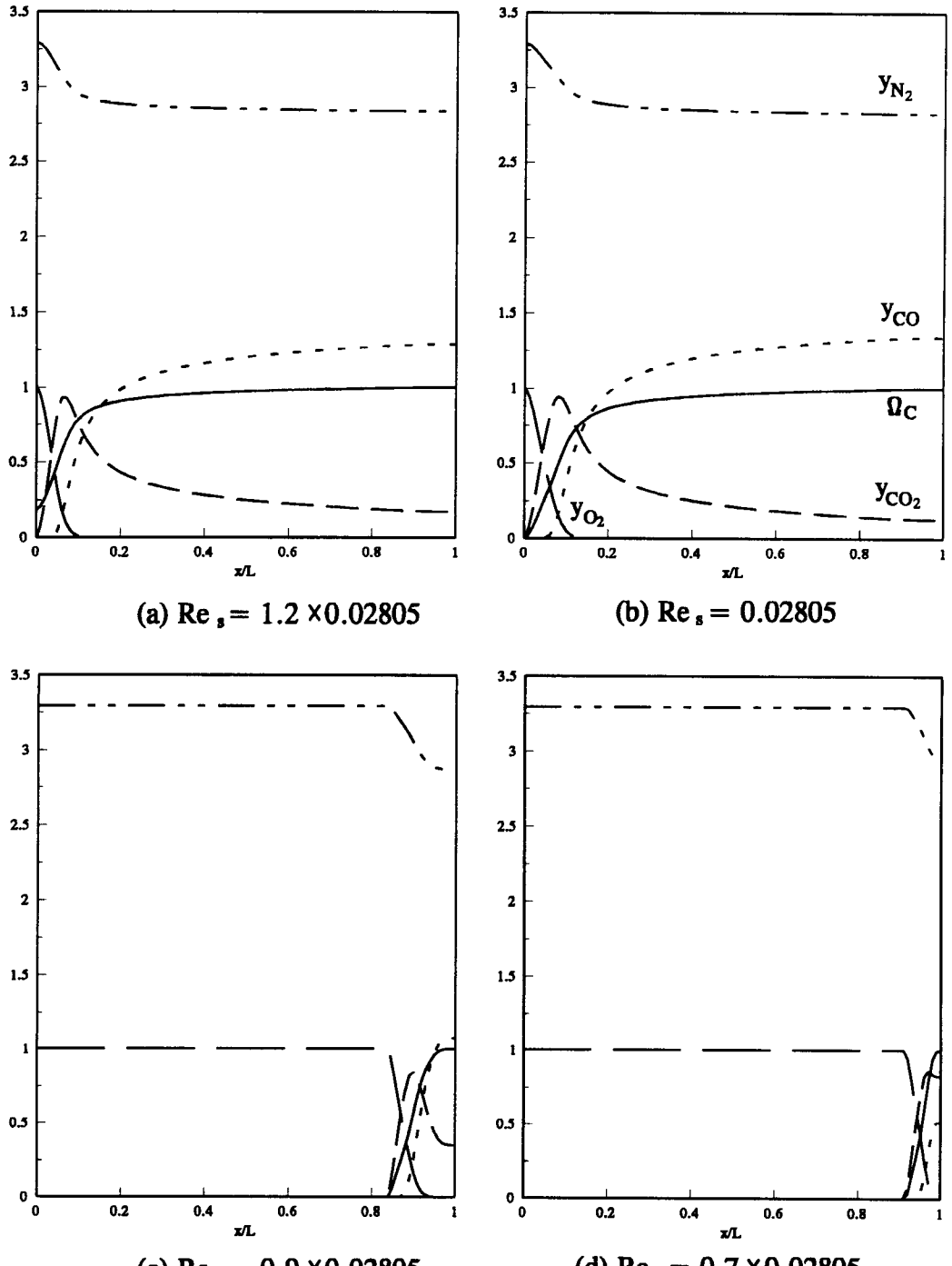

Fig. 10 Effect of solid supply rate on distributions of gas species concentrations and carbon content in solid for excess or deficient solid supply rate. (Re_{gin}=173.4)

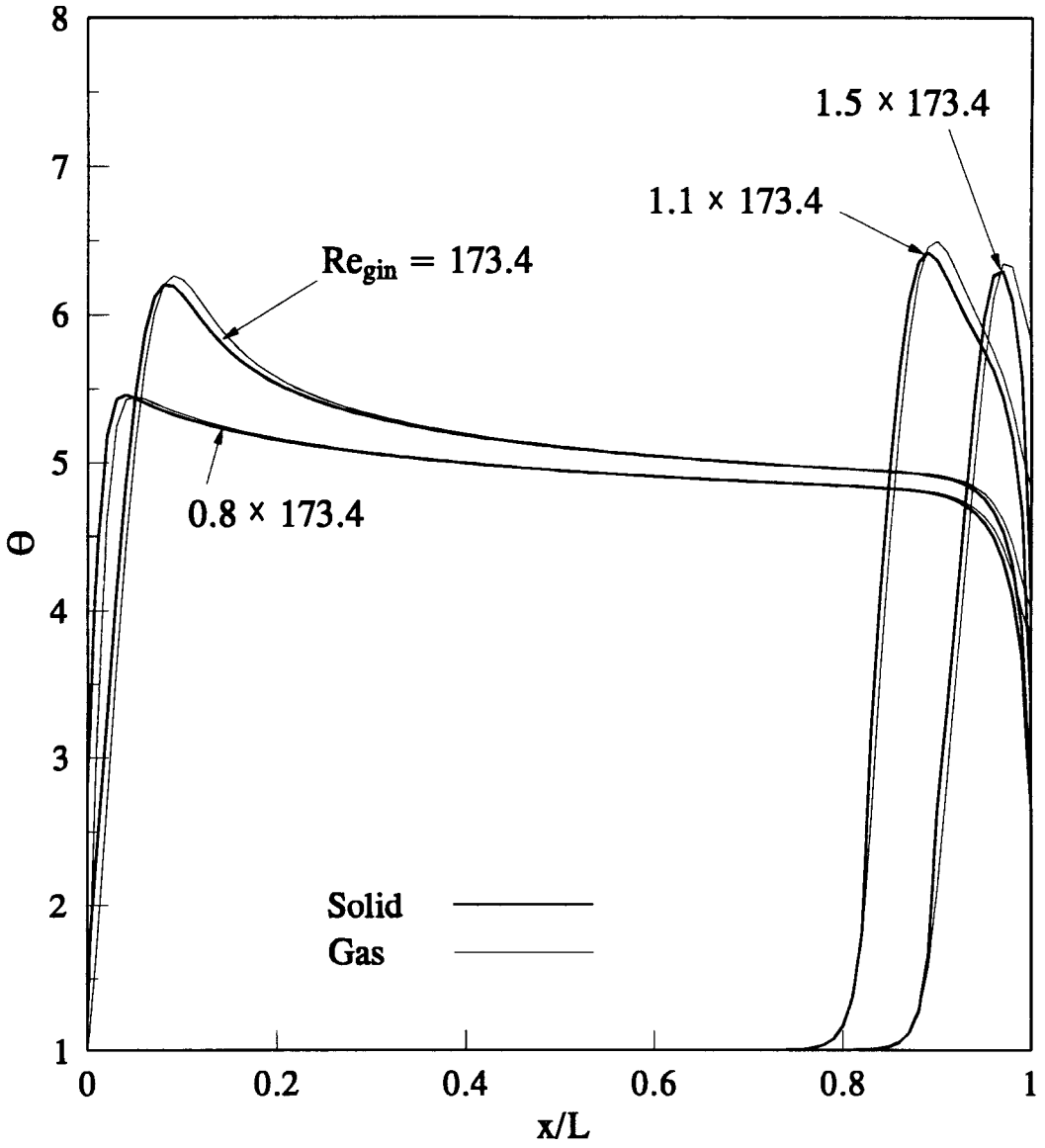

Fig. 11 Effect of gas supply rate on temperature distributions of solid and gas for deficient or excess gas supply rate. (Re_s=0.02805)

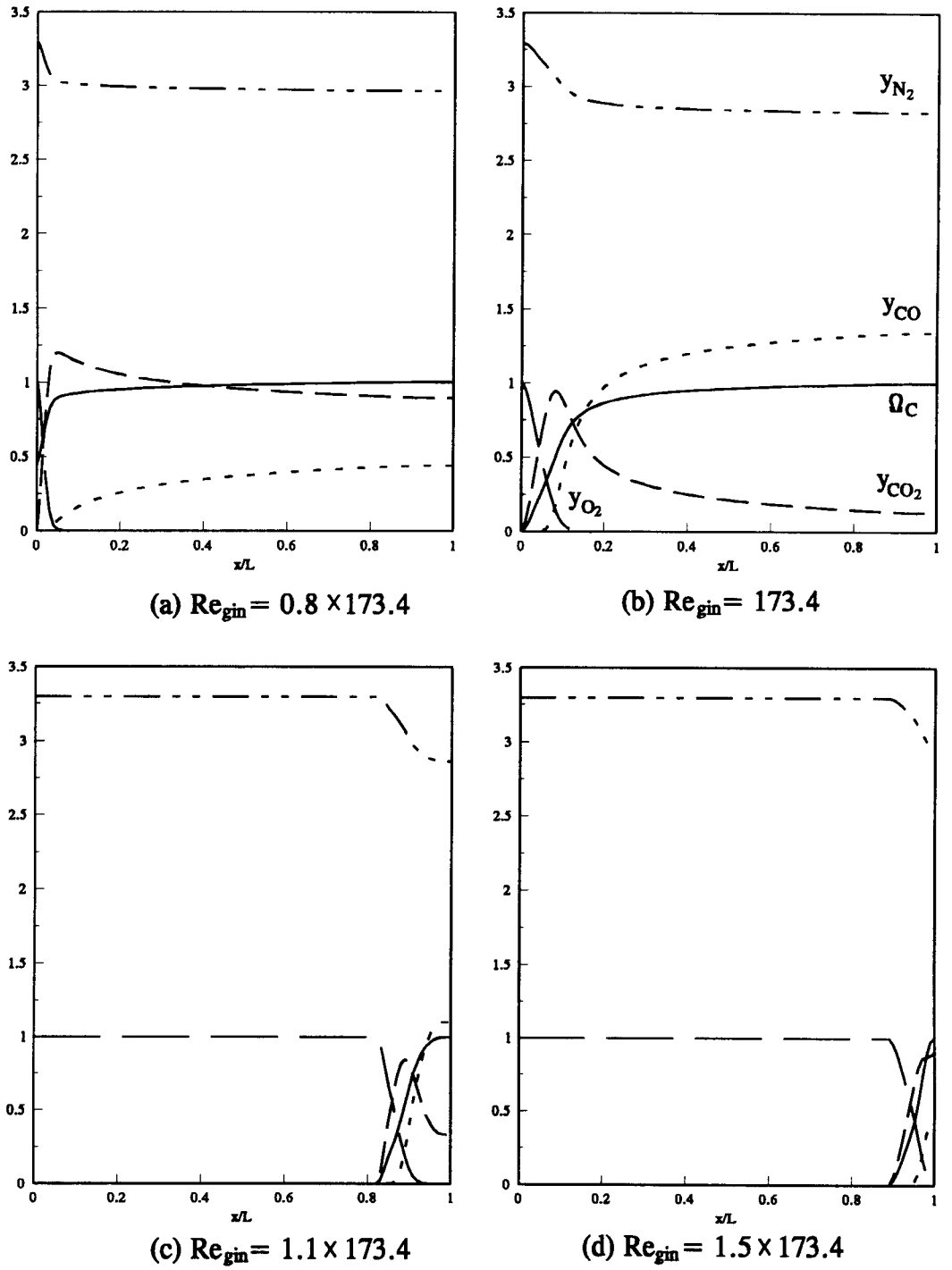

(a) Re_{gin}= 0.8 x 173.4

(b) Re_{gin}= 173.4

(c) Re_{gin}= 1.1 x 173.4

(d) Re_{gin}= 1.5 x 173.4

Fig. 12 Effect of gas supply rate on distributions of gas species concentrations and carbon content in solid for deficient or excess gas supply rate. (Re_s=0.02805)

peak temperature (or combustion zone) is shifted downward and the carbon content in solid at the bottom of the bed is not completely consumed. The corresponding distributions of gas species concentrations are also shifted downward. When the gas supply rate is higher than the stoichiometric rate, the peak temperature of the bed (or the combustion zone) is shifted upward and the carbon content in solid is depleted to zero at the upper portion of the bed. The corresponding distributions of gas species concentrations are also shifted upward.

A decrease in solid supply rate while keeping the gas supply rate fixed is equivalent to an increase in gas supply rate while keeping the solid supply rate fixed. When the air supply rate is even slightly higher than the eigenvalue, the combustion zone is shifted upward, the carbon is depleted to zero at the upper portion, and the corresponding distributions of gas species concentrations are also shifted upward. The concentration of carbon monoxide at the top of the bed for excess gas supply is lower but the corresponding concentration of carbon dioxide for excess gas supply is higher than that for eigenvalue gas supply. It is quite clear that furnishing air even if only slightly higher than the eigenvalue, gasification is minimized and the length of the reactor required for complete combustion is greatly reduced.

Figures 13-17 show the effects of stoichiometric solid and gas supply rates on the distributions of solid and gas temperatures, of carbon content in solid, of gas species concentrations, of velocity and density of gas mixture. The temperature of the bed except at the bottom portion of the bed is higher for higher solid and gas supply rates. The combustion zone is thicker for higher solid and gas supply rates as shown in Figures 13-15 because the increase in the rate of carbon combustion is relatively

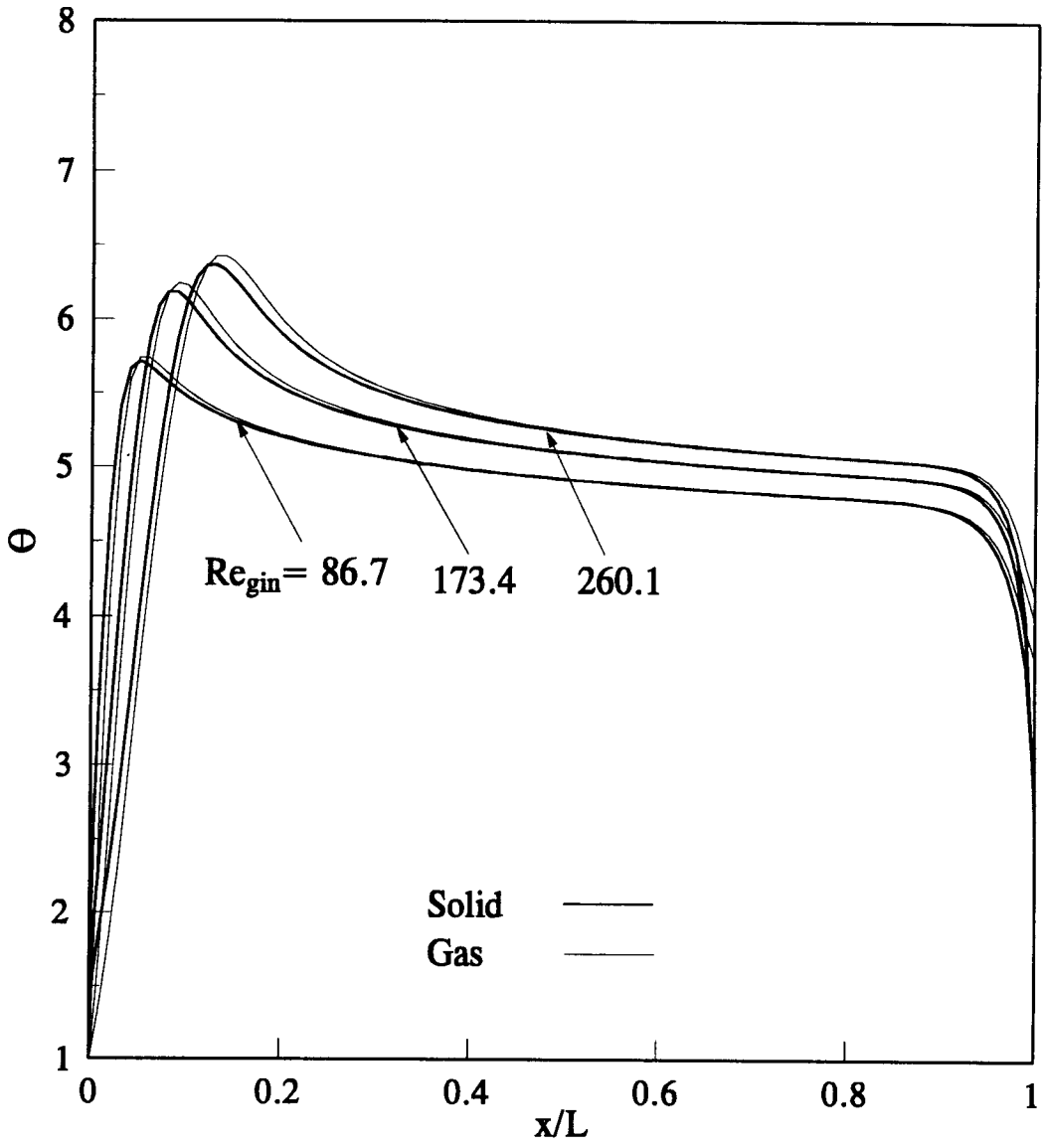

Fig. 13 Effect of stoichiometric solid and gas supply rates on temperature distributions of solid and gas.

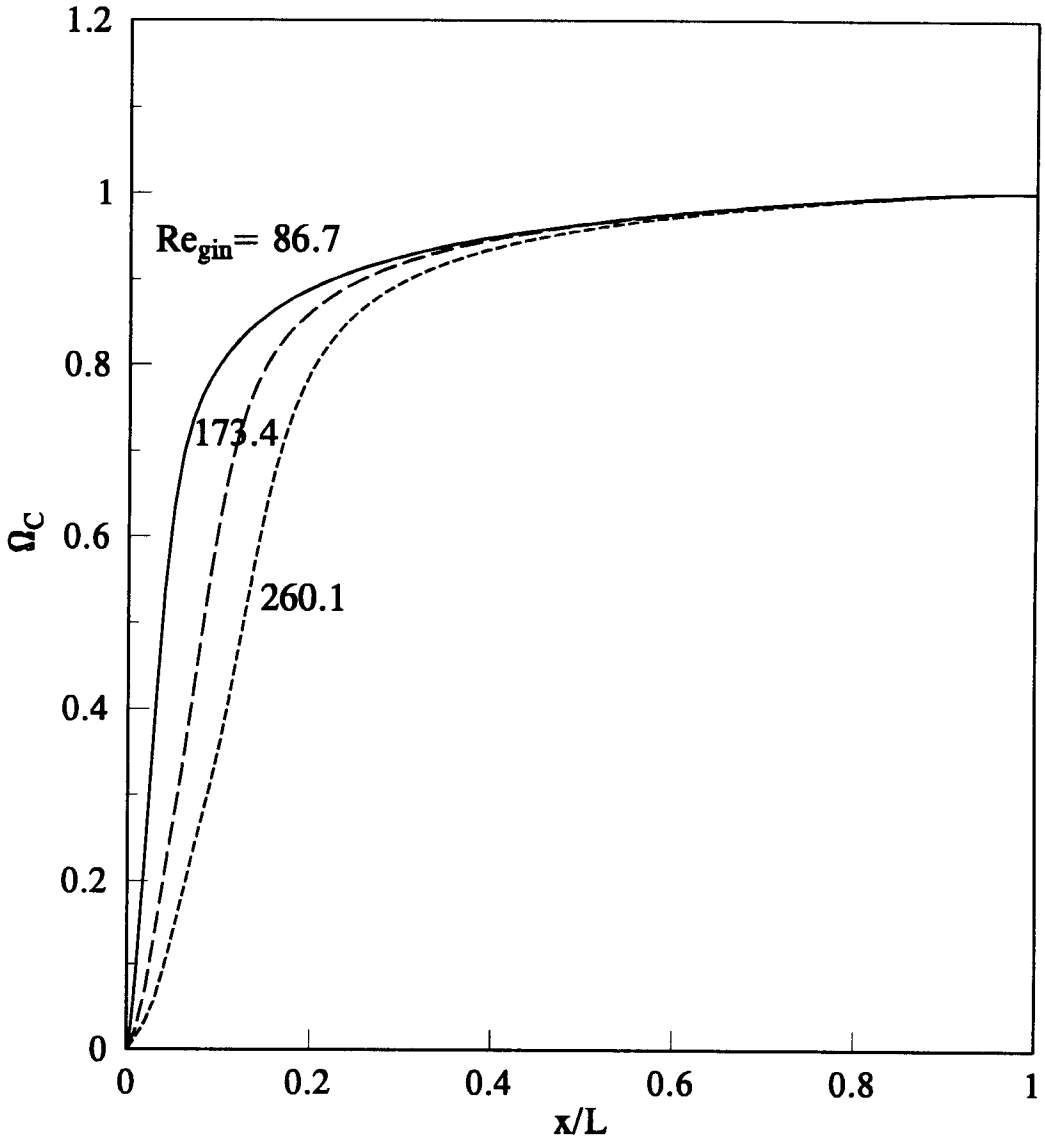

Fig. 14 Effect of stoichiometric solid and gas supply rates on distribution of carbon content in solid.

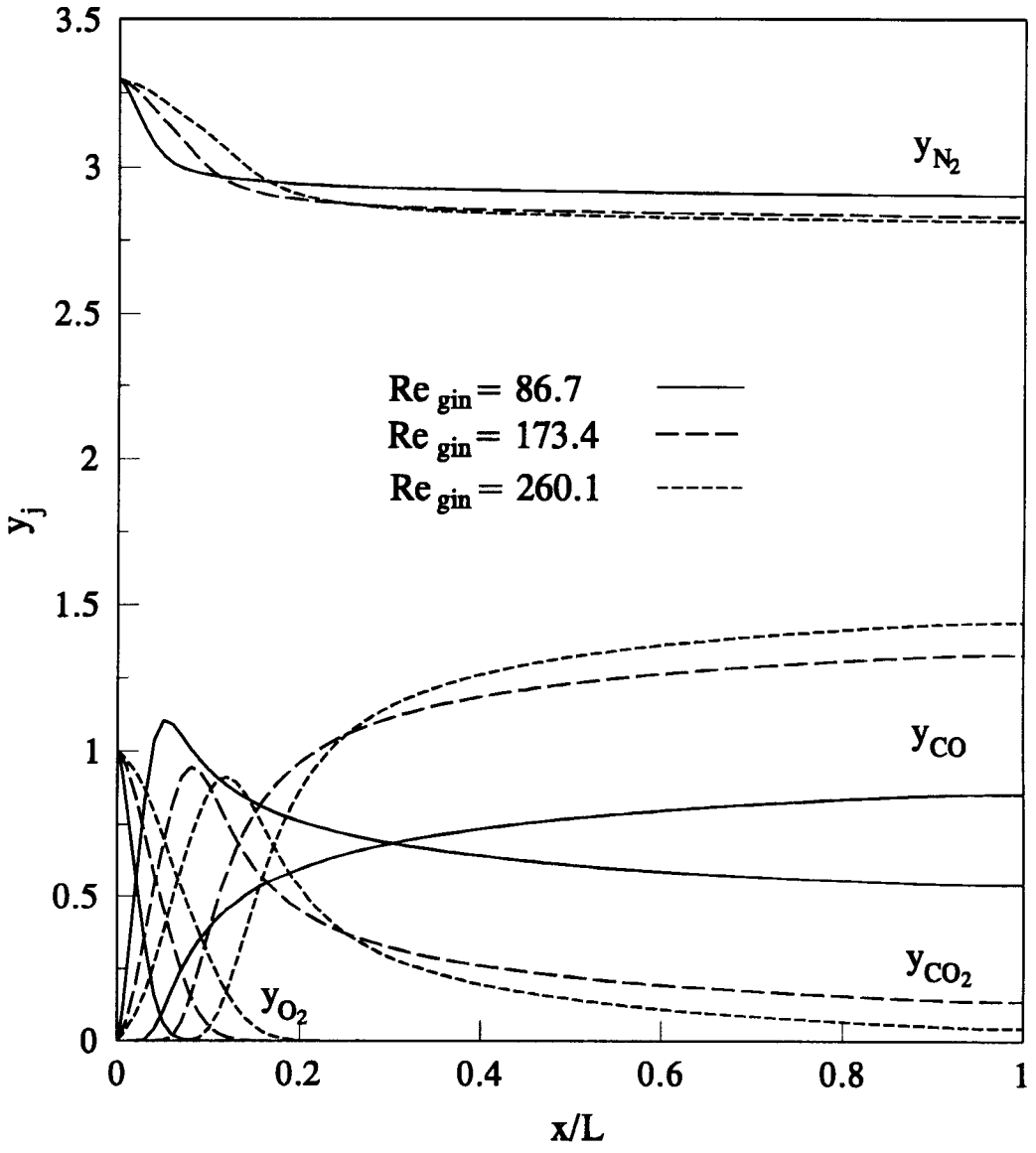

Fig. 15 Effect of stoichiometric solid and gas supply rates on concentration distributions of gas species.

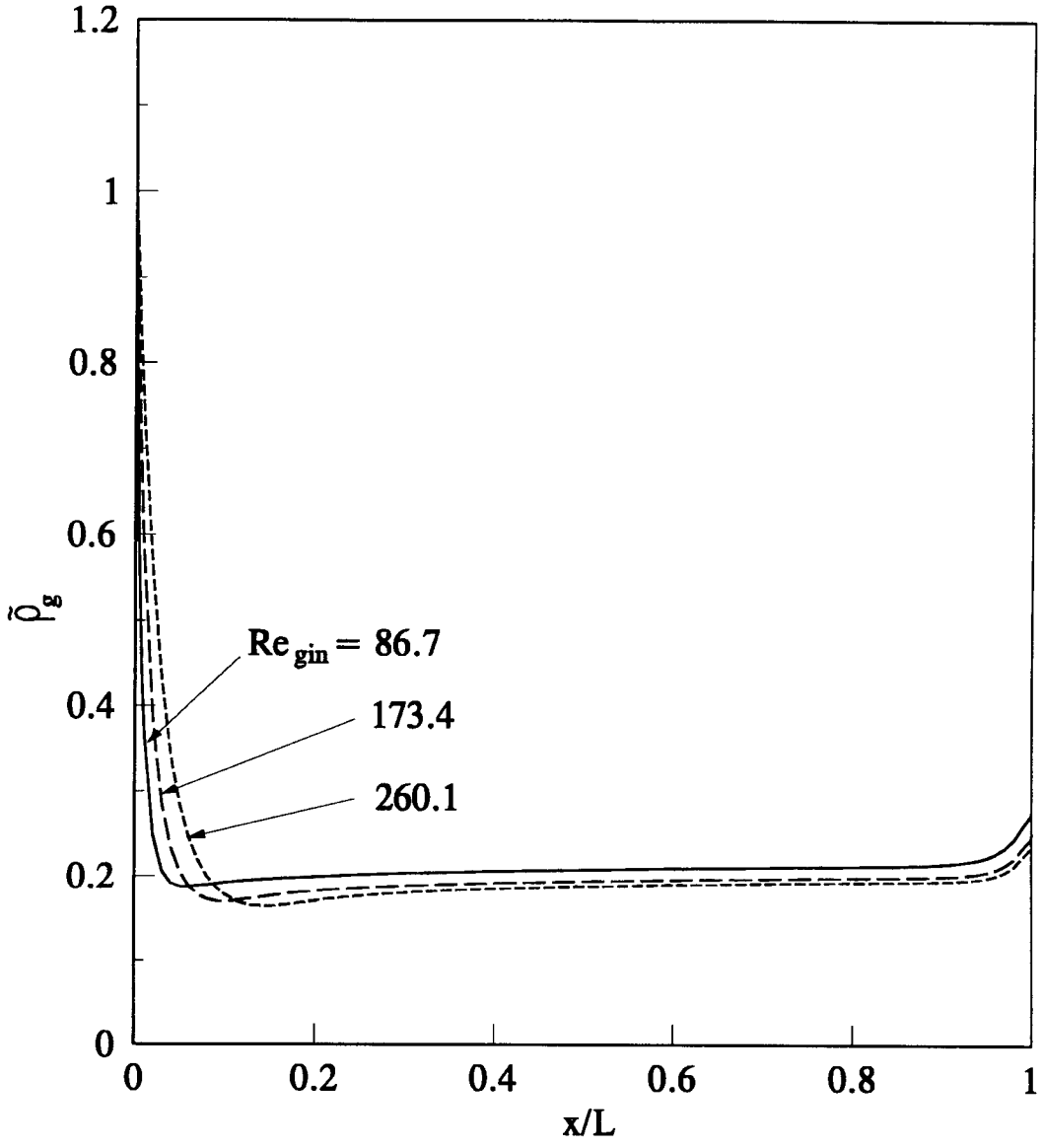

Fig. 16 Effect of stoichiometric solid and gas supply rates on density distribution of gas mixture.

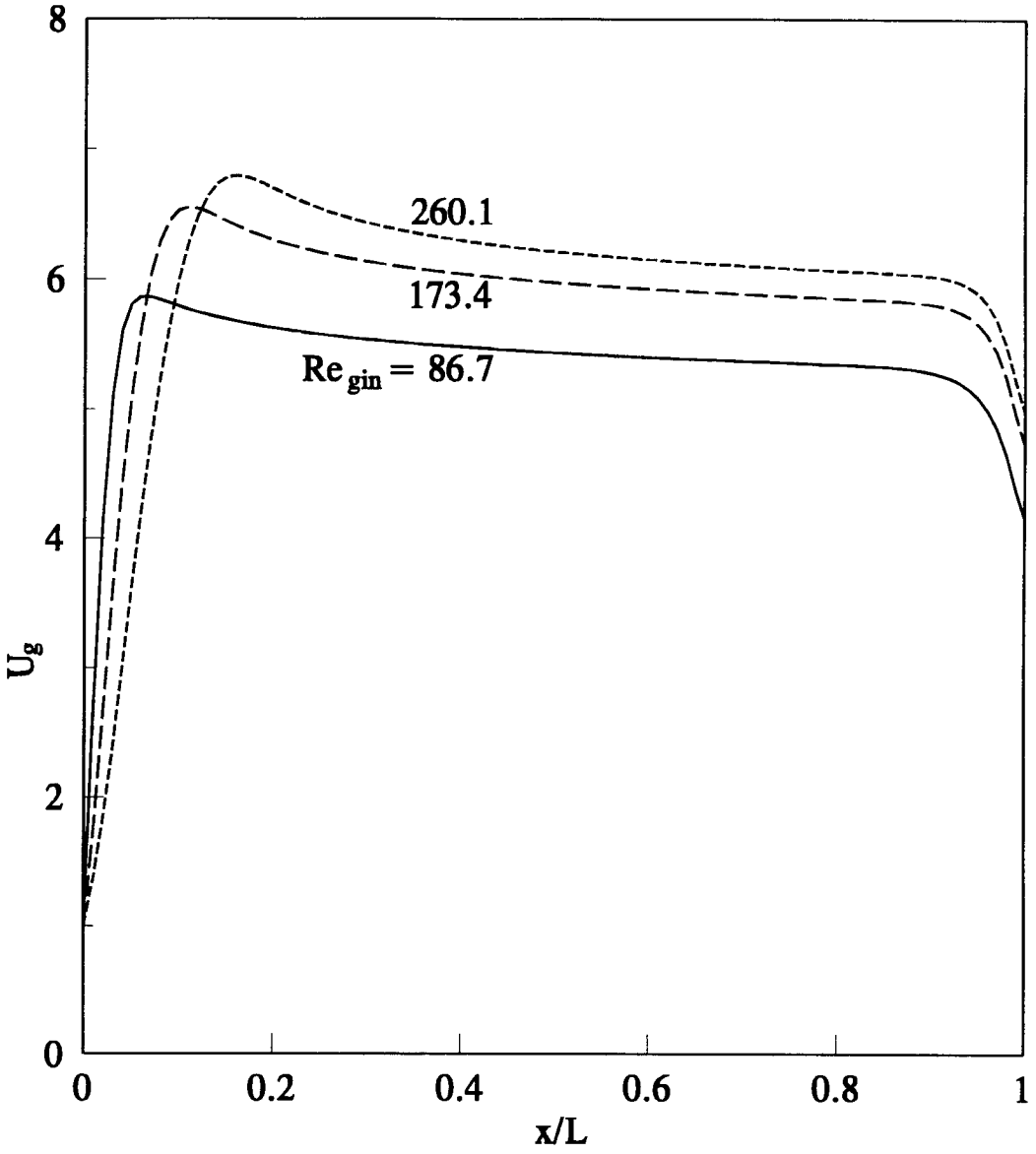

Fig. 17 Effect of stoichiometric solid and gas supply rates on gas velocity distribution.

slower than the increase in gas supply rate even though the absolute magnitude of the combustion reaction rate is higher for higher supply rate. When the gas supply rate becomes ten-fold higher, the gas supply Reynolds number becomes ten-fold higher. On the other hand, the rate of carbon combustion becomes about $10^{0.563}$ times higher because the carbon combustion is mainly controlled by mass transfer of oxygen from the bulk gas to particle surface and the mass transfer coefficient is proportional to the 0.563 power of the gas Reynolds number. Figure 14 shows that the carbon in solid is consumed completely at the bottom of the bed for stoichiometric solid and gas supply rates.

Figure 15 shows the effects of stoichiometric solid and gas supply rates on the concentration distributions of gas species in the bed. Oxygen is depleted at the higher location of the bed, that is, the region of combustion reaction is thicker for higher solid and gas supply rates. For higher solid and gas supply rates, the concentration of carbon dioxide is lower and that of carbon monoxide is higher at the top portion of the bed because the rate of gasification reaction of carbon with carbon dioxide is mostly controlled by reaction kinetics rather than mass transfer and the temperature of the bed is higher.

Figures 16 and 17 show the effects of stoichiometric solid and gas supply rates on the density and velocity distributions of gas mixture. For higher solid and gas supply rates, the density of gas mixture except at the bottom portion of the bed is lower because the density of gas mixture is inversely proportion to the temperature as described in the equation of state and temperature of the bed is higher. The velocity of gas mixture depends on two factors. First, the velocity of gas mixture is inversely

proportional to the density of gas mixture, that is, it is proportional to the temperature of the bed. The second factor is mass loss or generation of gas species due to the chemical reaction. The velocity of gas mixture for higher solid and gas supply rates is higher except at the bottom portion of the bed.

4.4 EFFECT OF GAS SUPPLY TEMPERATURE

The values of stoichiometric solid supply rate for several given gas supply rates and gas supply temperatures are calculated by numerical calculation to be as shown in Figure 18. Figure 18(a) shows the relation of stoichiometric solid and gas supply rates in terms of the Reynolds number whereas Figure 18(b) shows in terms of mass velocity. The lines in the figure represent the relation of stoichiometric solid and gas supply rates. When the relation of solid and gas supply rates falls in the upper left region of the line, the combustion zone is shifted to the upper portion of the bed. On the other hand, when the relation falls in the lower right region of the line, the combustion zone is shifted downward in the bed and unburnt residue carbon is discharged at the bottom of the bed. When the gas supply temperature is higher, more solid fuel particles can be consumed at the same rate of gas supply because of the higher reaction rate at higher temperature.

The effects of gas supply temperature on distributions of solid and gas temperatures, of carbon content in solid, and of gas species concentrations for a given gas supply rate are shown in Figures 19-21. The temperature of the bed for higher gas supply temperature becomes higher. The peak temperature of the bed is slightly shifted downward and the region of combustion is thinner for higher gas

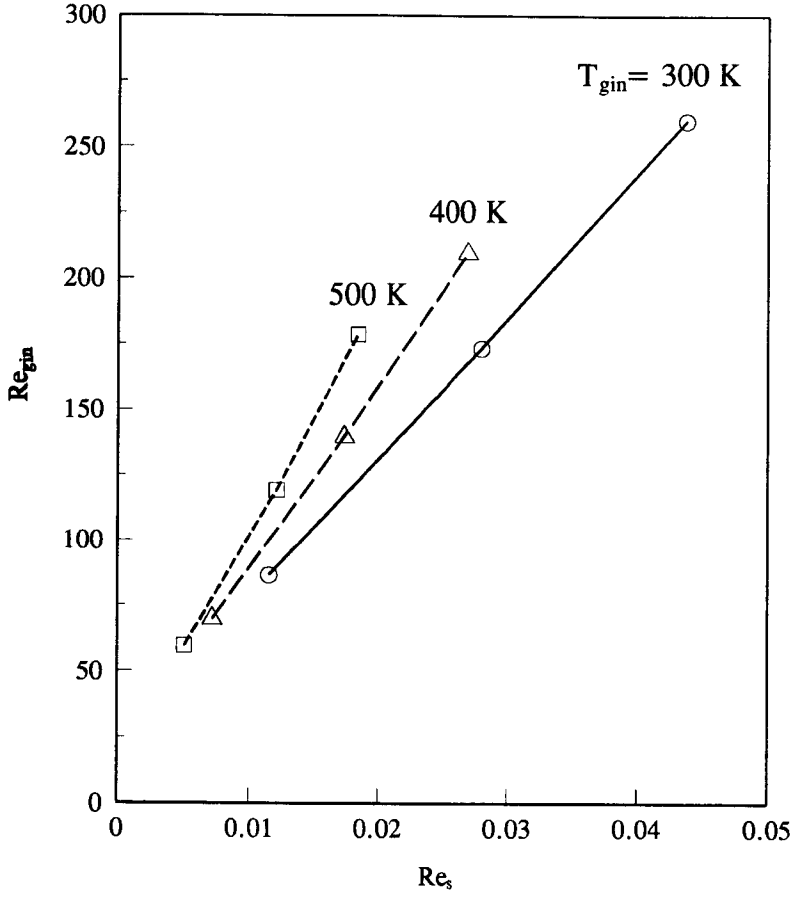

(a) Stoichiometric relation of Reynolds numbers

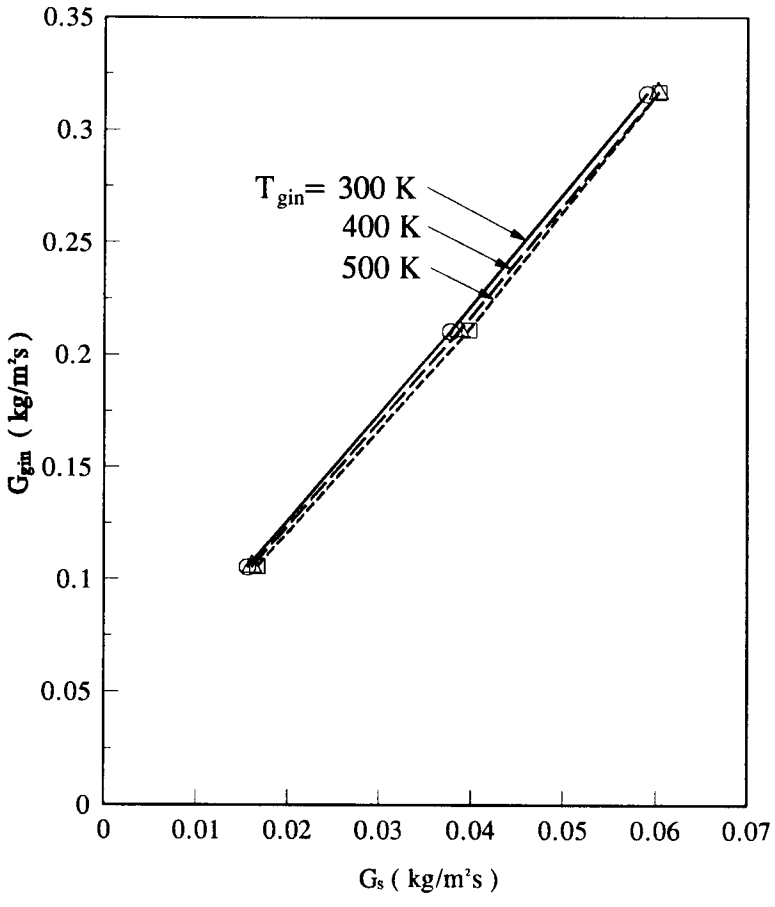

(b) Stoichiometric relation of mass velocities

Fig. 18 Effect of gas supply temperature on stoichiometric solid and gas supply rates. (T_{sin}=300 K, ϕ=0.26, ϕ_h=0.3, L=0.6096 m, d=0.015 m, ω_{Cin}=0.913)

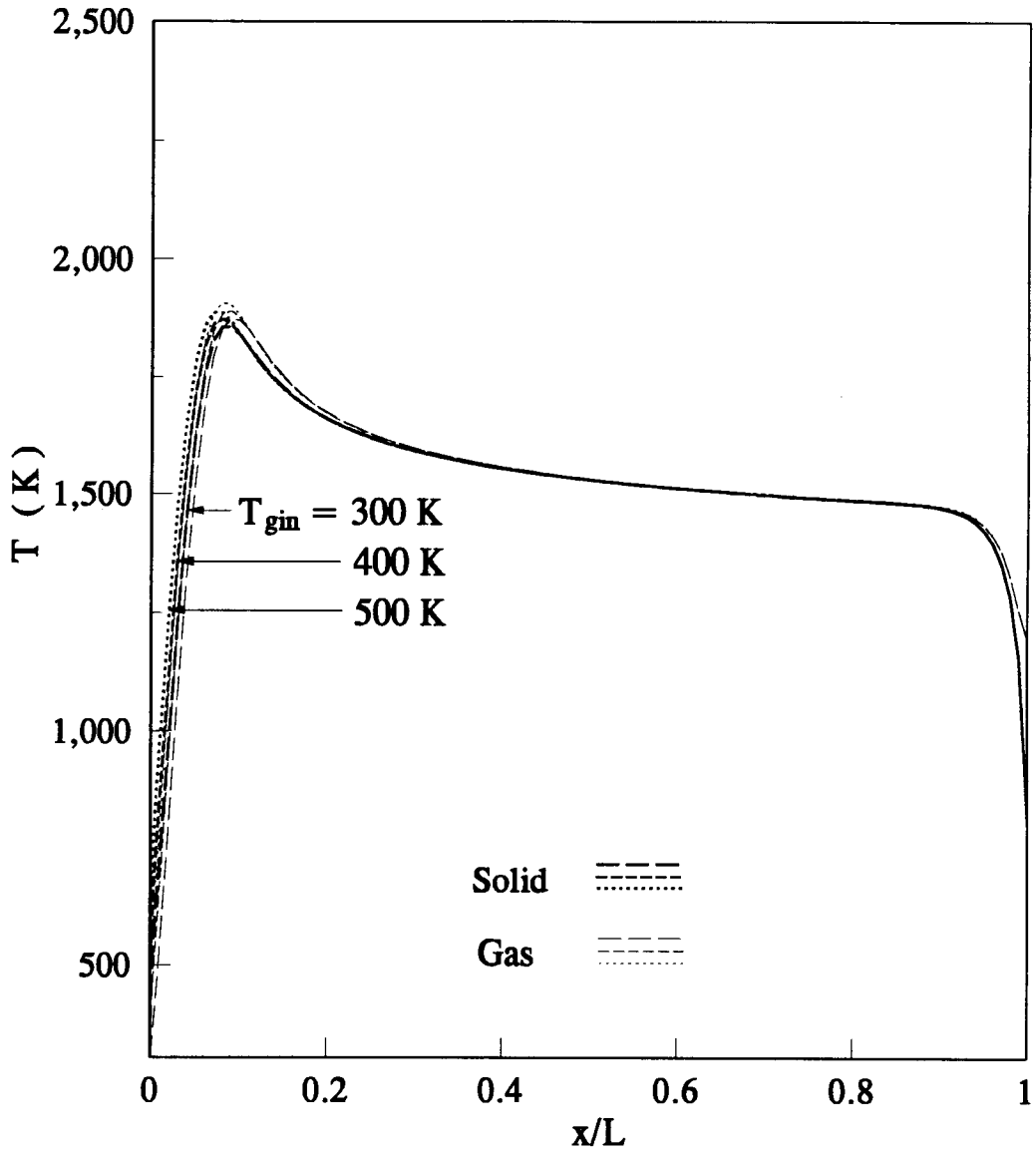

Fig. 19 Effect of gas supply temperature on temperature distributions of solid and gas for stoichiometric solid and gas supply rates. (G_{gin}=0.21074 kg/m^{2}s)

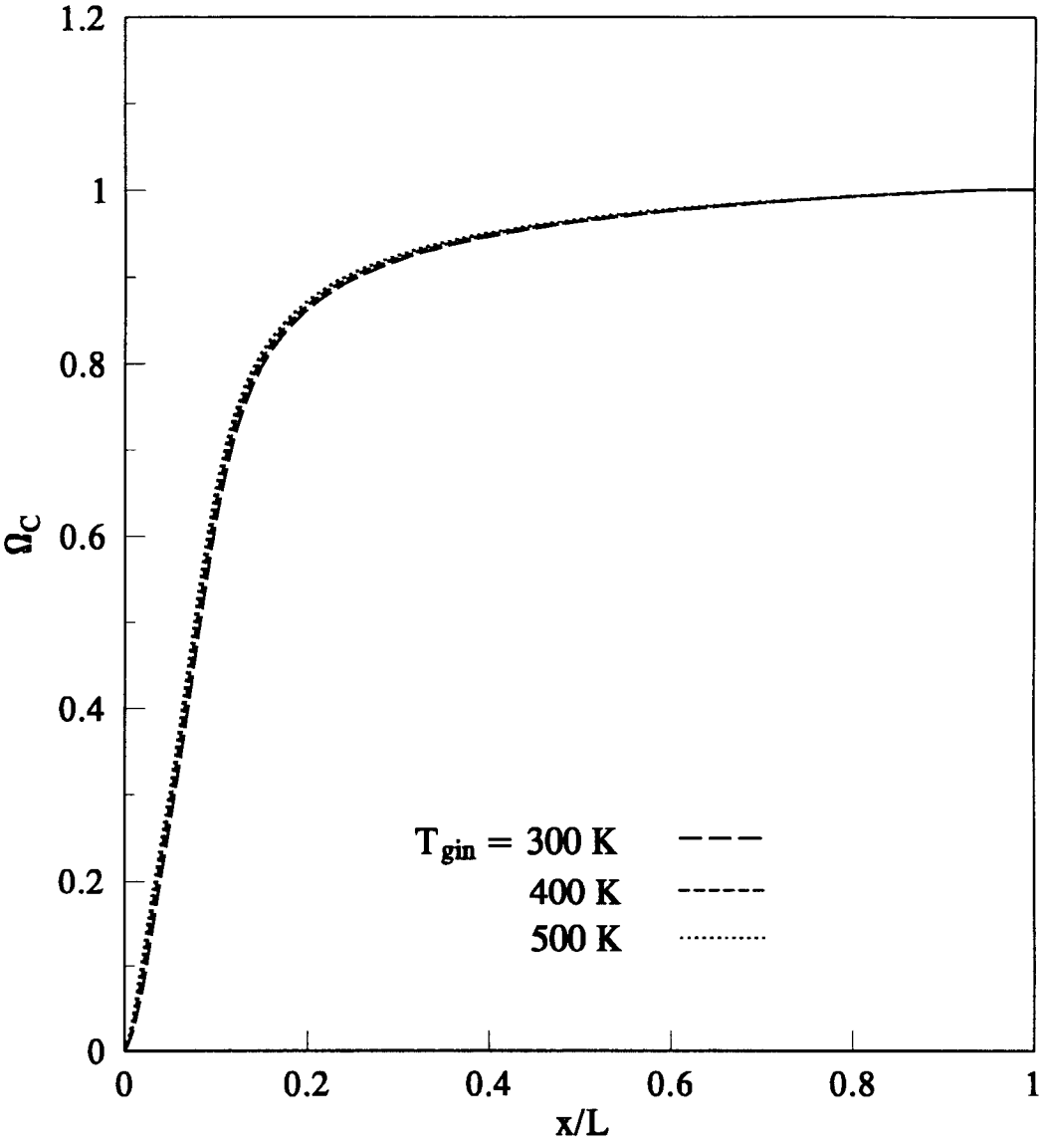

Fig. 20 Effect of gas supply temperature on distribution of carbon content in solid for stoichiometric solid and gas supply rates. (G_{gin}=0.21074 kg/m^{2}s)

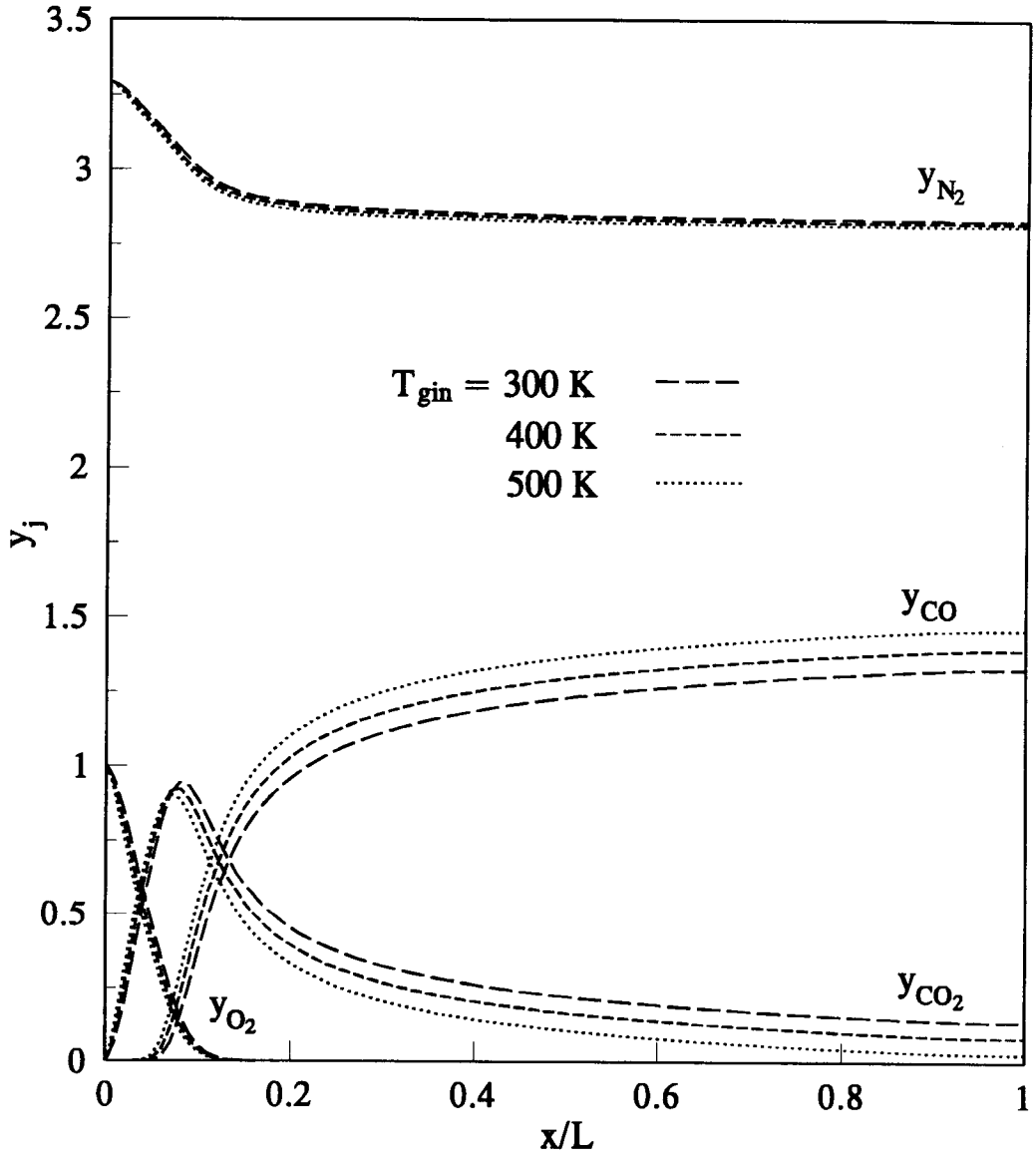

Fig. 21 Effect of gas supply temperature on concentration distributions of gas species for stoichiometric solid and gas supply rates. (G_{gin}=0.21074 kg/m^{2}s)

supply temperature because of the higher temperature of the bed. In addition, the oxygen concentration becomes zero at the lower location of the bed and the location of maximum carbon dioxide concentration is lower in the bed for higher gas supply temperature. The concentration of carbon dioxide is lower and the concentration of carbon monoxide is higher for higher gas supply temperature because of the higher temperature of the bed and the corresponding higher gasification reaction rate.

4.5 EFFECT OF PARTICLE DIAMETER

The values of stoichiometric solid supply rate for several given gas supply rates and particle diameters are calculated to be as shown in Figure 22. Figure 22(a) shows the relation of stoichiometric solid and gas supply rates in terms of the Reynolds number whereas Figure 22(b) shows in terms of mass velocity. The lines in the figure represent the relation of stoichiometric solid and gas supply rates. At a given gas supply rate, the solid supply rate becomes higher, that is, more solid fuel particles can be consumed for larger particle size because the temperature of the bed except at the bottom of the bed is higher as shown in Figure 23 and more carbon dioxide is consumed by the gasification reaction of carbon with carbon dioxide to carbon monoxide as shown in Figure 25.

The effects of solid particle size on the distributions of solid and gas temperatures, of carbon content in solid, and of gas species concentrations for a given gas supply rate are shown in Figures 23-25. The terms which are affected by the solid particle diameter in the governing equations are heat and mass transfer coefficients, molecular diffusion through the ash layer, and total surface area of solid

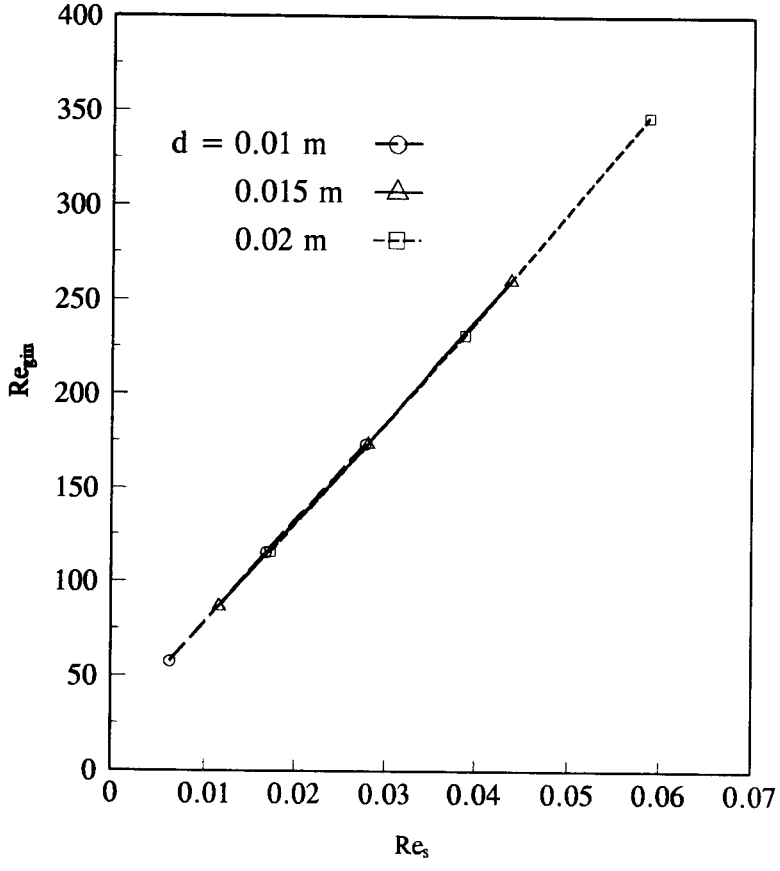

(a) Stoichiometric relation of Reynolds numbers

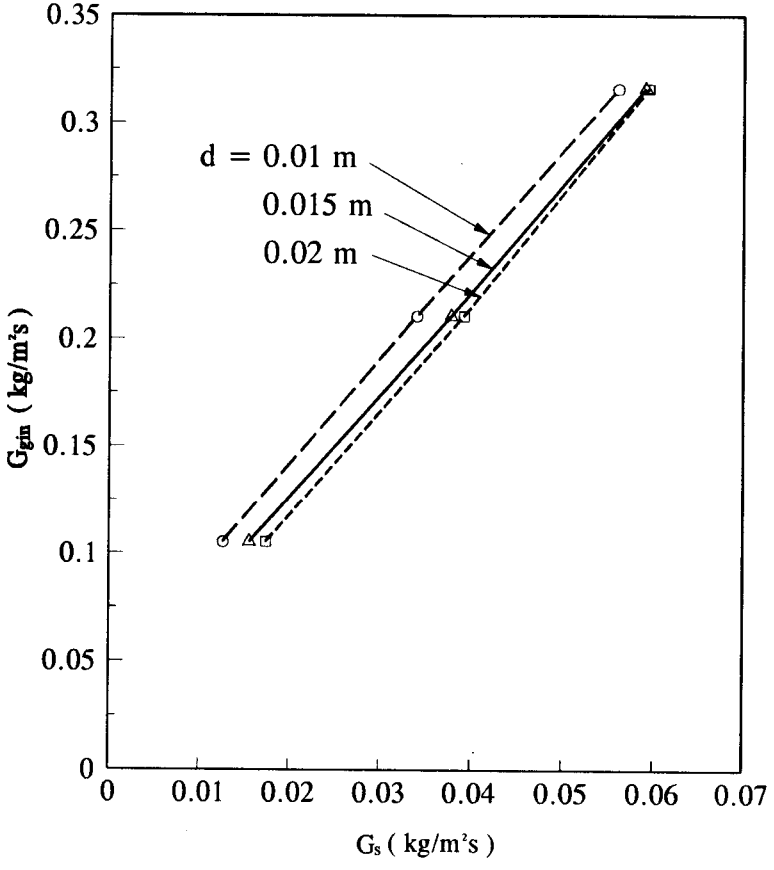

(b) Stoichiometric relation of mass velocities

Fig. 22 Effect of solid particle diameter on stoichiometric solid and gas supply rates. (T_{gin}=300 K,T_{sin}=300 K, ϕ=0.26, ϕ_h=0.3, L=0.6096 m, ω_{Cin}=0.913)

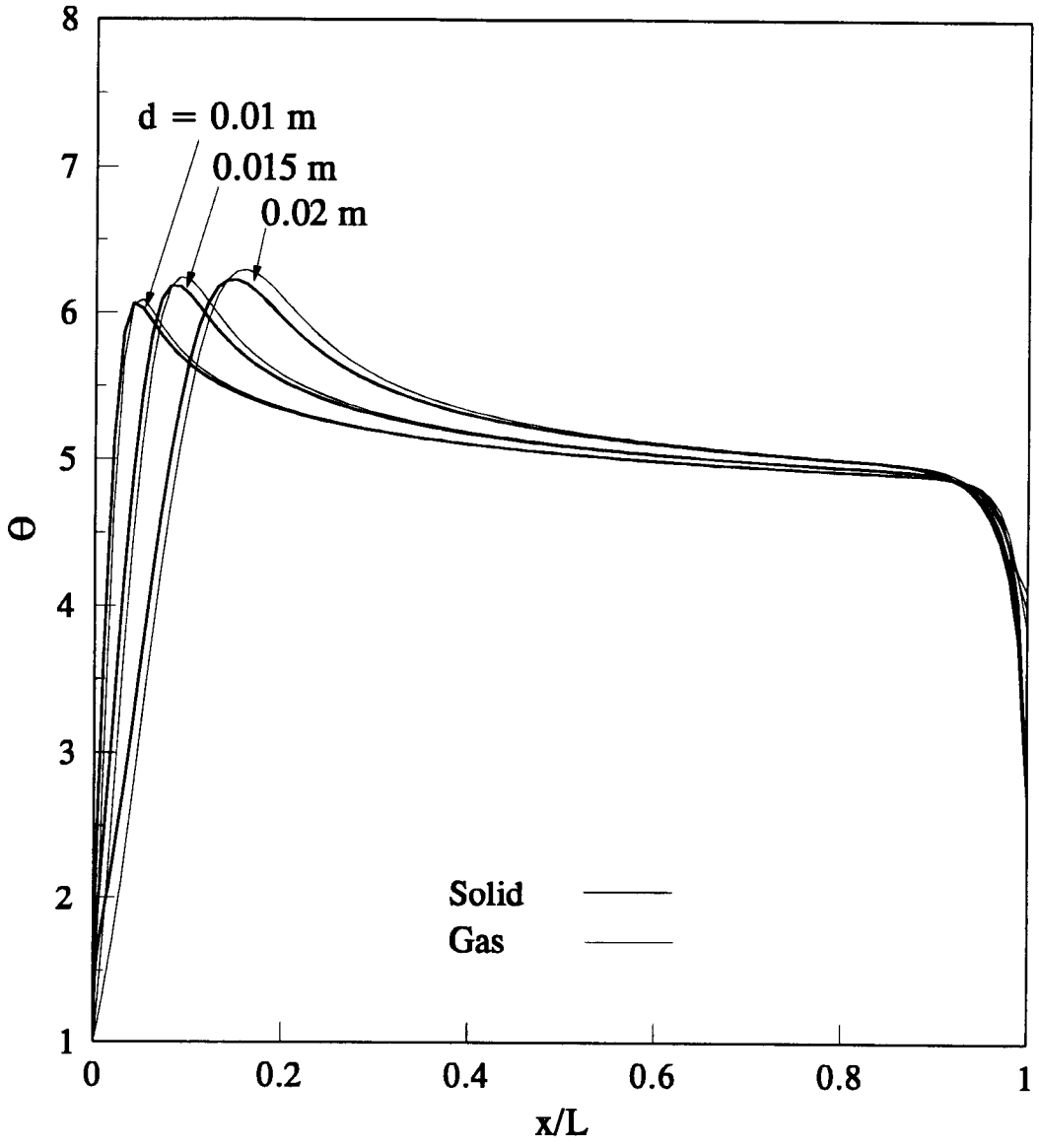

Fig. 23 Effect of solid particle diameter on temperature distributions of solid and gas for stoichiometric solid and gas supply rates. (G_{gin}=0.21074 kg/m^{2}s)

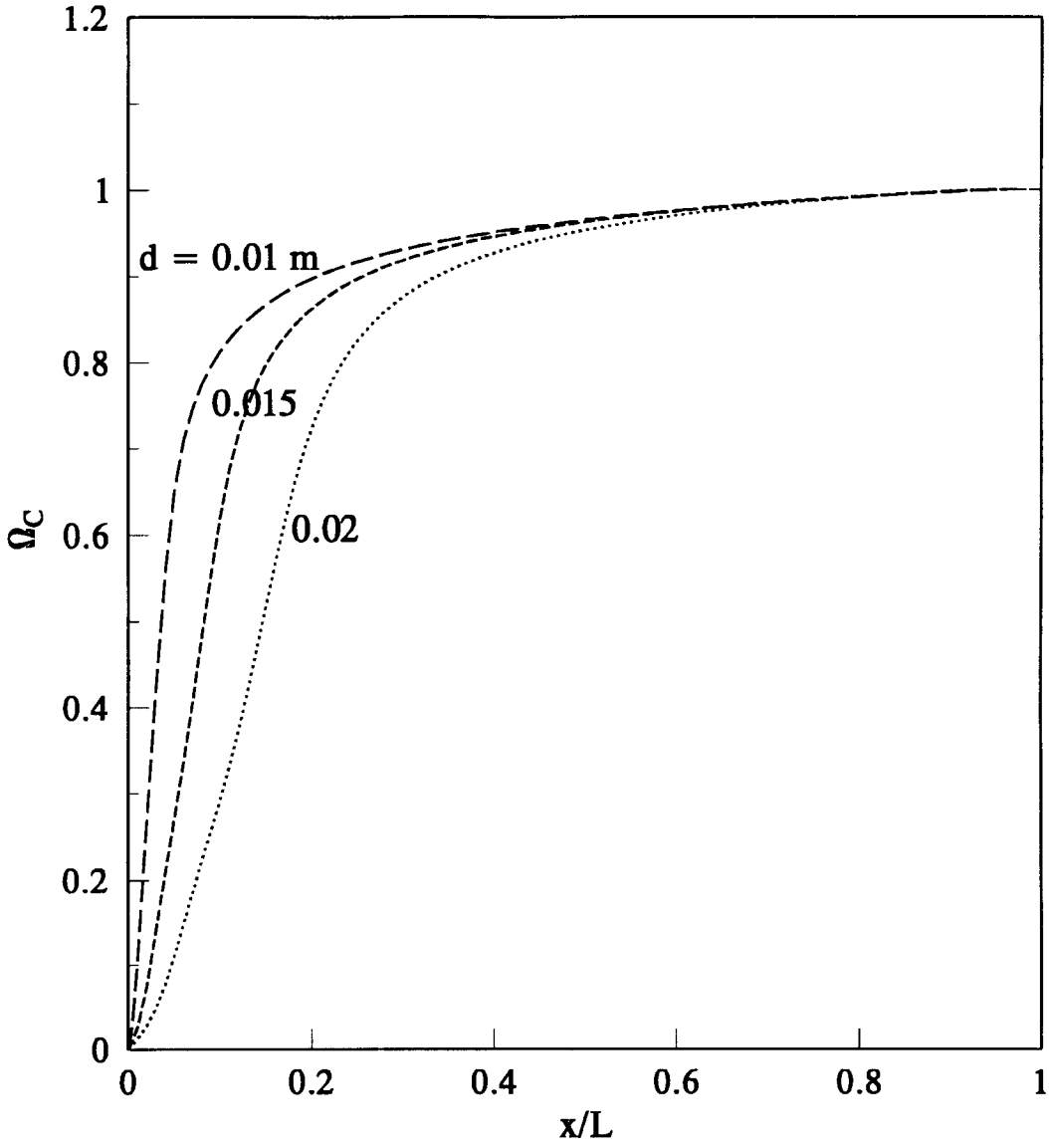

Fig. 24 Effect of solid particle diameter on distribution of carbon content in solid for stoichiometric solid and gas supply rates. (G_{gin}=0.21074 kg/m^{2}s)

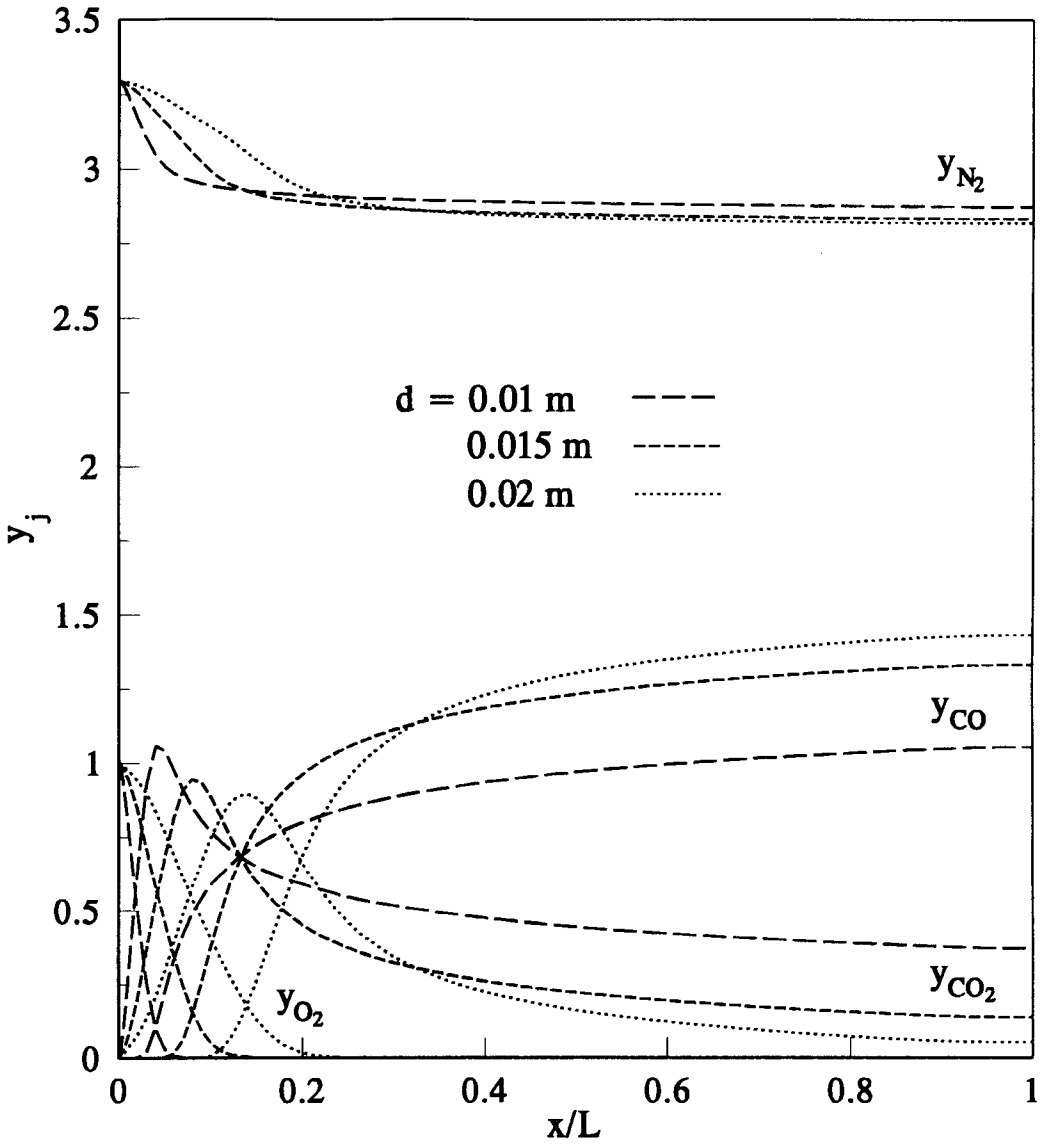

Fig. 25 Effect of solid particle diameter on concentration distributions of gas species for stoichiometric solid and gas supply rates. (G_{gin}=0.21074 kg/m^{2}s)

particles per unit volume of bed. On the other hand, the void fraction of the bed depends not on the particle diameter but on the method of packing. The heat and mass transfer coefficients, molecular diffusion through the ash layer, and total surface area of solid particles per unit volume of bed become smaller for larger solid particle diameter. The local combustion rate is lower for larger particle diameter but it is distributed along a wider portion of the bed. Therefore, the peak temperature of the bed for larger particle sizes is located at the upper portion of the bed as shown in Figure 23. The temperature difference between solid and gas is larger for larger particle diameter because of the lower convective heat transfer coefficient and smaller surface area of solid particle per unit volume of the bed. The peak temperature of the bed is higher for larger particle size because less heat is lost at the bottom of the bed. The combustion zone is thicker and oxygen is depleted at the higher location of the bed for larger particle size as shown in Figure 25. The carbon content in solid decreases more slowly in the combustion zone for larger particle diameter as shown in Figure 24. When the diameter of solid particles becomes larger than some critical size, the region of carbon combustion is wider than the bed length, unburnt carbon is discharged out of the bed.

The temperature except at the bottom portion of the bed is higher for larger particle size. The rate of gasification reaction is mostly controlled by reaction kinetics except at very high temperature and it is higher at higher temperature. The concentration of carbon dioxide at the top portion of the bed is lower for larger particle size because of the higher gasification reaction rate at higher temperature.

The corresponding concentration of carbon monoxide at the top portion of the bed is higher for larger particle diameter.

Naturally, as pointed out earlier, the basic assumption of the temperature of the solid being uniform within the particle holds satisfactorily only for small particles. When the particles are large enough to yield a Biot number greater than about 0.1, large errors may be encountered. The issue of nonuniform particle temperature cannot be addressed without much complication of the model. It is not now clear to what extent the results presented in Figures 23-25 will be altered by these nonuniformities within the particle.

4.6 EFFECT OF INITIAL CARBON CONTENT IN SOLID PARTICLES

The values of stoichiometric solid supply rate for several gas supply rates and initial carbon contents in solid particles are estimated by numerical calculation to be as shown in Figure 26. For a given gas supply rate, the stoichiometric solid supply rate is higher for lower initial carbon content in solid particles because the same amount of carbon is needed for the complete consumption of carbon at the bottom of the bed, the temperature of the bed except at the bottom of the bed is higher, the concentration of carbon dioxide is lower, and the concentration of carbon monoxide is higher at the top of the bed.

The effects of initial carbon content in solid on the distributions of solid and gas temperatures, of gas species concentrations, and of carbon content in solid for a given gas supply rate are shown in Figures 27-29 when the solid supply rates are stoichiometric. The porosity of the ash layer of particles is assumed to be same as the

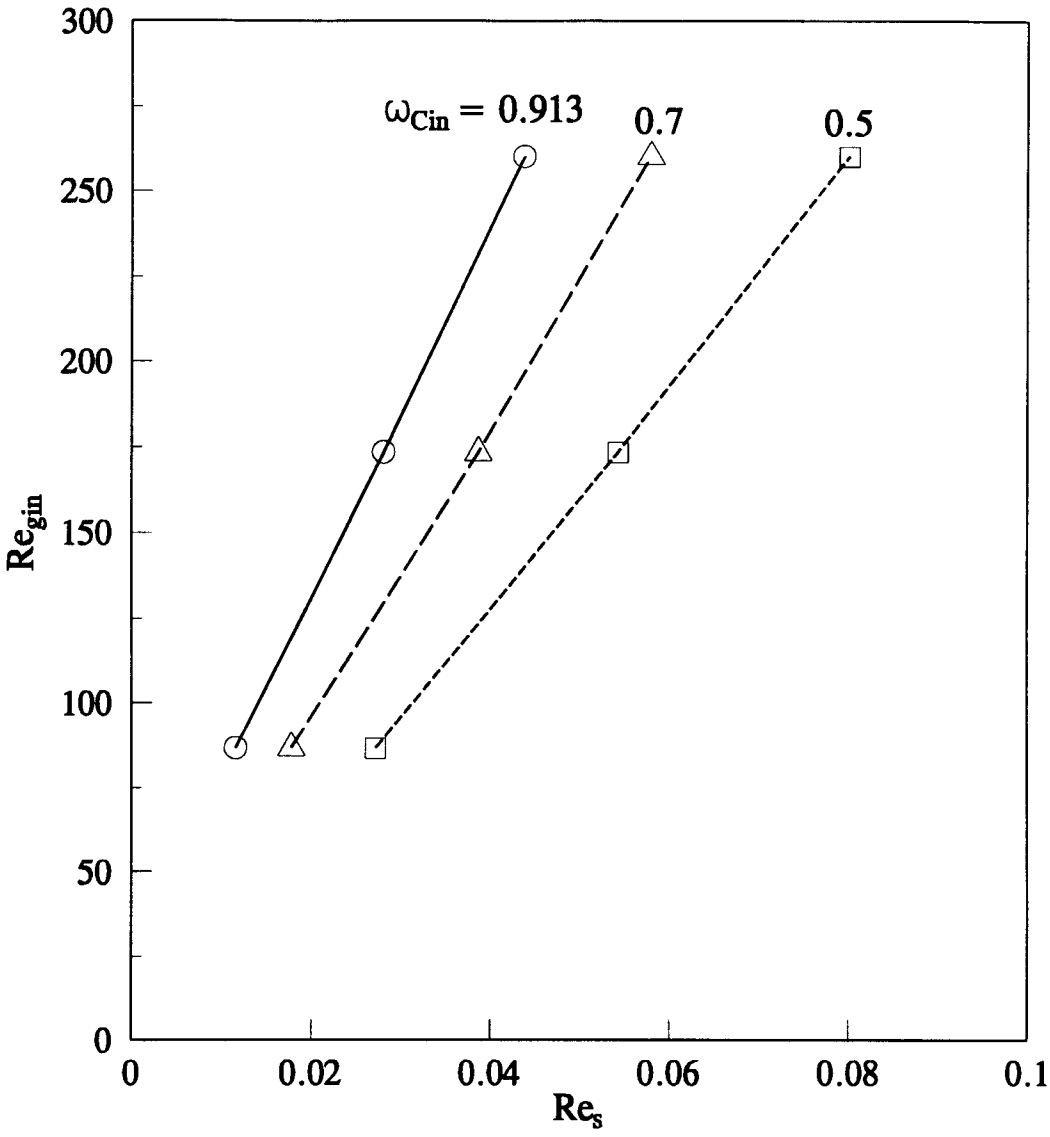

Fig. 26 Effect of initial carbon content in solid on stoichiometric solid and gas supply rates. (T_{gin}=300 K,T_{sin}=300 K, ϕ=0.26, ϕ_h=0.3, L=0.6096 m, d=0.015 m)

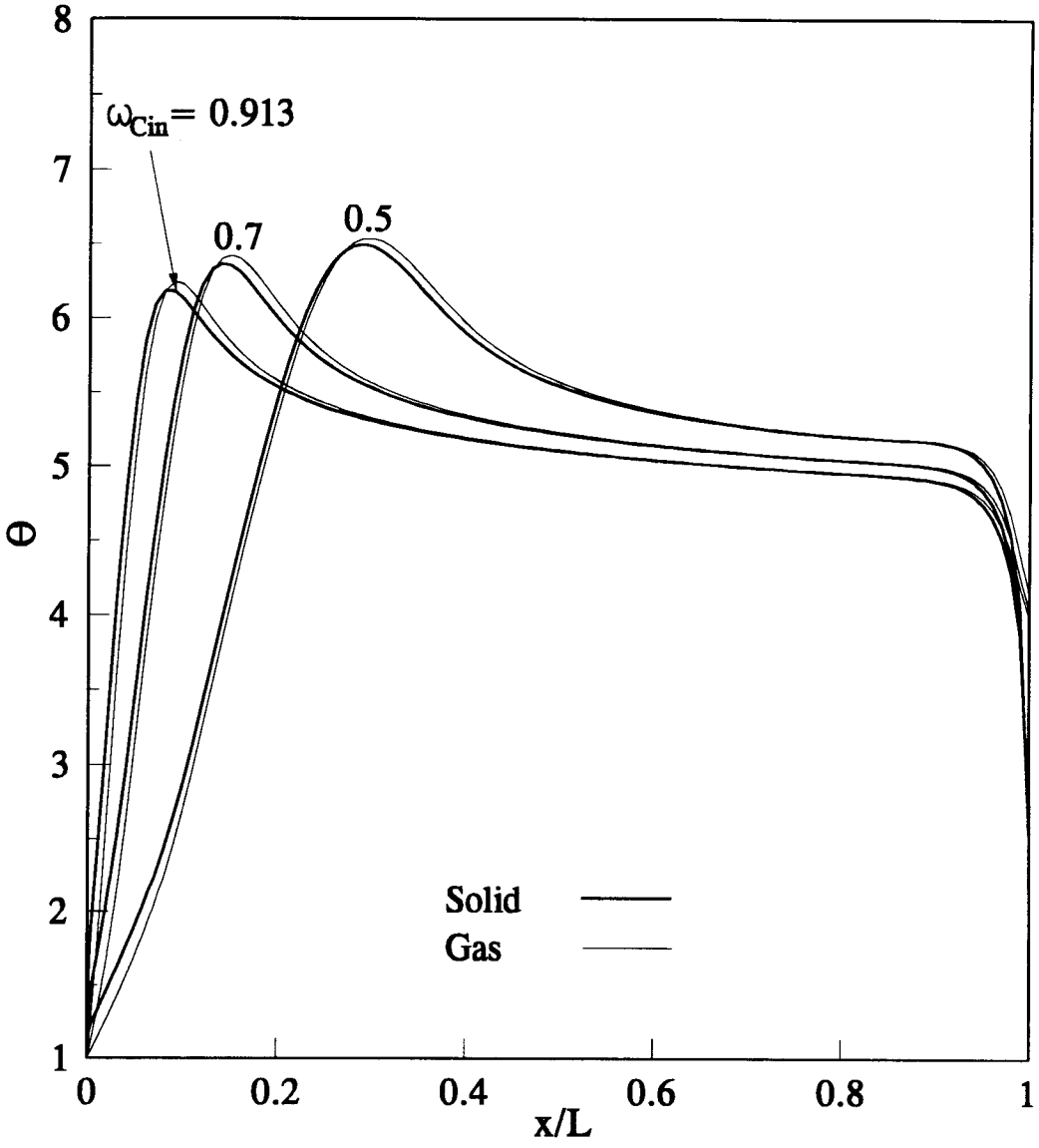

Fig. 27 Effect of initial carbon content in solid on temperature distributions of solid and gas for stoichiometric solid and gas supply rates. (Re_{gin}=173.4)

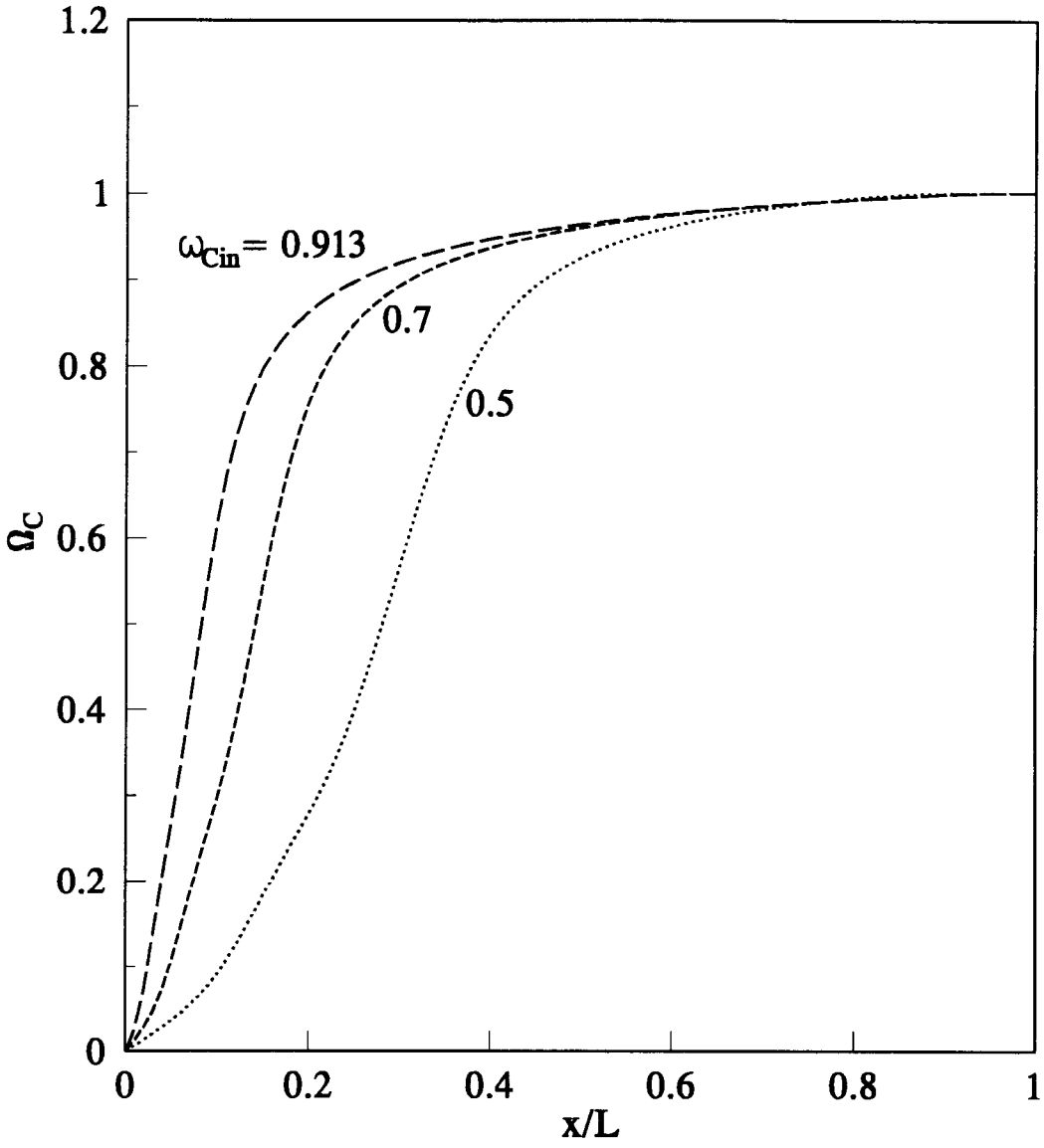

Fig. 28 Effect of initial carbon content in solid on distribution of carbon content in solid for stoichiometric solid and gas supply rates. (Re_{gin}=173.4)

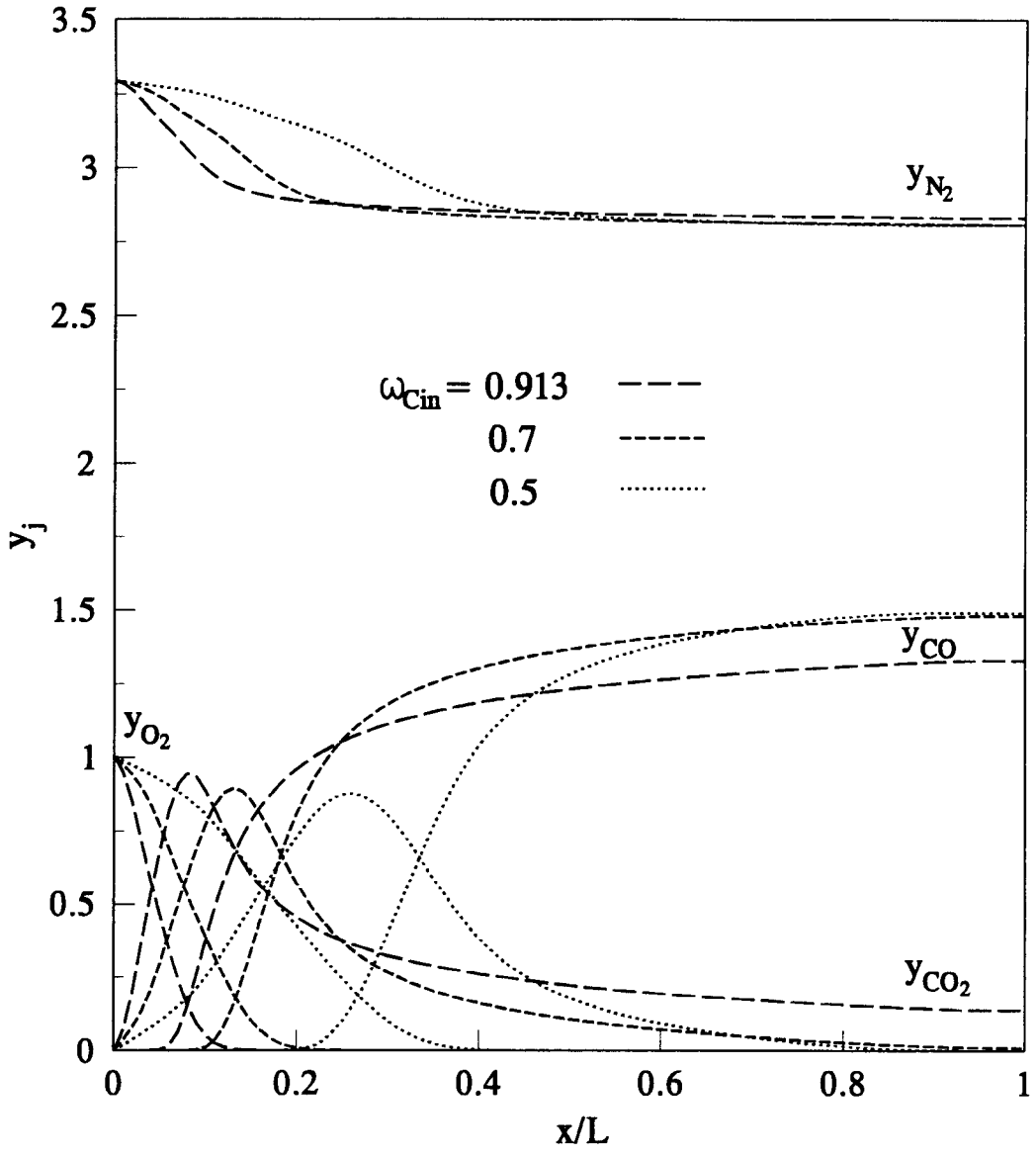

Fig.29 Effect of initial carbon content in solid on concentration distributions of gas species for stoichiometric solid and gas supply rates. (Re_{gin}=173.4)

initial carbon content in solid. The diffusion resistance through the ash layer becomes higher for lower carbon content in solid because the ash layer is less porous. The corresponding rate of combustion reaction which is controlled by molecular diffusion and convective mass transfer is lower. The combustion zone is thicker for lower initial carbon content in solid because more solid particles are supplied as shown in Figure 26 but the combustion rate is lower. The peak temperature is located at the upper portion of the bed because of this lower rate but wider distribution of combustion reaction. In addition, the temperature gradient at the bottom portion of the bed is lower so that less heat is lost through the bottom of the bed. Therefore, the temperature of the bed for lower initial carbon content in solid is higher except at the bottom portion of the bed. When the initial carbon content in solid is less than some critical value, the reaction rate may be so low and the region of carbon combustion may be so wide that supplied carbon cannot be completely consumed, unburned carbon is discharged at the bottom of the bed, and the temperature of the bed becomes low. Further study is necessary to verify this discussion.

The local carbon content in solid particles decreases more slowly in the combustion zone for lower initial carbon content in solid. The oxygen concentration becomes zero at the upper location of the bed for lower initial carbon content in solid. The concentration of carbon dioxide becomes lower and the corresponding concentration of carbon monoxide becomes higher at the top portion of the bed for lower initial carbon content in solid because of the higher temperature and higher rate of gasification reaction of carbon with carbon dioxide to carbon monoxide.

4.7 EFFECTIVE THERMAL CONDUCTIVITY

In addition to the thermal conductivities of the solid and gas themselves, the effects of void fraction, radiation heat transfer, and enhanced heat transfer due to the eddy diffusion by fluid flow around solid particles are accounted in the effective thermal conductivities of solid and gas in the present study. Figure 30 shows the comparison of effective thermal conductivities with and without the effects of radiation heat transfer and enhanced heat transfer due to the eddy diffusion by fluid flow. The effective thermal conductivities of solid and gas with the effect of radiation heat transfer and enhanced heat transfer due to the eddy diffusion by fluid flow are higher than those without the effects. The increase in the effective thermal conductivity of gas by the effect of the enhanced heat transfer due to the eddy diffusion by fluid flow is higher than the increase in effective thermal conductivity of solid by the effect of radiation heat transfer.

In this chapter, five different reaction models are investigated and compared with experiment from literature. The relation of the stoichiometric solid and gas supply rates and the distributions of solid and gas temperatures, of gas species concentrations, of carbon content in solid particles are discussed as obtained by numerical calculation. The effects of several parameters are also investigated in this chapter.

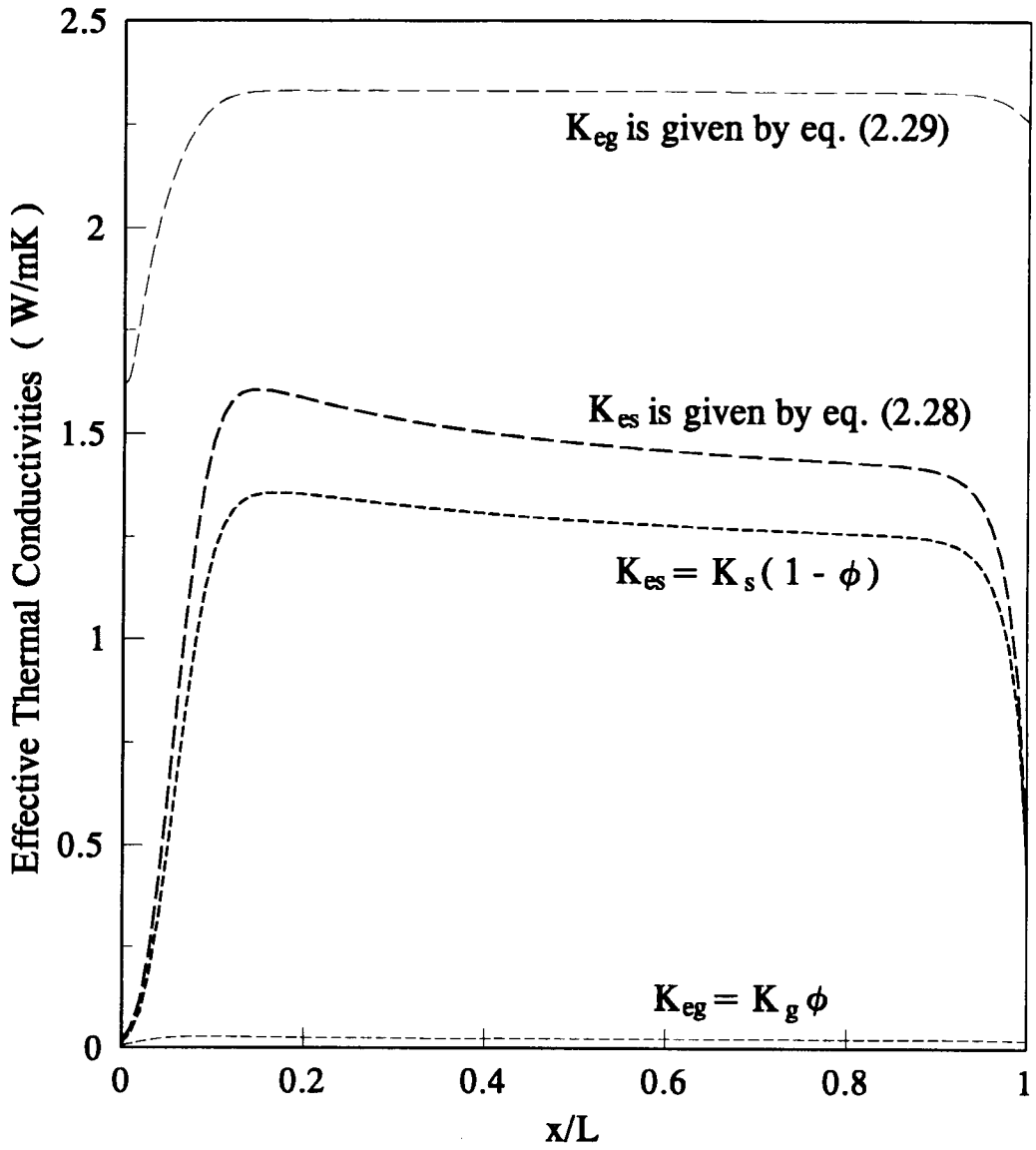

Fig. 30 Comparison of effective thermal conductivities with and without the effects of radiation heat transfer and enhanced heat transfer due to the eddy diffusion by fluid flow for standard run.

CHAPTER 5

CONCLUSIONS AND RECOMMENDATIONS

5.1 CONCLUSIONS

A one-dimensional steady-state computational model for combustion of a bed of solid fuel particles with a counterflowing oxidant gas has been developed. The values of stoichiometric solid and gas supply rates for various given conditions are estimated and the effects of solid and gas supply rates, gas supply temperature, solid particle diameter, and initial carbon content in solid particles are investigated. The following conclusions are drawn.

(1) The temperature of the bed and concentrations of gas species calculated by the three reaction model agree best with the experimental result from literature when the fraction of carbon monoxide in the products of the reaction of carbon with oxygen is given as a function of temperature.

(2) The stoichiometric solid supply rate is higher when gas supply rate is higher.

(3) When more excess air is supplied, the reaction zone is more shifted towards the top of the bed. When more excess solid fuel particles are supplied, more unburned carbon is discharged at the bottom of the bed.

(4) At a given gas supply rate, the stoichiometric solid supply rate becomes higher when the gas supply temperature is higher, the size of the particle is larger, and the initial carbon content in solid is lower.

(5) When the stoichiometric solid and gas supply rates become higher, the temperature of the bed becomes higher, the region of carbon combustion becomes

thicker, the concentration of carbon dioxide at the top of the bed becomes lower, and the concentration of carbon monoxide becomes higher.

(6) When the gas supply temperature becomes higher at a given gas supply rate, the temperature of the bed becomes higher, the region of carbon combustion becomes thinner, the concentration of carbon dioxide becomes lower, and concentration of carbon monoxide becomes higher.

(7) When the solid particle diameter becomes larger at a given gas supply rate, the temperature of the bed becomes higher, the region of carbon combustion becomes thicker, the concentration of carbon dioxide becomes lower, and the concentration of carbon monoxide becomes higher.

(8) When the initial carbon content in solid particles becomes lower at a given gas supply rate, the temperature of the bed becomes higher, the region of carbon combustion becomes thicker, the concentration of carbon dioxide becomes lower, and the concentration of carbon monoxide becomes higher.

(9) The effective thermal conductivities of solid and gas with the effects of radiation heat transfer and enhanced heat transfer due to the eddy diffusion by fluid flow are higher than those without the effects.

5.2 RECOMMENDATIONS

The Biot numbers obtained through the numerical calculation in this study ranges from 0.75 to 2.3 which are relatively high so that the error caused by the uniform temperature assumption may not be negligible. Incorporation of temperature

distribution in solid particle to the present model may make the results better but the model becomes much more complex.

Nitrogen in gas supply is assumed to be inert in the present study. On the other hand, the temperature of the most commercial moving bed combustors is sufficiently high to make nitrogen react with oxygen to produce nitrogen oxide and this product is a notorious source of pollution. The reaction of nitrogen with oxygen must be considered in the design of practical combustors.

The volume fraction of carbon monoxide in product gas is about 30%. This carbon monoxide can be consumed to carbon dioxide by additional supply of oxygen or secondary air at the top of the bed. The concentration of carbon monoxide in products can be reduced and additional heat can be obtained by this additional reaction. Present model can be made more realistic by introducing this additional reaction.

Real coal combustion involves: (a) pyrolysis in which a variety of combustible gases are released from solid to burn in gas phase; and (b) drying in which moisture is released. The present coke (or carbon char) combustion problem needs to be extended to account for such pyrolytic process, drying process, and gas phase combustion. This extended model appears suitable also for a study of biomass particle bed combustion.

Under deficient air conditions, the present model represents an idealized gasifier problem. Upon incorporation of the appropriate chemistry, accounting for the chemical reactions in which carbon, water, hydrogen, and hydrocarbons are involved,

the present model can be extended to a coal gasification problem. Gas supplied to the coal gasifier usually contains deficient air (or oxygen) and steam.

By some modification, the present model can also be adapted for drying of moist inert particle beds and catalytic combustion of low BTU gaseous fuels in a bed of inert particles whose surface serves as the site of reaction.

REFERENCES

1. Winslow, A. M., "Numerical Model of Coal Gasification in a Packed Bed," *16th Symp. (International) on Combustion*, The Combustion Institute, Pittsburgh, PA, pp. 503-514, 1976.

2. Amundson, N. R. and L. E. Arri, "Char Gasification in a Countercurrent Reactor," *AIChE Journal*, Vol. 24, No. 1, pp. 87-101, 1978.

3. Yoon, H., J. Wei, and M. M. Denn, "A Model for Moving-Bed Coal Gasification Reactors," *AIChE Journal*, Vol. 24, No. 5, pp. 885-903, 1978.

4. Cho, Y. S. and B. Joseph, "Heterogeneous Model for Moving-Bed Coal Gasification Reactors," *Ind. Eng. Chem. Process Des. Dev.*, Vol. 20, No. 2, pp. 314-318, 1981.

5. Gibbs, R. T. and L. S. Soo, "Heat Transfer and Reaction Rate in Steam Gasification of Coal," *ASME Paper*, 80-WA/HT-14, 1980.

6. Caram, H. S. and C. Fuentes, "Simplified Model for a Countercurrent Char Gasifier, "*Ind. Eng. Chem. Fundam.*, Vol. 21, No. 4, pp. 464-472, 1982.

7. Bhattacharya, A., L. Salam, M. P. Duduković, and B. Joseph, "Experimental and Modeling Studies in Fixed-Bed Char Gasification," *Ind. Eng. Chem. Process Des. Dev.*, Vol. 25, No. 4, pp. 988-996, 1986.

8. Nicholls, P. and M. G. Eilers, "The Principles of Underfeed Combustion and the Effect of Preheated Air on Overfeed and Underfeed Fuel Beds," *Trans. ASME*, Vol. 56, No. 5, pp. 321-336, 1934.

9. Mayers, M. A., "Temperature and Combustion Rates in Fuel Beds," *Trans. ASME*, Vol. 59, pp. 279-288, 1937.

10. Kuwata, M., T. J. Kuo, and R. H. Essenhigh, "Burning Rates and Operational Limits in a Solid-Fuel Bed," *Proceeding of the 4th National Incinerator Conference*, ASME, pp. 272-287, 1970.

11. Eapen, T., R. Blackadar, and R. H. Essenhigh, "Kinetics of Gasification in a Combustion Pot : A Comparison of Theory and Experiment," *16th Symp. (International) on Combustion*, The Combustion Institute, Pittsburgh, PA, pp. 515-522, 1977.

12. Barriga, A. and R. H. Essenhigh, "A Mathematical Model of a Combustion Pot : Comparison of Theory and Experiment," *ASME Paper*, 80-WA/HT-32, 1980.

13. Lawson, D. A. and J. Norbury, "Porous Medium Combustion," *Numerical Methods in Heat Transfer*, John Wiley and Sons, Vol. III, pp. 173-193, 1985.

14. Bodle, W. W. and F. C. Schora, "Coal Gasification Technology Overview," in *Advances in Coal Utilization Technology* (Symposium Paper), Institute of Gas Technology, Chicago, Illinois, (Presented May 14-18, 1979 at Louisville, Kentucky), pp. 11-34, 1979.

15. Smoot, L. D. and P. J. Smith, *Coal Combustion and Gasification*, Plenum Press, New York, N. Y., pp. 184, 1985.

16. Thring, M. W., "Physics of fuel bed combustion," *Fuel*, Vol. 31, pp. 355, 1952.

17. Arthur, J. R., "Reactions between Carbon and Oxygen," *Transactions of the Faraday Society*, Vol. 47, pp. 164-178, 1951.

18. Levenspiel, O., *Chemical Reaction Engineering*, John Wiley and Sons, New York, N. Y., 1972.

19. Gadsby, J., F. J. Long, P. Sleightholm, and K. W. Sykes, "The Mechanism of the Carbon Dioxide-Carbon Reaction," *Royal Society, Proceedings Ser. A.*, Vol. 193, pp. 357-376, 1948.

20. Walker, P. L., Jr., F. Rusinko, Jr., and L. G. Austin, "Gas Reactions of Carbon," *Advances in Catalysis*, Vol. XI, pp. 133, 1959.

21. Richards, M. B. and S. S. Penner, "Oxidation of a Porous Graphite Cylinder with Airflow Through a Coaxial Hole," *Dynamics of Deflagrations and Reactive Systems: Heterogeneous Combustion, Progress in Astronautics and Aeronautics*, Vol. 132, pp. 223-247, 1991.

22. Dixon-Lewis, G. and D. J. Williams, "The Oxidation of Hydrogen and Carbon Monoxide," *Comprehensive Chemical Kinetics*, edited by C. H. Bamford and C. F. H. Tipper, Elsevier Scientific, Amsterdam, The Netherlands, Vol. 17, pp. 1-248, 1977.

23. Howard, J. B., G. C. Williams, and D. H. Fine, "Kinetics of Carbon Monoxide Oxidation in Postflame Gases," *14th Symp. (International) on Combustion*, The Combustion Institute, Pittsburgh, PA, pp. 975-986, 1973.

24. Dryer F. L. and I. Glassman, "High-Temperature Oxidation of CO and CH_4," *14th Symp. (International) on Combustion*, The Combustion Institute, Pittsburgh, PA, pp. 987-1003, 1973.

25. Hottel, H. C., G. C. Williams, N. M. Nerheim, and G. R. Schneider, "Kinetic Studies in Stirred Reactors: Combustion of Carbon Monoxide and Propane," *10th Symp. (International) on Combustion*, The Combustion Institute, Pittsburgh, PA, pp. 111-121, 1965.

26. Wicks, C. E. and F. E. Block, "Thermodynamic Properties of 65 Elements-Their Oxides, Halides, Carbides, and Nitrides," *Bulletin 605, Bureau of Mines*, U.S. Government Printing Office, Washington DC, 1963.

27. Gupta, A. S. and G. Thodos, "Direct Analogy between Mass and Heat Transfer to Beds of Spheres," *AIChE Journal*, Vol. 9, No. 6, pp. 751-754, 1963.

28. Malling, G. F. and Thodos G., "Analogy between Mass and Heat Transfer in Beds of Spheres : Contributions due to End Effects," *Int. J. Heat and Mass Transfer*, Vol. 10, pp. 489-498, 1967.

29 Kunii, D. and J. M. Smith, "Heat Transfer Characteristics of Porous Rocks," *AIChE Journal,* Vol. 6, No. 1, pp. 71-78, 1960.

30. Yagi, S., D. Kunii, and N. Wakao, "Studies on Axial Effective Thermal Conductivities in packed Beds," *AIChE Journal,* Vol. 6, No. 4, pp. 543-546, 1960.

31. Wakao, N. and K. Kato, "Effective Thermal Conductivity of Packed Beds," *Journal of Chemical Engineering of Japan,* Vol. 2, No. 1, pp. 24-33, 1968.

32. Wakao, N. and S. Kaguei, *Heat and Mass Transfer in packed Beds*, Gordon and Breach, New York, NY, 1982.

33. Wen, C. Y. and Y. H. Yu, "Mechanics of Fluidization," *Chemical Engineering Progress Symposium Series*, Vol. 62, No. 62, pp. 100-111, 1966.

34. Wen, C. Y. and Y. H. Yu, "A Generalized Method for Predicting the Minimum Fluidization Velocity," *AIChE Journal,* Vol. 12, No. 3, pp. 610-612, 1966.

35. Saxena, S. C. and G. J. Vogel, "The Measurement of Incipient Fluidisation Velocities in a Bed of Coarse Dolomite at Temperature and Pressure," *Transactions Institute Chemical Engineering*, Vol. 55, pp. 184-189, 1977.

36. Botterill, J. S. M., Y. Teoman, and K. R. Yüregir, "The Effect of Operating Temperature on the Velocity of Minimum Fluidization, Bed Voidage and General Behavior," *Power Technology*, Vol. 32, pp. 101-110, 1982.

37. Rose, J. W. and J. R. Cooper, *Technical Data on Fuel*, John Wiley and sons, New York, N.Y., 1977.

38. Reid, R. C. et al., *The Properties of Gases and Liquids*, McGraw Hill, 4th Ed. New York, N.Y., 1987.

39. Van Wylen, G. J. and R. E. Sonntag, *Fundamentals of Classical Thermodynamics*, 3rd Ed., John Wiley and Sons, New York, N. Y., 1985.

40. Chung, T. H., M. Ajlan, L. L. Lee, and K. E. Starling, "Generalized Multiparameter Correlation for Nonpolar and Polar Fluid Transport Properties," *Ind. Eng. Chem. Res.*, Vol. 27, pp. 671-679, 1988.

41. Chung, T. H., L. L. Lee, and K. E. Starling, "Application of Kinetic Gas Theories and Multiparameter Correlation for Prediction of Dilute Gas Viscosity and Thermal Conductivity," *Ind. Eng. Chem.Fundam.*, Vol. 23, pp. 8-13, 1984.

42. Fuller, E. N., K. Ensley, and J. C. Giddings, "Diffusion of Halogenated Hydrocarbons in Helium. The Effect of Structure on Collision Cross Sections," *J. Phys. Chem.*, Vol. 75, pp. 3679, 1969.

43. Essenhigh R. H., "Coal Combustion," *Coal conversion Technology*, edited by C. Y. Wen and E. S. Lee, Addison-Wesley, Reading, Massachusetts, 1979.

APPENDIX

APPENDIX

FORTRAN PROGRAM FOR NUMERICAL CALCULATION

CFP.FOR

```
      IMPLICIT REAL *8 (A-H,O-Z)
      IMPLICIT INTEGER *4 (I-N)
      PARAMETER ( NMAX  = 501   )
      PARAMETER ( N     = 500   )
C      PARAMETER ( NMAX  = 1001   )
C      PARAMETER ( N     = 1000   )
      PARAMETER ( NKMAX = 5      )
      PARAMETER ( ITMAX = 2000   )
      PARAMETER ( EPS   = 1.0D-7 )
      SAVE
```

CFD.FOR

```
C INDEPENDENT VARIABLE
      COMMON XI(NMAX),XXX(NMAX),XXI(NMAX)
C DEPENDENT VARIABLES
      COMMON ROG(NMAX),ROS(NMAX)
      COMMON THEG(NMAX),THEGG(NMAX),THEGOLD(NMAX),TG(NMAX),TGG(NMAX),
     *       THES(NMAX),THESOLD(NMAX),TS(NMAX),TSS(NMAX)
      COMMON THESOL(NMAX),THEGOL(NMAX)
      COMMON DTHESH,DTHEGH
      COMMON COMCOL(NMAX),YO2OL(NMAX),YCO2OLD(NMAX),YCOOLD(NMAX)
      COMMON DCOMCMM,DYO2MM,DYCO2M,KCO2,DYCOM,KCO
      COMMON YO2(NMAX),YO2OLD(NMAX),YN2(NMAX),YCO2(NMAX),YCO(NMAX),
     *       YH2O(NMAX),
     *       YY(NKMAX,NMAX),Y(NKMAX,NMAX),XX(NKMAX,NMAX),YYM(NMAX)
      COMMON COMC(NMAX),COMCOLD(NMAX),COMA(NMAX),UG(NMAX),
     *       TROG(NMAX),TROS(NMAX)
C GEOMETRY
      COMMON D,VL,VL0,XVL0,XVL0P,POR,PORS,AVD,RD
      COMMON DXI(NMAX)
C FLOW
      COMMON ROSIN,ROGIN,TROIN,REGIN,RES
      COMMON REG(NMAX),VI(NKMAX,NMAX),VIG(NMAX),TVIG(NMAX),
     *       VIO2(NMAX),VIN2(NMAX),VICO2(NMAX),VICO(NMAX),VIH2O(NMAX)
C ENERGY CONSERVATION
      COMMON TSIN,TGIN,RT,PRGIN,CB1,CB2
      COMMON CP(NKMAX,NMAX),VK(NKMAX,NMAX),AA(NKMAX,NKMAX,NMAX),
     *       CPS(NMAX),TCPS(NMAX),VKS(NMAX),
     *       CPO2(NMAX),CPN2(NMAX),CPCO2(NMAX),CPCO(NMAX),CPH2O(NMAX),
     *       VKO2(NMAX),VKN2(NMAX),VKCO2(NMAX),VKCO(NMAX),VKH2O(NMAX),
     *       CPG(NMAX),TCPG(NMAX),VKG(NMAX),TKG(NMAX),
     *       PRG(NMAX),VNUG(NMAX),BI(NMAX),QS(NMAX),QG(NMAX),
     *       RK(NMAX),PSI(NMAX),TAVE(NMAX),HRS(NMAX),
     *       EKG(NMAX),EKS(NMAX),EKGG(NMAX),EKSS(NMAX),EKT(NMAX),
     *       TKEG(NMAX),TKES(NMAX)
      COMMON CS1(NMAX),CS2(NMAX),CS3(NMAX),CS4(NMAX),CS5(NMAX),
     *       CG1(NMAX),CG2(NMAX),CG3(NMAX),CG4(NMAX),CG5(NMAX)
C SPECIES CONSERVATION
      COMMON YO2IN,YN2IN,YH2OIN,REHU,VMC,VMO2,VMN2,VMCO2,VMCO,VMH2O,
     *       TMC,TMO2,TMN2,TMCO2,TMCO,TMH2O,SCO2IN,SIGM,EOK,
     *       PG,PH2O,PO2,PN2
      COMMON VMJ(NKMAX),VMG(NMAX),TMJ(NKMAX),TMG(NMAX),
     *       TST(NMAX),OMD(NMAX),
     *       DI(NKMAX,NKMAX,NMAX),DJM(NKMAX,NMAX),TDJM(NKMAX,NMAX),
     *       DO2(NMAX),DN2(NMAX),DCO2(NMAX),DCO(NMAX),DH2O(NMAX),
     *       TDO2(NMAX),TDN2(NMAX),TDCO2(NMAX),TDCO(NMAX),TDH2O(NMAX),
     *       TDEO2(NMAX),TDECO2(NMAX),
     *       W1(NMAX),W2(NMAX),W3(NMAX),WK3(NMAX),WC(NMAX),WA(NMAX),
     *       WO2(NMAX),WN2(NMAX),WCO2(NMAX),WCO(NMAX),WH2O(NMAX),
     *       CONJ1(NKMAX,NMAX),CONJ2(NKMAX,NMAX),CONJ3(NKMAX,NMAX),
     *       CONJ4(NKMAX,NMAX),CONJ5(NKMAX,NMAX),CB(NKMAX),
     *       SCO2(NMAX),SCCO2(NMAX),SHO2(NMAX),SHCO2(NMAX)
C SOLID SPECIES CONSERVATION
      COMMON OMCIN,OMAIN,CONCA
```

```
C CARBON COMBUSTION
      COMMON DCD0,R,VK01,E1,DA1,AR1,
     *       VK021,E21,DA21,AR21,VK022,E22,DA22,AR22,
     *       VK023,E23,DA23,AR23,VK03,E3,DA3,AR3,VA,VB,VC,CFCO
      COMMON DH1A(NMAX),DH1B(NMAX),DH2(NMAX),DH3(NMAX),
     *       H1A(NMAX),H1B(NMAX),H2(NMAX),H3(NMAX),FCO(NMAX),
     *       WCONA(NMAX),WCONB(NMAX),DCD(NMAX),
     *       WCON1(NMAX),WCON2(NMAX),WCON3(NMAX),
     *       WCON4(NMAX),WCON5(NMAX),WCON6(NMAX),WCON7(NMAX),
     *       WMASS1(NMAX),WDIFF1(NMAX),WCOMB1(NMAX),
     *       WMASS2(NMAX),WDIFF2(NMAX),WCOMB2(NMAX),
     *       WW1(NMAX),WW2(NMAX),WW3(NMAX),WWK3(NMAX)
C CONTINUITY
      COMMON P,PP,PPP,CCON
      COMMON SOCON(NMAX)
C NUMERICAL
      COMMON ITER,NKIND
      COMMON DTHEGM,DTHESM,DCOMCM,DYO2M,KCM,KO2M,KTSH,KTGH,
     *       KTS,KTG,KC,KO2
C       COMMON VINT1(NMAX),VINT2(NMAX),VINT3(NMAX),VINT4(NMAX)
      COMMON A1(NMAX),B1(NMAX),C1(NMAX),F1(NMAX),
     *       A2(NMAX),B2(NMAX),C2(NMAX),F2(NMAX),
     *       AM(NMAX),BM(NMAX),CM(NMAX),FM(NMAX)
C VALUES USED TO FIND PROPERTIES OF GAS SPECIES
      COMMON SIGVJ(NKMAX),VMIJ(NKMAX,NKMAX)
      COMMON TC(NKMAX),VVC(NKMAX),OM(NKMAX),DMV(NKMAX),BETA(NKMAX)
      COMMON TR(NKMAX,NMAX),TSTAR(NKMAX,NMAX),COMV(NKMAX,NMAX),
     *       DDMV(NKMAX,NMAX),FC(NKMAX,NMAX),Z(NKMAX,NMAX),
     *       CV(NKMAX,NMAX),ALP(NKMAX,NMAX),PSAI(NKMAX,NMAX)
```

CF.FOR

```
      PROGRAM CF
C COMBUSTION OF SPHERICAL CARBON PARTICLES IN A MOVING BED    1/ 7/93
C EFFECTIVE THERMAL CONDUCTIVITY FOR SOLID AND GAS PHASE      2/19/93
C SOLID ENTRANCE AND EXIT ; CONVECTION BOUNDARY               4/12/93
C GAS INLET ; CONSTANT TEMPERATURE                            5/23/93
C GAS EXIT ; ZERO GRADIENT BOUNDARY                           7/17/93
C SUBROUTINE IS TRIDIA
C HEAT TRANSFER COEFFICIENT BY MALLING & THODOS
C CONVECTION TERM BY UPWIND METHOD
C ALL PROPERTIES OF GAS ARE TEMPERATURE DEPENDENT
C ALL PROPERTIES OF SOLID ARE TEMPERATURE DEPENDENT EXCEPT DENSITY
      INCLUDE 'CFP.FOR'
      INCLUDE 'CFD.FOR'
      OPEN(5,FILE='CF.DAT',STATUS='OLD')
      OPEN(6,FILE='CF.OUT',STATUS='UNKNOWN')
      OPEN(7,FILE='CFG.OUT',STATUS='UNKNOWN')
C      OPEN(8,FILE='CFA.OUT',STATUS='UNKNOWN')
C INPUT AND CONSTANT KNOWN PARAMETERS
      CALL INPUT
C INITIALIZATION AND GUESSING
      CALL INIT
C ***************************************************************
C ITERATION BEGIN
      DO 5 ITER=1,ITMAX
      WRITE(*,*) '    ITER = ',ITER
      DO 6 K=1,NMAX
         THESOLD(K)=THES(K)
         THEGOLD(K)=THEG(K)
         COMCOLD(K)=COMC(K)
         YO2OLD(K)=YO2(K)
         YCO2OLD(K)=YCO2(K)
         YCOOLD(K)=YCO(K)
6     CONTINUE
C CALCULATTE PROPERTIES OF SOLID AND GAS
      CALL PROP
C CALCULATE DIMENSIONLESS PARAMETERS
      CALL PARA
C EQUATION OF STATE TO FIND DENSITY OF GAS
      CALL STATE
C CALCULATE GAS REYNOLDS NUMBER BY GAS CONTINUITY
      CALL CONT
C CALCULATE HEAT AND MASS TRANSFER COEFFICIENT
      CALL HMTR
C ****************************** SPECIES EQUATIONS
C CALCULATE CONSTANTS FOR SPECIES CONSERVATION
      CALL MTJ
C ****************** GAS SPECIES
C CALCULATE O2 CONCENTRATION IN GAS
      CALL MTO2
C CALCULATE CO2 CONCENTRATION IN GAS
      CALL MTCO2
C CALCULATE CO CONCENTRATION IN GAS
      CALL MTCO
C CALCULATE N2 CONCENTRATION IN GAS
      CALL MTN2
C CALCULATE H2O CONCENTRATION IN GAS
      CALL MTH2O
C CALCULATE MODIFIED MASS LOSS OR GENERATION OF GAS SPECIES
      CALL W123
```

```
C ****************** SOLID SPECIES
C CALCULATE CARBON CONCENTRATION IN GAS
      CALL MTCA
C CALCULATE ASH CONCENTRATION IN GAS
      CALL MTAS
C ************************************************
C ****************************** ENERGY EQUATIONS
C CALCULATE EFFECTIVE THERMAL CONDUCTIVITY
      CALL EFFK
C CALCULATE TEMPERATURE DISTRIBUTION IN GAS PHASE
      CALL HTGAS
C CALCULATE TEMPERATURE DISTRIBUTION IN SOLID PHASE
C WITH CONVECTIVE BOUNDARY CONDITION FOR SOLID AT X=L
      CALL HTSOL
C ************************************************
C CHECK CONVERGENCE
      CALL DAX(THESOLD,THES,DTHESM,KTS)
      CALL DAX(THEGOLD,THEG,DTHEGM,KTG)
      CALL DAX(COMCOLD,COMC,DCOMCM,KC)
      CALL DAX(YO2OLD,YO2,DYO2M,KO2)
      CALL DAX(YCO2OLD,YCO2,DYCO2M,KCO2)
      CALL DAX(YCOOLD,YCO,DYCOM,KCO)
      NH=N/2
      WRITE(*,*) 'COMC(1)=',COMC(1),'YCO2(NMAX)=',YCO2(NMAX)
      WRITE(*,211)
      WRITE(*,212) THES(NH),THEG(NH),YO2(NH),YCO2(NH),YCO(NH)
211   FORMAT(4X,'THES',8X,'THEG',8X,'YO2',9X,'YCO2',9X,'YCO')
212   FORMAT(2F10.5,3D13.5)
      WRITE(*,111) KTS,KTG,KC,KO2,KCO2
      WRITE(*,112) DTHESM,DTHEGM,DCOMCM,DYO2M,DYCO2M
111   FORMAT(1X,'DTHESM(',I4,')',1X,'DTHEGM(',I4,')',1X,
     *       'DCOMCM(',I4,')',1X,'DYO2M(',I4,')',1X,'DYCO2M(',I4,')')
112   FORMAT(5D13.5)
      IF(DTHESM.LT.EPS.AND.DTHEGM.LT.EPS.AND.DCOMCM.LT.EPS) GO TO 8
5     CONTINUE
8     CONTINUE
C ************************************************************
C PRINT OUT THE RESULTS
      CALL OUTPUT
C CHECK TEMERATURE DEPENDENT PROPERTIES
C      CALL CHECK
C ********************************************
      STOP
      END
```

```
C ************************** SUBROUTINE
C INPUT AND CONSTANT KNOWN PARAMETERS
C AND SOME DIMENSIONLESS PARAMETERS
      SUBROUTINE INPUT
      INCLUDE 'CFP.FOR'
      INCLUDE 'CFD.FOR'
C INPUT
      READ(5,*) NKIND,OMCIN,OMAIN,VK021,E21,CFCO,REHU
      READ(5,*) REGIN,RES,TGIN,TSIN,D,VL,VL0
      READ(5,*) VA,VB,VC,VK03,E3
CC KNOWN OR GIVEN CONSTANT PARAMETERS
C PRESSURE(P in Pa, PP in atm, PPP in bar) AND UNIVERSAL GAS CONSTANT
      PPP=1.01325
      PP=1.0
      P=1.0132D5*PP
      R=8.314D3
C SPECIES PARAMETERS
      VMC=12.0
      VMO2=32.0
      VMN2=28.016
      VMCO2=44.01
      VMCO=28.010
      VMH2O=18.015
C INITIAL MASS FRACTION OF O2, N2, H2O
      PG=3.567D3
      PH2O=REHU*PG
      PO2=0.21*(P-PH2O)
      PN2=0.79*(P-PH2O)
      VMG(1)=(PO2*VMO2+PN2*VMN2+PH2O*VMH2O)/P
      YO2IN=PO2*VMO2/(P*VMG(1))
      YN2IN=PN2*VMN2/(P*VMG(1))
      YH2OIN=PH2O*VMH2O/(P*VMG(1))
C COMBUSTION PARAMETERS
C C + 0.5 O2 = CO
      VK01=2.013D-3
      E1=7.981D7
C C + CO2 = 2 CO
C      E21=5.4D8
      VK022=6.229D-13
      E22=-2.051D8
      VK023=156.5
      E23=1.109D8
C CO + 0.5 O2 = CO2 : REFER DATA INPUT
C SOME DIMENSIONLESS PARAMETERS ; GEOMETRIC PARAMETERS
      POR=0.26
      PORS=OMCIN
      RD=D/VL
      AVD=6.0*(1.0-POR)
C DIMENSIONLESS AXIAL LOCATION
      DO 10 K=1,NMAX
         DXI(K)=1.0/N
         XI(K)=(K-1)*DXI(K)
10    CONTINUE
      RETURN
      END
```

```
C ************************** SUBROUTINE
C INITIALIZATION AND GUESSING
      SUBROUTINE INIT
      INCLUDE 'CFP.FOR'
      INCLUDE 'CFD.FOR'
      DO 20 K=1,NMAX
         A1(K)=0.0
         B1(K)=0.0
         C1(K)=0.0
         F1(K)=0.0
         A2(K)=0.0
         B2(K)=0.0
         C2(K)=0.0
         F2(K)=0.0
         AM(K)=0.0
         BM(K)=0.0
         CM(K)=0.0
         FM(K)=0.0
         THES(K)=TSIN/TGIN
         THEG(K)=TSIN/TGIN
         YO2(K)=1.0
         YN2(K)=YN2IN/YO2IN
         YCO2(K)=0.0
         YCO(K)=0.0
         YH2O(K)=YH2OIN/YO2IN
         COMC(K)=1.0
         COMA(K)=1.0
         UG(K)=1.0
         TROG(K)=1.0
         TROS(K)=1.0
         WMASS1(K)=0.0
         WDIFF1(K)=0.0
         WCOMB1(K)=0.0
         WMASS2(K)=0.0
         WDIFF2(K)=0.0
         WCOMB2(K)=0.0
         W1(K)=0.0
         W2(K)=0.0
         W3(K)=0.0
         WC(K)=0.0
         WA(K)=0.0
         WO2(K)=0.0
         WN2(K)=0.0
         WCO2(K)=0.0
         WCO(K)=0.0
         WH2O(K)=0.0
         QS(K)=0.0
         QG(K)=0.0
20    CONTINUE
      XVL0=(VL-VL0)/VL
      XVL0P=XVL0+0.1
      DO 30 K=1,NMAX
         IF(XI(K).GT.XVL0.AND.XI(K).LT.XVL0P) GO TO 40
         THES(K)=5.0
         THEG(K)=5.0
30    CONTINUE
40    CONTINUE
      RETURN
      END
```

```
C ************************** SUBROUTINE
C CALCULATE PROPERTIES OF SOLID AND GAS
C PROPERTIES OF SOLID ARE CONSTANT EXCEPT VARIABLE DENSITY
C OF SOLID AT EACH LOCATION OF BED
C PROPERTIES OF GAS ARE ALL TEMPERATURE DEPENDENT
      SUBROUTINE PROP
      INCLUDE 'CFP.FOR'
      INCLUDE 'CFD.FOR'
C ***************** PROPERTIES OF SOLID
C CONSTANT PROPERTIES OF SOLID
C      ROSIN=1.5D3
      ROSIN=1.75D3
C VARIABLE PROPERTIES OF SOLID
      DO 1 K=1,NMAX
         TSS(K)=THES(K)*TGIN-273.15
C SPECIFIC HEAT OF GRAPHITE ; ROSE AND COOPER
         CPS(K)=(0.75+29.3D-5*TSS(K))*1000.0
C THERMAL CONDUCTIVITY OF COAL ; ROSE AND COOPER
         VKS(K)=(130.0+0.54*TSS(K)+0.00063*(TSS(K)**2))/1000.0
         VKS(K)=VKS(K)*(COMC(K)*OMCIN+COMA(K)*OMAIN)
1     CONTINUE
C ***************** PROPERTIES OF GAS
CC KNOWN CONSTANTS AND PROPERTIES OF EACH GAS SPECIES
      CALL PROPGS
CC PROPERTIES OF GAS MIXTURE
      DO 5 K=1,NMAX
C Y(I,K) : DIMENSIONLESS MASS FRACTION
         Y(1,K)=YO2(K)
         Y(2,K)=YN2(K)
         Y(3,K)=YCO2(K)
         Y(4,K)=YCO(K)
         Y(5,K)=YH2O(K)
C YY(I,K) : MASS FRACTION
      DO 10 J=1,NKIND
         YY(J,K)=Y(J,K)*YO2IN
10    CONTINUE
C VMG(K) : MIXTURE MOLAR MASS
         SUMM=0.0
         DO 510 J=1,NKIND
            SUMM=SUMM+YY(J,K)/VMJ(J)
510      CONTINUE
         VMG(K)=1.0/SUMM
C XX(I,J) : MOLE FRACTION
         DO 520 J=1,NKIND
            XX(J,K)=YY(J,K)*VMG(K)/VMJ(J)
520      CONTINUE
5     CONTINUE
C GAS DENSITY AT THE BOTTOM OF THE BED BY EQUATION OF STATE
      ROGIN=P*VMG(1)/(R*TGIN)
C SPECIFIC HEAT
      DO 100 K=1,NMAX
         SUMCP=0.0
         DO 90 J=1,NKIND
            SUMCP=SUMCP+YY(J,K)*CP(J,K)
90       CONTINUE
         CPG(K)=SUMCP
100    CONTINUE
```

```
C AA(I,J,K)
      DO 110 K=1,NMAX
         DO 120 I=1,NKIND
            DO 130 J=1,NKIND
               AA1=SQRT(VI(I,K)/VI(J,K))
               AA2=(VMJ(J)/VMJ(I))**0.25
               AA3=1.0+VMJ(I)/VMJ(J)
               AA(I,J,K)=((1.0+AA1*AA2)**2)/SQRT(8.0*AA3)
130         CONTINUE
120      CONTINUE
110   CONTINUE
C DYNAMIC VISCOSITY
      DO 140 K=1,NMAX
         SUMVI1=0.0
         DO 150 I=1,NKIND
            SUMVI2=0.0
            DO 160 J=1,NKIND
               SUMVI2=SUMVI2+XX(J,K)*AA(I,J,K)
160         CONTINUE
            SUMVI1=SUMVI1+(XX(I,K)*VI(I,K))/SUMVI2
150      CONTINUE
         VIG(K)=SUMVI1
140   CONTINUE
C THERMAL CONDUCTIVITY
      DO 170 K=1,NMAX
         SUMVK1=0.0
         DO 180 I=1,NKIND
            SUMVK2=0.0
            DO 190 J=1,NKIND
               SUMVK2=SUMVK2+XX(J,K)*AA(I,J,K)
190         CONTINUE
            SUMVK1=SUMVK1+(XX(I,K)*VK(I,K))/SUMVK2
180      CONTINUE
         VKG(K)=SUMVK1
170   CONTINUE
C MIXTURE DIFFUSION COEFFICIENT
      DO 50 K=1,NMAX
        DO 60 I=1,NKIND
            SUM=0.0
            DO 70 J=1,NKIND
               IF(I.EQ.J) GO TO 70
               DSUM=XX(J,K)/DI(I,J,K)
               SUM=SUM+DSUM
70          CONTINUE
         DJM(I,K)=(1.0-XX(I,K))/SUM
60       CONTINUE
50    CONTINUE
      DO 410 K=1,NMAX
         DO2(K)=DJM(1,K)
         DN2(K)=DJM(2,K)
         DCO2(K)=DJM(3,K)
         DCO(K)=DJM(4,K)
         DH2O(K)=DJM(5,K)
410   CONTINUE
      RETURN
      END
```

```
C ************************** SUBROUTINE
C KNOWN CONSTANTS AND PROPERTIES OF EACH GAS SPECIES
      SUBROUTINE PROPGS
      INCLUDE 'CFP.FOR'
      INCLUDE 'CFD.FOR'
C CONSTANTS FOR VISCOSITY AND THERMAL CONDUCTIVITY CALCULATION
      TC(1)=154.6
      TC(2)=126.2
      TC(3)=304.1
      TC(4)=132.9
      TC(5)=647.3
      VVC(1)=73.4
      VVC(2)=89.8
      VVC(3)=93.9
      VVC(4)=93.2
      VVC(5)=57.1
      OM(1)=0.025
      OM(2)=0.039
      OM(3)=0.239
      OM(4)=0.066
      OM(5)=0.344
      DMV(1)=0.0
      DMV(2)=0.0
      DMV(3)=0.0
      DMV(4)=0.1
      DMV(5)=1.8
C MOLAR MASS OF EACH GAS SPECIES
      VMJ(1)=VMO2
      VMJ(2)=VMN2
      VMJ(3)=VMCO2
      VMJ(4)=VMCO
      VMJ(5)=VMH2O
      DO 10 K=1,NMAX
C TG(K) : DIMENSIONAL TEMPERATURE OF GAS
         TG(K)=TGIN*THEG(K)
C The above line is switched to the next line to investigate
C the case of constant properties of gas.
C         tg(k)=tgin
10    CONTINUE
C ************************** SPECIFIC HEAT
C DIMENSIONAL TEMPERATURE FOR SPECIFIC HEAT CALCULATION
      DO 100 K=1,NMAX
         TGG(K)=TG(K)/100.0
100   CONTINUE
C SPECIFIC HEAT IN J/kgK BY WYLEN AND SONNTAG
      DO 110 K=1,NMAX
      CPO2(K) =(37.432+0.020102*(TGG(K)**1.5)-178.57*(TGG(K)**(-1.5))
     *          +236.88*(TGG(K)**(-2.0)))*1000.0/VMO2
      CPN2(K) =(39.060-512.79*(TGG(K)**(-1.5))+1072.70*(TGG(K)**(-2))
     *          -820.40*(TGG(K)**(-3)))*1000.0/VMN2
      CPCO2(K)=(-3.7357+30.529*(TGG(K)**0.5)-4.1034*TGG(K)
     *          +0.024198*(TGG(K)**2))*1000.0/VMCO2
      CPCO(K) =(69.145-0.70463*(TGG(K)**0.75)-200.77*TGG(K)**(-0.5)
     *          +176.76*TGG(K)**(-0.75))*1000.0/VMCO
      CPH2O(K)=(143.05-183.54*(TGG(K)**0.25)+82.751*(TGG(K)**0.5)
     *          -3.6989*TGG(K))*1000.0/VMH2O
      CP(1,K)=CPO2(K)
      CP(2,K)=CPN2(K)
      CP(3,K)=CPCO2(K)
      CP(4,K)=CPCO(K)
      CP(5,K)=CPH2O(K)
110   CONTINUE
```

```
C ************************** DYNAMIC VISCOSITY
C CALCULATE VISCOSITY BY REID ET AL.
C DIMENSIONLESS TEMPERATURE AND COMV
      DO 210 K=1,NMAX
         DO 220 J=1,NKIND
            TR(J,K)=TG(K)/TC(J)
            TSTAR(J,K)=1.2593*TR(J,K)
            COMV(J,K)=1.16145*TSTAR(J,K)**(-0.14874)
     *              +0.52487*DEXP(-0.77320*TSTAR(J,K))
     *              +2.16178*DEXP(-2.43787*TSTAR(J,K))
220      CONTINUE
210   CONTINUE
C DIMENSIONLESS DIPOLE MOMENT AND FC
      DO 230 K=1,NMAX
         DO 240 J=1,NKIND
            DDMV(J,K)=131.3*DMV(J)/((VVC(J)*TC(J))**0.5)
            FC(J,K)=1.0-0.2756*OM(J)+0.059035*(DDMV(J,K)**4)
240      CONTINUE
230   CONTINUE
C DYNAMIC VISCOSITY IN Pa s
      DO 250 K=1,NMAX
         DO 260 J=1,NKIND
            VI(J,K)=4.0785D-6*FC(J,K)*(VMJ(J)*TG(K))**0.5/
     *           (VVC(J)**(2.0/3.0)*COMV(J,K))
260      CONTINUE
         VIO2(K)=VI(1,K)
         VIN2(K)=VI(2,K)
         VICO2(K)=VI(3,K)
         VICO(K)=VI(4,K)
         VIH2O(K)=VI(5,K)
250   CONTINUE
C ************************** THERMAL CONDUCTIVITY
C CALCULATE THERMAL CONDUCTIVITY BY REID ET AL.
C BETA
      DO 310 J=1,NKIND
         BETA(J)=0.7862-0.7109*OM(J)+1.3168*(OM(J)**2)
310   CONTINUE
C Z, CV, ALPHA, AND PSAI
      DO 320 K=1,NMAX
         DO 330 J=1,NKIND
            Z(J,K)=2.0+10.5*TR(J,K)**2
            CV(J,K)=CP(J,K)*VMJ(J)-R
            ALP(J,K)=CV(J,K)/R-1.5
            PSAI(J,K)=1.0+ALP(J,K)*((0.215+0.28288*ALP(J,K)-1.061
     *              *BETA(J)+0.26665*Z(J,K))/(0.6366+BETA(J)
     *              *Z(J,K)+1.061*ALP(J,K)*BETA(J)))
330      CONTINUE
320   CONTINUE
C THERMAL CONDUCTIVITY IN W/mK
      DO 340 K=1,NMAX
         DO 350 J=1,NKIND
            VK(J,K)=3.75*R*VI(J,K)*PSAI(J,K)/VMJ(J)
350      CONTINUE
         VKO2(K)=VK(1,K)
         VKN2(K)=VK(2,K)
         VKCO2(K)=VK(3,K)
         VKCO(K)=VK(4,K)
         VKH2O(K)=VK(5,K)
340   CONTINUE
```

```
C ************************** BINARY DIFFUSION COEFFICIENT
C CALCULATE BINARY DIFFUSION COEFFICIENT BY REID ET AL.
C CONSTANTS FROM TABLE 11-1 IN REID ET AL.
      SIGVJ(1)=16.3
      SIGVJ(2)=18.5
      SIGVJ(3)=26.9
      SIGVJ(4)=18.0
      SIGVJ(5)=13.1
C BINARY DIFFUSION COEFFICIENT
      DO 440 K=1,NMAX
         DO 450 J=1,NKIND
            DO 460 I=1,NKIND
            IF(I.EQ.J) GO TO 460
            VMIJ(I,J)=2.0/(1.0/VMJ(I)+1.0/VMJ(J))
            DI(I,J,K)=1.43D-7*(TG(K)**1.75)/(PPP*(VMIJ(I,J)**0.5)
     *                 *(SIGVJ(I)**(1.0/3.0)+SIGVJ(J)**(1.0/3.0))**2)
460         CONTINUE
450      CONTINUE
440   CONTINUE
      RETURN
      END
```

```
C ************************** SUBROUTINE
C CALCULATE DIMENSIONLESS PARAMETERS
      SUBROUTINE PARA
      INCLUDE 'CFP.FOR'
      INCLUDE 'CFD.FOR'
CC CONSTANT PARAMETERS
C FLOW-RELATED PARAMETERS
      TROIN=ROSIN/ROGIN
C     REGIN is given at SUBROUTINE INPUT.
C     RES is given at SUBROUTINE INPUT.
C ENERGY CONSERVATION PARAMETERS
      RT=TSIN/TGIN
      PRGIN=VIG(1)*CPG(1)/VKG(1)
C SPECIES CONSERVATION PARAMETERS
      SCO2IN=VIG(1)/(ROGIN*DO2(1))
C DIMENSIONLESS MOLAR MASS RATIO : TMJ(J)
      DO 530 J=1,NKIND
         TMJ(J)=VMJ(J)/VMG(1)
530   CONTINUE
      TMC=VMC/VMG(1)
      TMO2=TMJ(1)
      TMN2=TMJ(2)
      TMCO2=TMJ(3)
      TMCO=TMJ(4)
      TMH2O=TMJ(5)
C COMBUSTION PARAMETERS
C C + 0.5 O2 = CO2
      DA1=VK01*P*D/(ROGIN*DO2(1))
      AR1=E1/(R*TGIN)
C C + CO2 = 2CO
      DA21=VK021*P*(D**2)*VMC/DO2(1)
      AR21=E21/(R*TGIN)
      DA22=VK022*P
      AR22=E22/(R*TGIN)
      DA23=VK023*P
      AR23=E23/(R*TGIN)
C CO + 0.5 O2 = CO2
      DA3=ROGIN**(VA+VB+VC-1.0)*VK03*D**2/
     *     (DO2(1)*VMG(1)**(VA+VB+VC-1.0))
      AR3=E3/(R*TGIN)
CC VARIABLE PARAMETERS
C ENERGY CONSERAVTION PARAMETERS
      DO 10 K=1,NMAX
         TCPS(K)=CPS(K)/CPG(1)
         TKG(K)=VKG(K)/VKG(1)
         TCPG(K)=CPG(K)/CPG(1)
10    CONTINUE
C SPECIES CONSERVATION PARAMETERS
      DO 20 K=1,NMAX
         TVIG(K)=VIG(K)/VIG(1)
         DO 30 J=1,NKIND
            TDJM(J,K)=DJM(J,K)/DJM(1,1)
30       CONTINUE
      TDO2(K)=TDJM(1,K)
      TDN2(K)=TDJM(2,K)
      TDCO2(K)=TDJM(3,K)
      TDCO(K)=TDJM(4,K)
      TDH2O(K)=TDJM(5,K)
      TDEO2(K)=TDO2(K)*(PORS**2)
      TDECO2(K)=TDCO2(K)*(PORS**2)
20    CONTINUE
```

```
C     DIMENSIONLESS MOLAR MASS RATIO : TMG(K)
      DO 540 K=1,NMAX
         TMG(K)=VMG(K)/VMG(1)
540   CONTINUE
C VARIABLE DENSITY OF SILID PARTICLES
      DO 200 K=1,NMAX
         TROS(K)=COMC(K)*OMCIN+COMA(K)*OMAIN
200   CONTINUE
      RETURN
      END
```

```
C ************************** SUBROUTINE
      SUBROUTINE STATE
      INCLUDE 'CFP.FOR'
      INCLUDE 'CFD.FOR'
C GAS DENSITY BY EQUATION OF STATE
      DO 10 K=1,NMAX
         TROG(K)=TMG(K)/THEG(K)
10    CONTINUE
      RETURN
      END
```

```
C ************************** SUBROUTINE
C SOLUTION OF GAS CONTINUITY FOR DIMENSIONLESS GAS VELOCITY
      SUBROUTINE CONT
      INCLUDE 'CFP.FOR'
      INCLUDE 'CFD.FOR'
C CALCULATE INTEGRATION
      CCON=RD*YO2IN/(REGIN*SCO2IN)
      DO 100 K=1,NMAX
         SOCON(K)=WO2(K)+WCO2(K)+WCO(K)
100   CONTINUE
C DIMENSIONLESS GAS VELOCITY
      UG(1)=1.0
      DO 200 K=2,NMAX
         UG(K)=(TROG(K-1)*UG(K-1)+CCON*DXI(K-1)
     *          *(SOCON(K-1)+SOCON(K))/2.0)/TROG(K)
200   CONTINUE
      RETURN
      END
```

```
C ************************** SUBROUTINE
C HEAT AND MASS TRANSFER COEFFICIENT IN A MOVING BED
C AND RELATED DIMENSIONLESS PARAMETERS
      SUBROUTINE HMTR
      INCLUDE 'CFP.FOR'
      INCLUDE 'CFD.FOR'
CC DEPENDENT DIMENSIONLESS PARAMETERS
      DO 30 K=1,NMAX
C GAS REYNOLDS NUMBER AND PRANTDL AND OXYGEN SCHMIDT NUMBER
         REG(K)=REGIN*TROG(K)*UG(K)/TVIG(K)
         PRG(K)=PRGIN*TVIG(K)*TCPG(K)/TKG(K)
         SCO2(K)=SCO2IN*TVIG(K)/(TROG(K)*TDO2(K))
         SCCO2(K)=SCO2IN*TVIG(K)/(TROG(K)*TDCO2(K))
30    CONTINUE
      DO 40 K=1,NMAX
C CONVECTIVE HEAT AND MASS TRANSFER COEFFICIENT
      VNUG(K)=0.539*(REG(K)**0.563)*(PRG(K)**(1.0/3.0))/(POR**1.19)
      SHO2(K)=0.539*(REG(K)**0.563)*(SCO2(K)**(1.0/3.0))/(POR**1.19)
      SHCO2(K)=0.539*(REG(K)**0.563)*(SCCO2(K)**(1.0/3.0))/(POR**1.19)
40    CONTINUE
      RETURN
      END
```

```
C ************************** SUBROUTINE
C EFFECTIVE THERMAL CONDUCTIVITY OF SOLID AND GAS,
C EHTHALPY OF REACTION, AND RELATED DIMENSIONLESS PARAMETERS
      SUBROUTINE EFFK
      INCLUDE 'CFP.FOR'
      INCLUDE 'CFD.FOR'
C SOME CONSTANTS FOR EFFECTIVE THERMAL CONDUCTIVITY
      BET=0.894
      GAM=2.0/3.0
      SIG=5.729D-8
      TDIF=0.95
      DELTA=0.5
      DO 50 K=1,NMAX
         RK(K)=VKS(K)/VKG(K)
50    CONTINUE
      DO 100 K=1,NMAX
      PSI(K)=0.072*(1.0-1.0/RK(K))**2/(LOG(RK(K)-0.925*(RK(K)-1.0))-
     *       0.075*(1.0-1.0/RK(K)))-2.0/(3.0*RK(K))
100   CONTINUE
      DO 150 K=1,NMAX
C EFFECTIVE THERMAL CONDUCTIVITY OF SOLID
         TS(K)=THES(K)*TGIN
         HRS(K)=8.0*SIG*(TS(K)**3)/((2.0/TDIF)-0.264)
         EKS(K)=VKG(K)*BET*(1.0-POR)/(1.0/(1.0/PSI(K)+D*HRS(K)/VKG(K))+
     *          GAM/RK(K))
C EFFECTIVE THERMAL CONDUCTIVITY OF GAS
         EKG(K)=VKG(K)*(POR+DELTA*REG(K)*PRG(K))
C The above three lines is switched to the next two lines
C to investigate the case of constant thermal conductivity
C in stead of the effective thermal conductivity
         EKSS(K)=VKS(K)*(1.0-POR)
         EKGG(K)=VKG(K)*POR
C TOTAL EFFECTIVE THERMAL CONDUCTIVITY
         EKT(K)=EKS(K)+EKG(K)
150   CONTINUE
      DO 200 K=1,NMAX
C DIMENSIONLESS EFFECTIVE THERMAL CONDUCTIVITY
         TKEG(K)=EKG(K)/VKG(1)
         TKES(K)=EKS(K)/VKG(1)
C BIOT NUMBER
         BI(K)=VNUG(K)*(1.0-POR)*VKG(K)/EKS(K)
200   CONTINUE
C ENTHALPY OF REACTION
      DO 300 K=1,NMAX
         DH1A(K)=-1.0624D8-3.73D3*TS(K)-1.130*(TS(K)**2)-9.17D8/TS(K)
         DH1B(K)=-3.9200D8-2.97D3*TS(K)+0.293*(TS(K)**2)-1.93D8/TS(K)
         DH2(K)= 1.7952D8-4.49D3*TS(K)-2.553*(TS(K)**2)-1.641D9/TS(K)
         DH3(K)=-2.8576D8+0.76D3*TG(K)+1.423*(TG(K)**2)+7.240D8/TG(K)
300   CONTINUE
      DO 400 K=1,NMAX
         H1A(K)=-DH1A(K)/(CPG(1)*TGIN*VMC)
         H1B(K)=-DH1B(K)/(CPG(1)*TGIN*VMC)
         H2(K)=-DH2(K)/(CPG(1)*TGIN*VMC)
         H3(K)=-DH3(K)/(CPG(1)*TGIN*VMCO)
400   CONTINUE
      RETURN
      END
```

```
C ************************** SUBROUTINE
C CALCULATE CONSTANTS FOR CONCENTRATION OF SPECIES J IN GAS PHASE
      SUBROUTINE MTJ
      INCLUDE 'CFP.FOR'
      INCLUDE 'CFD.FOR'
CC CONSTANTS FOR MASS TRANSFER OF SPECIES J IN GAS PHASE
C  FRACTION OF CARBON MONOXIDE FOR THE REACTION OF CARBON WITH OXYGEN
      DO 10 K=1,NMAX
         IF(CFCO.LE.1.0) THEN
            FCO(K)=CFCO
         ELSEIF(CFCO.GT.1.0.OR.CFCO.LT.0.0) THEN
            ABC=2512.0*DEXP(-6240.0/(THES(K)*TGIN))
            FCO(K)=ABC/(1.0+ABC)
         ENDIF
10    CONTINUE
C  CONSTANTS FOR BOUNDARY CONDITIONS
      CB(1)=1.0
      CB(2)=YN2IN/YO2IN
      CB(3)=0.0
      CB(4)=0.0
      CB(5)=YH2OIN/YO2IN
C  CONSTANTS
      DO 100 J=1,NKIND
      DO 200 K=2,N
         CONJ1(J,K)=(TROG(K-1)*TDJM(J,K-1)+TROG(K)*TDJM(J,K))*POR
     *              +(DXI(K-1)+DXI(K))*REGIN*SCO2IN*TROG(K-1)
     *              *UG(K-1)/RD
         CONJ2(J,K)=DXI(K-1)/DXI(K)*(TROG(K)*TDJM(J,K)
     *              +TROG(K+1)*TDJM(J,K+1))*POR+(TROG(K-1)*TDJM(J,K-1)
     *              +TROG(K)*TDJM(J,K))*POR+(DXI(K-1)+DXI(K))
     *              *REGIN*SCO2IN*TROG(K)*UG(K)/RD
         CONJ3(J,K)=DXI(K-1)/DXI(K)*(TROG(K)*TDJM(J,K)
     *              +TROG(K+1)*TDJM(J,K+1))*POR
200   CONTINUE
         CONJ1(J,NMAX)=(TROG(N)*TDJM(J,N)+TROG(NMAX)*TDJM(J,NMAX))*POR
     *                 +2.0*DXI(N)*REGIN*SCO2IN*TROG(N)*UG(N)/RD
         CONJ2(J,NMAX)=(TROG(N)*TDJM(J,N)+3.0*TROG(NMAX)*TDJM(J,NMAX))
     *                 *POR+2.0*DXI(N)*REGIN*SCO2IN*TROG(NMAX)
     *                 *UG(NMAX)/RD
         CONJ3(J,NMAX)=2.0*TROG(NMAX)*TDJM(J,NMAX)*POR
100   CONTINUE
      RETURN
      END
```

```
C ************************** SUBROUTINE
C  MASS LOSS OR GENERATION DUE TO CARBON COMBUSTION : C + 0.5 O2 = CO2
      SUBROUTINE SOURCE1
      INCLUDE 'CFP.FOR'
      INCLUDE 'CFD.FOR'
C  MASS LOSS OR GENERATION DUE TO CARBON COMBUSTION
      DO 5 K=1,NMAX
         DCD(K)=COMC(K)**(1.0/3.0)
         IF(DCD(K).GT.0.99999) DCD(K)=0.99999
         IF(DCD(K).LT.0.6382) DCD(K)=0.6382
C         IF(DCD(K).LT.0.6) DCD(K)=0.6
C         IF(DCD(K).LT.0.00001) DCD(K)=0.00001
5     CONTINUE
      DO 10 K=1,NMAX
         WCONA(K)=-AVD/((RD**2)*(1.0-FCO(K)/2.0))
         IF(XI(K).LT.XVL0) WCONA(K)=0.0
         WCON1(K)=TROG(K)*TDO2(K)*SHO2(K)*TMC/TMO2
         WCON2(K)=2.0*TROG(K)*TDEO2(K)*DCD(K)/(1.0-DCD(K))*TMC/TMO2
         WCON3(K)=(DCD(K)**2)*DA1*DEXP(-AR1/THES(K))*TMG(K)/TMO2
         WMASS1(K)=WCONA(K)*WCON1(K)
         WDIFF1(K)=WCONA(K)*WCON2(K)
         WCOMB1(K)=WCONA(K)*WCON3(K)
C         WW1(K)=WCONA(K)/(1.0/WCON1(K)+1.0/WCON2(K)+1.0/WCON3(K))
         WW1(K)=WCONA(K)/(1.0/WCON1(K)+1.0/WCON2(K))
10    CONTINUE
      RETURN
      END
```

```
C ************************** SUBROUTINE
C  MASS LOSS OR GENERATION DUE TO CARBON COMBUSTION : C+CO2=2CO
      SUBROUTINE SOURCE2
      INCLUDE 'CFP.FOR'
      INCLUDE 'CFD.FOR'
C  MASS LOSS OR GENERATION DUE TO CARBON COMBUSTION
      IF(VK03.EQ.0.0) GO TO 20
      DO 10 K=1,NMAX
         WCONB(K)=-AVD/(RD**2)
         IF(XI(K).LT.XVL0) WCONB(K)=0.0
         WCON4(K)=TROG(K)*TDCO2(K)*SHCO2(K)*TMC/TMCO2
         WCON5(K)=2.0*TROG(K)*TDECO2(K)*DCD(K)/(1.0-DCD(K))*TMC/TMCO2
         WCON7(K)=1.0+DA22*DEXP(-AR22/THES(K))*YCO(K)*YO2IN*TMG(K)/TMCO
     *             +DA23*DEXP(-AR23/THES(K))*YCO2(K)*YO2IN*TMG(K)/TMCO2
         WCON6(K)=(1.0/6.0)*(DCD(K)**2)*TROS(K)*TROIN*DA21
     *             *DEXP(-AR21/THES(K))*TMG(K)/TMCO2/WCON7(K)
         IF(WCON6(K).LE.0.0) WCON6(K)=1.0D-30
         WMASS2(K)=WCONB(K)*WCON4(K)
         WDIFF2(K)=WCONB(K)*WCON5(K)
         WCOMB2(K)=WCONB(K)*WCON6(K)
         WW2(K)=WCONB(K)/(1.0/WCON4(K)+1.0/WCON5(K)+1.0/WCON6(K))
10    CONTINUE
20    CONTINUE
      RETURN
      END
```

```
C ************************** SUBROUTINE
C  MASS LOSS OR GENERATION DUE TO HOMOGENEOUS REACTION :
C  CO + 0.5 O2 = CO2
      SUBROUTINE SOURCE3
      INCLUDE 'CFP.FOR'
      INCLUDE 'CFD.FOR'
C  MASS LOSS OR GENERATION DUE TO HOMOGENEOUS REACTION
      DO 10 K=1,NMAX
C  REACTION RATE BY INTRINSIC KINETICS FOR COMPARISON
        WWK3(K)=-POR/(RD**2)*DA3*DEXP(-AR3/THEG(K))*(YH2O(K)**VC)*
     *          YO2IN**(VA+VB+VC-1.0)*TROG(K)**(VA+VB+VC)/
     *          (TMCO**(VA-1.0)*TMO2**VB*TMH2O**VC)
C  INTRINSIC REACTION RATE OF CO AND O2 IS SO HIGH THAT
C  THE RATE OF CO CONSUMPTION BY REACTION (3) IS SAME AS
C  THE RATE OF CO GENERATION BY REACTION (1)
        WW3(K)=FCO(K)*WW1(K)*TMCO/TMC
        IF(REHU.LE.0.0) WW3(K)=0.0
        IF(VK03.LE.0.0) WW3(K)=0.0
10    CONTINUE
      RETURN
      END
```

```
C ************************** SUBROUTINE
C CALCULATE CONCENTRATION OF O2 SPECIES IN GAS PHASE
      SUBROUTINE MTO2
      INCLUDE 'CFP.FOR'
      INCLUDE 'CFD.FOR'
C  MASS LOSS OR GENERATION TERM EXCEPT VOLATILE COMBUSTION
C  MASS LOSS OR GENERATION DUE TO CARBON COMBUSTION
      CALL SOURCE1
      CALL SOURCE3
C CONSTANTS FOR MASS LOSS OR GENERATION TERM
      DO 10 K=1,NMAX
      IF(YO2(K).LE.0.0) YO2(K)=1.0D-30
10    CONTINUE
      DO 20 K=2,N
         CONJ4(1,K)=(DXI(K-1)+DXI(K))*DXI(K-1)*((1.0-FCO(K)/2.0)*
     *               WW1(K)*TMO2/TMC+0.5*WW3(K)*TMO2/TMCO)
20    CONTINUE
      CONJ4(1,NMAX)=2.0*(DXI(N)**2)*((1.0-FCO(NMAX)/2.0)*WW1(NMAX)*
     *              TMO2/TMC+0.5*WW3(NMAX)*TMO2/TMCO)
C GENERATE COEFFICIENT MATRIX AND CONSTANT VECTOR
      BM(1)=-CONJ2(1,2)+CONJ4(1,2)
      CM(1)=CONJ3(1,2)
      FM(1)=-CONJ1(1,2)*CB(1)
      DO 100 K=2,N-1
         AM(K)=CONJ1(1,K+1)
         BM(K)=-CONJ2(1,K+1)+CONJ4(1,K+1)
         CM(K)=CONJ3(1,K+1)
         FM(K)=0.0
100   CONTINUE
      AM(N)=CONJ1(1,NMAX)+CONJ3(1,NMAX)
      BM(N)=-CONJ2(1,NMAX)+CONJ4(1,NMAX)
      FM(N)=0.0
C SOLVE THE SIMULTANEOUS EQUATION
      CALL TRIDIA(N,AM,BM,CM,FM,YYM)
      DO 200 K=1,N
         YO2(K+1)=YYM(K)
200   CONTINUE
      YO2(1)=CB(1)
      RETURN
      END
```

```
C ************************** SUBROUTINE
C CALCULATE CONCENTRATION OF CO2 SPECIES IN GAS PHASE
      SUBROUTINE MTCO2
      INCLUDE 'CFP.FOR'
      INCLUDE 'CFD.FOR'
C  MASS LOSS OR GENERATION DUE TO CARBON COMBUSTION
      CALL SOURCE2
C     CALL SOURCE3
C CONSTANTS FOR MASS LOSS OR GENERATION TERM
      DO 20 K=2,N
         CONJ4(3,K)=(DXI(K-1)+DXI(K))*DXI(K-1)*WW2(K)*TMCO2/TMC
         CONJ5(3,K)=-(DXI(K-1)+DXI(K))*DXI(K-1)*((1.0-FCO(K))*WW1(K)*
     *               YO2(K)*TMCO2/TMC+WW3(K)*YO2(K)*TMCO2/TMCO)
20    CONTINUE
      CONJ4(3,NMAX)=2.0*(DXI(N)**2)*WW2(NMAX)*TMCO2/TMC
      CONJ5(3,NMAX)=-2.0*(DXI(N)**2)*((1.0-FCO(NMAX))*WW1(NMAX)*
     *               YO2(NMAX)*TMCO2/TMC+WW3(NMAX)*YO2(NMAX)*TMCO2/TMCO)
C GENERATE COEFFICIENT MATRIX AND CONSTANT VECTOR
      BM(1)=-CONJ2(3,2)+CONJ4(3,2)
      CM(1)=CONJ3(3,2)
      FM(1)=-CONJ5(3,2)-CONJ1(3,2)*CB(3)
      DO 100 K=2,N-1
         AM(K)=CONJ1(3,K+1)
         BM(K)=-CONJ2(3,K+1)+CONJ4(3,K+1)
         CM(K)=CONJ3(3,K+1)
         FM(K)=-CONJ5(3,K+1)
100   CONTINUE
      AM(N)=CONJ1(3,NMAX)+CONJ3(3,NMAX)
      BM(N)=-CONJ2(3,NMAX)+CONJ4(3,NMAX)
      FM(N)=-CONJ5(3,NMAX)
C SOLVE THE SIMULTANEOUS EQUATION
      CALL TRIDIA(N,AM,BM,CM,FM,YYM)
      DO 200 K=1,N
         YCO2(K+1)=YYM(K)
200   CONTINUE
      YCO2(1)=CB(3)
      RETURN
      END
```

```
C ************************** SUBROUTINE
C CALCULATE CONCENTRATION OF CO SPECIES IN GAS PHASE
      SUBROUTINE MTCO
      INCLUDE 'CFP.FOR'
      INCLUDE 'CFD.FOR'
C  MASS LOSS OR GENERATION DUE TO CARBON COMBUSTION
C CONSTANTS FOR MASS LOSS OR GENERATION TERM
      DO 20 K=2,N
         CONJ5(4,K)=(DXI(K-1)+DXI(K))*DXI(K-1)*WW3(K)*YO2(K)
     *               -(DXI(K-1)+DXI(K))*DXI(K-1)*TMCO/TMC*
     *               (FCO(K)*WW1(K)*YO2(K)+2.0*WW2(K)*YCO2(K))
C          CONJ5(4,K)=-(DXI(K-1)+DXI(K))*DXI(K-1)*TMCO/TMC*
C     *                (2.0*WW2(K)*YCO2(K))
20    CONTINUE
      CONJ5(4,NMAX)=2.0*(DXI(N)**2)*WW3(NMAX)*YO2(NMAX)
     *               -2.0*(DXI(N)**2)*TMCO/TMC*
     *               (FCO(NMAX)*WW1(NMAX)*YO2(NMAX)+2.0*WW2(NMAX)*
     *              YCO2(NMAX))
C       CONJ5(4,NMAX)=-2.0*(DXI(N)**2)*TMCO/TMC*
C     *                (2.0*WW2(NMAX)*YCO2(NMAX))
C GENERATE COEFFICIENT MATRIX AND CONSTANT VECTOR
      BM(1)=-CONJ2(4,2)
      CM(1)=CONJ3(4,2)
      FM(1)=-CONJ5(4,2)-CONJ1(4,2)*CB(4)
      DO 100 K=2,N-1
         AM(K)=CONJ1(4,K+1)
         BM(K)=-CONJ2(4,K+1)
         CM(K)=CONJ3(4,K+1)
         FM(K)=-CONJ5(4,K+1)
100   CONTINUE
      AM(N)=CONJ1(4,NMAX)+CONJ3(4,NMAX)
      BM(N)=-CONJ2(4,NMAX)
      FM(N)=-CONJ5(4,NMAX)
C SOLVE THE SIMULTANEOUS EQUATION
      CALL TRIDIA(N,AM,BM,CM,FM,YYM)
      DO 200 K=1,N
         YCO(K+1)=YYM(K)
200   CONTINUE
      YCO(1)=CB(4)
      DO 10 K=1,NMAX
      IF(YCO(K).LE.0.0) YCO(K)=1.0D-30
10    CONTINUE
      RETURN
      END
```

```
C ************************** SUBROUTINE
C CALCULATE CONCENTRATION OF N2 SPECIES IN GAS PHASE
      SUBROUTINE MTN2
      INCLUDE 'CFP.FOR'
      INCLUDE 'CFD.FOR'
C  MASS LOSS OR GENERATION TERM EXCEPT VOLATILE COMBUSTION
      DO 10 K=1,NMAX
         WN2(K)=0.0
10    CONTINUE
C CONSTANTS FOR MASS LOSS OR GENERATION TERM
      DO 20 K=2,N
         CONJ4(2,K)=(DXI(K-1)+DXI(K))*DXI(K-1)*WN2(K)
20    CONTINUE
      CONJ4(2,NMAX)=2.0*(DXI(N)**2)*WN2(NMAX)
C GENERATE COEFFICIENT MATRIX AND CONSTANT VECTOR
      BM(1)=-CONJ2(2,2)
      CM(1)=CONJ3(2,2)
      FM(1)=-CONJ4(2,2)-CONJ1(2,2)*CB(2)
      DO 100 K=2,N-1
         AM(K)=CONJ1(2,K+1)
         BM(K)=-CONJ2(2,K+1)
         CM(K)=CONJ3(2,K+1)
         FM(K)=-CONJ4(2,K+1)
100   CONTINUE
      AM(N)=CONJ1(2,NMAX)+CONJ3(2,NMAX)
      BM(N)=-CONJ2(2,NMAX)
      FM(N)=-CONJ4(2,NMAX)
C SOLVE THE SIMULTANEOUS EQUATION
      CALL TRIDIA(N,AM,BM,CM,FM,YYM)
      DO 200 K=1,N
         YN2(K+1)=YYM(K)
200   CONTINUE
      YN2(1)=CB(2)
      RETURN
      END
```

```
C ************************** SUBROUTINE
C CALCULATE CONCENTRATION OF H2O SPECIES IN GAS PHASE
      SUBROUTINE MTH2O
      INCLUDE 'CFP.FOR'
      INCLUDE 'CFD.FOR'
C  MASS LOSS OR GENERATION TERM EXCEPT VOLATILE COMBUSTION
      DO 10 K=1,NMAX
         WH2O(K)=0.0
10    CONTINUE
C CONSTANTS FOR MASS LOSS OR GENERATION TERM
      DO 20 K=2,N
         CONJ4(5,K)=(DXI(K-1)+DXI(K))*DXI(K-1)*WH2O(K)
20    CONTINUE
      CONJ4(5,NMAX)=2.0*(DXI(N)**2)*WH2O(NMAX)
C GENERATE COEFFICIENT MATRIX AND CONSTANT VECTOR
      BM(1)=-CONJ2(5,2)
      CM(1)=CONJ3(5,2)
      FM(1)=-CONJ4(5,2)-CONJ1(5,2)*CB(5)
      DO 100 K=2,N-1
         AM(K)=CONJ1(5,K+1)
         BM(K)=-CONJ2(5,K+1)
         CM(K)=CONJ3(5,K+1)
         FM(K)=-CONJ4(5,K+1)
100   CONTINUE
      AM(N)=CONJ1(5,NMAX)+CONJ3(5,NMAX)
      BM(N)=-CONJ2(5,NMAX)
      FM(N)=-CONJ4(5,NMAX)
C SOLVE THE SIMULTANEOUS EQUATION
      CALL TRIDIA(N,AM,BM,CM,FM,YYM)
      DO 200 K=1,N
         YH2O(K+1)=YYM(K)
200   CONTINUE
      YH2O(1)=CB(5)
      RETURN
      END
```

```
C ************************** SUBROUTINE
C CALCULATE MODIFIED MASS LOSS OR GENERATION OF GAS SPECIES
      SUBROUTINE W123
      INCLUDE 'CFP.FOR'
      INCLUDE 'CFD.FOR'
C      write(6,*) 'yco'
C      write(6,*) yco
      DO 10 K=1,NMAX
         W1(K)=WW1(K)*YO2(K)
         W2(K)=WW2(K)*YCO2(K)
         W3(K)=WW3(K)*YO2(K)
         WK3(K)=WWK3(K)*YCO(K)**VA*YO2(K)**VB
         WO2(K)=(1.0-FCO(K)/2.0)*W1(K)*TMO2/TMC+0.5*W3(K)*TMO2/TMCO
         WCO2(K)=-(1.0-FCO(K))*W1(K)*TMCO2/TMC+W2(K)*TMCO2/TMC
     *           -W3(K)*TMCO2/TMCO
         WCO(K)=-FCO(K)*W1(K)*TMCO/TMC-2.0*W2(K)*TMCO/TMC+W3(K)
10    CONTINUE
      RETURN
      END
```

```
C ************************** SUBROUTINE
C CALCULATE CONCENTRATION OF CARBON SPECIES IN SOLID PHASE
      SUBROUTINE MTCA
      INCLUDE 'CFP.FOR'
      INCLUDE 'CFD.FOR'
C CONSTANTS FOR MASS LOSS OR GENERATION TERM
      CONCA=RD*YO2IN/((1.0-POR)*TROIN*RES*SCO2IN*OMCIN)
      DO 10 K=1,NMAX
         WC(K)=W1(K)+W2(K)
10    CONTINUE
C CARBON CONTENT IN SOLID PARTICLES
      COMC(NMAX)=1.0
      DO 30 K=N,1,-1
         COMC(K)=COMC(K+1)+CONCA*DXI(K)*(WC(K)+WC(K+1))/2.0
         IF(COMC(K).LT.0.0) THEN
            DO 40 KK=K,1,-1
               W1(KK)=0.0
               W2(KK)=0.0
               WC(KK)=0.0
               COMC(KK)=0.0
40          CONTINUE
            GO TO 50
         ENDIF
30    CONTINUE
50    CONTINUE
      RETURN
      END
```

```
C ************************** SUBROUTINE
C CALCULATE CONCENTRATION OF ASH SPECIES IN SOLID PHASE
      SUBROUTINE MTAS
      INCLUDE 'CFP.FOR'
      INCLUDE 'CFD.FOR'
C ASH CONTENT IN SOLID PARTICLES DOESN'T CHANGE
      DO 20 K=1,NMAX
         COMA(K)=1.0
20    CONTINUE
      RETURN
      END
```

```
C ************************** SUBROUTINE
C CALCULATE TEMPERATURE DISTRIBUTION IN GAS PHASE
      SUBROUTINE HTGAS
      INCLUDE 'CFP.FOR'
      INCLUDE 'CFD.FOR'
C HEAT SOURCE BY HOMOGENEOUS REACTION
      DO 100 K=1,NMAX
         QG(K)=-(PRGIN/SCO2IN)*YO2IN*H3(K)*W3(K)
100   CONTINUE
C CONSTANTS FOR GAS PHASE HEAT TRANSFER
      DO 150 K=2,N
         CG1(K)=TKEG(K-1)+TKEG(K)+(DXI(K-1)+DXI(K))
     *           *REGIN*PRGIN*TROG(K-1)*UG(K-1)*TCPG(K-1)/RD
         CG2(K)=DXI(K-1)/DXI(K)*(TKEG(K)+TKEG(K+1))+TKEG(K-1)+TKEG(K)
     *           +(DXI(K-1)+DXI(K))*REGIN*PRGIN*TROG(K)*UG(K)*TCPG(K)/RD
     *           +(DXI(K-1)+DXI(K))*DXI(K-1)*AVD*TKG(K)*VNUG(K)/(RD**2)
         CG3(K)=DXI(K-1)/DXI(K)*(TKEG(K)+TKEG(K+1))
         CG4(K)=(DXI(K-1)+DXI(K))*DXI(K-1)*AVD*TKG(K)*VNUG(K)/(RD**2)
         CG5(K)=(DXI(K-1)+DXI(K))*DXI(K-1)*QG(K)
150   CONTINUE
      CG1(NMAX)=TKEG(N)+TKEG(NMAX)+2.0*DXI(N)*REGIN*PRGIN
     *           *TROG(N)*UG(N)*TCPG(N)/RD
      CG2(NMAX)=TKEG(N)+3.0*TKEG(NMAX)+2.0*DXI(N)
     *           *REGIN*PRGIN*TROG(NMAX)*UG(NMAX)*TCPG(NMAX)/RD
     *           +2.0*(DXI(N)**2)*AVD*TKG(NMAX)*VNUG(NMAX)/(RD**2)
      CG3(NMAX)=2.0*TKEG(NMAX)
      CG4(NMAX)=2.0*(DXI(N)**2)*AVD*TKG(NMAX)*VNUG(NMAX)/(RD**2)
      CG5(NMAX)=2.0*(DXI(N)**2)*QG(NMAX)
C ***************************************************************
C GENERATE COEFFICIENT MATRIX AND CONSTANT VECTOR FOR GAS PHASE
      B2(1)=-CG2(2)
      C2(1)=CG3(2)
      F2(1)=-CG4(2)*THES(2)-CG5(2)-CG1(2)
      DO 200 K=2,N-1
         A2(K)=CG1(K+1)
         B2(K)=-CG2(K+1)
         C2(K)=CG3(K+1)
         F2(K)=-CG4(K+1)*THES(K+1)-CG5(K+1)
200   CONTINUE
      A2(N)=CG1(NMAX)+CG3(NMAX)
      B2(N)=-CG2(NMAX)
      F2(N)=-CG4(NMAX)*THES(NMAX)-CG5(NMAX)
C SOLVE THE SIMULTANEOUS EQUATION FOR GAS PHASE
      CALL TRIDIA(N,A2,B2,C2,F2,THEGG)
      DO 300 K=1,N
         THEG(K+1)=THEGG(K)
300   CONTINUE
      THEG(1)=1.0
      RETURN
      END
```

```
C ************************** SUBROUTINE
C CALCULATE TEMPERATURE DISTRIBUTION IN SOLID PHASE
      SUBROUTINE HTSOL
      INCLUDE 'CFP.FOR'
      INCLUDE 'CFD.FOR'
C HEAT SOURCE BY CARBON COMBUSTION
      DO 100 K=1,NMAX
         QS(K)=-(PRGIN/SCO2IN)*YO2IN*(FCO(K)*H1A(K)*W1(K)
     *          +(1.0-FCO(K))*H1B(K)*W1(K)+H2(K)*W2(K))
100   CONTINUE
C CONSTANTS FOR SOLID PHASE HEAT TRANSFER
      CS1(1)=2.0*TKES(1)
      CS2(1)=3.0*TKES(1)+TKES(2)
     *        +2.0*DXI(1)*(1.0-POR)*TROS(1)*TCPS(1)*RES*PRGIN*TROIN/RD
     *        +2.0*(DXI(1)**2)*AVD*TKG(1)*VNUG(1)/(RD**2)
      CS3(1)=TKES(1)+TKES(2)+2.0*DXI(1)*(1.0-POR)
     *        *TROS(2)*TCPS(2)*RES*PRGIN*TROIN/RD
      CS4(1)=2.0*(DXI(1)**2)*AVD*TKG(1)*VNUG(1)/(RD**2)
      CS5(1)=2.0*(DXI(1)**2)*QS(1)
      DO 130 K=2,N
         CS1(K)=TKES(K-1)+TKES(K)
         CS2(K)=DXI(K-1)/DXI(K)*(TKES(K)+TKES(K+1))+TKES(K-1)+TKES(K)
     *           +(DXI(K-1)+DXI(K))*DXI(K-1)/DXI(K)*(1.0-POR)*TROS(K)
     *           *TCPS(K)*RES*PRGIN*TROIN/RD+(DXI(K-1)+DXI(K))*DXI(K-1)
     *           *AVD*TKG(K)*VNUG(K)/(RD**2)
         CS3(K)=DXI(K-1)/DXI(K)*(TKES(K)+TKES(K+1))
     *           +(DXI(K-1)+DXI(K))*DXI(K-1)/DXI(K)*(1.0-POR)
     *           *TROS(K+1)*TCPS(K+1)*RES*PRGIN*TROIN/RD
         CS4(K)=(DXI(K-1)+DXI(K))*DXI(K-1)*AVD*TKG(K)*VNUG(K)/(RD**2)
         CS5(K)=(DXI(K-1)+DXI(K))*DXI(K-1)*QS(K)
130   CONTINUE
      CS1(NMAX)=TKES(N)+TKES(NMAX)
      CS2(NMAX)=TKES(N)+3.0*TKES(NMAX)+2.0*DXI(N)
     *           *(1.0-POR)*TROS(NMAX)*TCPS(NMAX)*RES*PRGIN*TROIN/RD
     *           +2.0*(DXI(N)**2)*AVD*TKG(NMAX)*VNUG(NMAX)/(RD**2)
      CS3(NMAX)=2.0*TKES(NMAX)+2.0*DXI(N)*(1.0-POR)*TROS(NMAX)
     *           *TCPS(NMAX)*RES*PRGIN*TROIN/RD
      CS4(NMAX)=2.0*(DXI(N)**2)*AVD*TKG(NMAX)*VNUG(NMAX)/(RD**2)
      CS5(NMAX)=2.0*(DXI(N)**2)*QS(NMAX)
      CB1=2.0*DXI(1)*(1.0-POR)*TKG(1)*VNUG(1)/(TKES(1)*RD)
      CB2=2.0*DXI(N)*(1.0-POR)*TKG(NMAX)*VNUG(NMAX)/(TKES(NMAX)*RD)
C ***************************************************************
C GENERATE COEFFICIENT MATRIX AND CONSTANT VECTOR FOR SOLID PHASE
      B1(1)=-(CS1(1)*CB1+CS2(1))
      C1(1)=CS1(1)+CS3(1)
      F1(1)=-CS4(1)*THEG(1)-CS5(1)-CS1(1)*CB1
      DO 500 K=2,N
         A1(K)=CS1(K)
         B1(K)=-CS2(K)
         C1(K)=CS3(K)
         F1(K)=-CS4(K)*THEG(K)-CS5(K)
500   CONTINUE
      A1(NMAX)=CS1(NMAX)+CS3(NMAX)
      B1(NMAX)=-(CS2(NMAX)+CS3(NMAX)*CB2)
      F1(NMAX)=-CS4(NMAX)*THEG(NMAX)-CS5(NMAX)-CS3(NMAX)*CB2*RT
C SOLVE THE SIMULTANEOUS EQUATION FOR SOLID PHASE
      CALL TRIDIA(NMAX,A1,B1,C1,F1,THES)
      RETURN
      END
```

```
C ************************** SUBROUTINE
C PRINT OUT THE RESULTS FOR CARBON COMBUSTION
      SUBROUTINE OUTPUT
      INCLUDE 'CFP.FOR'
      INCLUDE 'CFD.FOR'
C ************************** CONVERGED SOLUTION
      WRITE(6,*) '  ERROR CRITERION  AT THE FINAL ITERATION'
      WRITE(6,*) 'COMC(1)=',COMC(1),'YCO2(NMAX)=',YCO2(NMAX)
      WRITE(6,111) KTS,KTG,KC,KO2
      WRITE(6,112) DTHESM,DTHEGM,DCOMCM,DYO2M
111   FORMAT(1X,'DTHESM(',I4,')',1X,'DTHEGM(',I4,')',1X,
     *       'DCOMCM(',I4,')',1X,'DYO2M(',I4,')')
112   FORMAT(4D13.5)
      WRITE(6,*) ' '
      WRITE(6,*) '*************** FINAL SOLUTION ***************'
      WRITE(6,*) ' '
      WRITE(6,*) '***** INPUT PARAMETERS ***** '
      WRITE(6,*) '  REGIN  = ',REGIN  ,'  RES    = ',RES
      WRITE(6,*) '  TGIN   = ',TGIN   ,'  TSIN   = ',TSIN
      WRITE(6,*) '  d      = ',D      ,'  L      = ',VL
      WRITE(6,*) '  NKIND  = ',NKIND
      WRITE(6,*) '  OMCIN  = ',OMCIN  ,'  OMAIN  = ',OMAIN
      WRITE(6,*) '  VK01   = ',VK01   ,'  E1     = ',E1
      WRITE(6,*) ' '
      WRITE(6,*) '***** RESULT OUTPUT ***** '
      WRITE(6,*) '  ITER = ',ITER
      WRITE(6,*) '  VMG(1) = ',VMG(1) ,'  BI(1)  = ',BI(1)
      WRITE(6,*) '  PRGIN  = ',PRGIN  ,'  SCO2IN = ',SCO2IN
      WRITE(6,*) '  VNUG(1)= ',VNUG(1),'  SHO2(1)= ',SHO2(1)
      WRITE(6,*) '  DA1    = ',DA1    ,'  AR1    = ',AR1
      WRITE(6,*) '  CFCO   = ',CFCO
      WRITE(6,*) '  YO2IN  = ',YO2IN  ,'  YN2IN  = ',YN2IN
      WRITE(6,*) '  YH2OIN = ',YH2OIN
      WRITE(6,*) ' '
C OUTPUT FOR RESULT PRINT OUT

      WRITE(6,2010)
C      DO 1000 K=1,10
      DO 1000 K=1,5
         WRITE(6,2020) K,XI(K),THES(K),THEG(K),UG(K),TROG(K),TROS(K),
     *                 FCO(K)
1000  CONTINUE
C      DO 1010 K=11,NMAX,10
      DO 1010 K=6,NMAX,5
         WRITE(6,2020) K,XI(K),THES(K),THEG(K),UG(K),TROG(K),TROS(K),
     *                 FCO(K)
1010  CONTINUE
      WRITE(6,2010)
2010  FORMAT(/3X,'K',5X,'XI',5X,'THES',6X,'THEG',8X,'UG',7X,'TROG',
     *       6X,'TROS',6X,'FCO',/)
2020  FORMAT(I4,F8.4,6F10.6)
```

```
      WRITE(6,2030)
C      DO 1020 K=1,10
      DO 1020 K=1,5
         WRITE(6,2040) K,XI(K),COMC(K),
     *                 YO2(K),YCO2(K),YCO(K),YN2(K),YH2O(K)
1020  CONTINUE
C      DO 1030 K=11,NMAX,10
      DO 1030 K=6,NMAX,5
         WRITE(6,2040) K,XI(K),COMC(K),
     *                 YO2(K),YCO2(K),YCO(K),YN2(K),YH2O(K)
1030  CONTINUE
      WRITE(6,2030)
2030  FORMAT(/3X,'K',3X,'XI',5X,'COMC',8X,'YO2',8X,'YCO2',8X,'YCO',
     *       9X,'YN2',8X,'YH2O',/)
2040  FORMAT(I4,F7.3,F9.5,5E12.4)

      WRITE(6,2050)
C      DO 1040 K=1,10
      DO 1040 K=1,5
         WRITE(6,2060) K,XI(K),WCOMB1(K),WMASS1(K),WDIFF1(K),
     *                           WCOMB2(K),WMASS2(K),WDIFF2(K)
1040  CONTINUE
C      DO 1050 K=11,NMAX,10
      DO 1050 K=6,NMAX,5
         WRITE(6,2060) K,XI(K),WCOMB1(K),WMASS1(K),WDIFF1(K),
     *                           WCOMB2(K),WMASS2(K),WDIFF2(K)
1050  CONTINUE
      WRITE(6,2050)
2050  FORMAT(/3X,'K',4X,'XI',5X,'WCOMB1',5X,'WMASS1',5X,'WDIFF1',
     *                        5X,'WCOMB2',5X,'WMASS2',5X,'WDIFF2',/)
2060  FORMAT(I4,F8.4,6E11.3)

      WRITE(6,2070)
C      DO 1060 K=1,10
      DO 1060 K=1,5
         WRITE(6,2080) K,XI(K),W1(K),W2(K),W3(K),WK3(K),BI(K)
1060  CONTINUE
C      DO 1070 K=11,NMAX,10
      DO 1070 K=6,NMAX,5
         WRITE(6,2080) K,XI(K),W1(K),W2(K),W3(K),WK3(K),BI(K)
1070  CONTINUE
      WRITE(6,2070)
2070  FORMAT(/3X,'K',4X,'XI',8X,'W1',11X,'W2',11X,'W3',
     *       10X,'WK3',5X,'BI(K)',/)
2080  FORMAT(I4,F8.4,5E13.5)

C OUTPUT FOR GRAPH
C      DO 1200 K=1,10
      DO 1200 K=1,5
         WRITE(7,2230) XI(K),THES(K),THEG(K),UG(K),TROG(K),TROS(K)
C         WRITE(7,2230) XI(K),TS(K),TG(K),UG(K),TROG(K),TROS(K)
1200  CONTINUE
C      DO 1201 K=11,NMAX,10
      DO 1201 K=6,NMAX,5
         WRITE(7,2230) XI(K),THES(K),THEG(K),UG(K),TROG(K),TROS(K)
C         WRITE(7,2230) XI(K),TS(K),TG(K),UG(K),TROG(K),TROS(K)
1201  CONTINUE
2230  FORMAT(F8.4,5E13.5)
```

```
      WRITE(7,*) ' '
C      DO 1202 K=1,10
      DO 1202 K=1,5
         WRITE(7,2240) XI(K),COMC(K),YO2(K),YCO2(K),YCO(K),
     *                 YH2O(K),YN2(K)
C          WRITE(7,2240) XI(K),COMC(K),XX(1,K),XX(3,K),XX(4,K),XX(5,K),
C     *                  XX(2,K)
1202  CONTINUE
C      DO 1203 K=11,NMAX,10
      DO 1203 K=6,NMAX,5
         WRITE(7,2240) XI(K),COMC(K),YO2(K),YCO2(K),YCO(K),
     *                 YH2O(K),YN2(K)
C          WRITE(7,2240) XI(K),COMC(K),XX(1,K),XX(3,K),XX(4,K),XX(5,K),
C     *                  XX(2,K)
1203  CONTINUE
2240  FORMAT(F7.3,6E12.4)

      WRITE(7,*) ' '
C      DO 1204 K=1,10
      DO 1204 K=1,5
         WRITE(7,2250) XI(K),W1(K),W2(K),W3(K),WK3(K),BI(K)
1204  CONTINUE
C      DO 1205 K=11,NMAX,10
      DO 1205 K=6,NMAX,5
         WRITE(7,2250) XI(K),W1(K),W2(K),W3(K),WK3(K),BI(K)
1205  CONTINUE
2250  FORMAT(F8.4,5E13.5)

      WRITE(7,*) ' '
C      DO 1206 K=1,10
      DO 1206 K=1,5
         WRITE(7,2260) XI(K),EKS(K),EKG(K),EKSS(K),EKGG(K)
1206  CONTINUE
C      DO 1207 K=11,NMAX,10
      DO 1207 K=6,NMAX,5
         WRITE(7,2260) XI(K),EKS(K),EKG(K),EKSS(K),EKGG(K)
1207  CONTINUE
2260  FORMAT(F8.4,4E13.5)

      RETURN
      END
```

```
C ************************** SUBROUTINE
C PRINT OUT THE RESULTS TO CHECK CONVERGENCE
      SUBROUTINE OUTPUT6
      INCLUDE 'CFP.FOR'
      INCLUDE 'CFD.FOR'
      write(6,111) KTS,KTG,KC,KO2
      write(6,112) dthesm,dthegm,dcomcm,dyo2m
111   format(1x,'dthesm(',I4,')',1x,'dthegm(',I4,')',1x,
     *       'dcomcm(',I4,')',1x,'dyo2m(',I4,')')
112   format(4d13.5)
      WRITE(6,1010)
C      DO 1000 K=1,10,2
      DO 1000 K=1,5
         WRITE(6,1020) K,XI(K),THES(K),THEG(K),COMC(K),YO2(K),
     *                 YCO2(K),YCO(K),WCOMB1(K),WMASS1(K),WDIFF1(K),
     *                 W1(K),WCOMB2(K),WMASS2(K),WDIFF2(K),W2(K),
     *                 WO2(K),WCO2(K),WCO(K)
1000  CONTINUE
C      DO 1100 K=11,NMAX,10
      DO 1100 K=6,NMAX,5
         WRITE(6,1020) K,XI(K),THES(K),THEG(K),COMC(K),YO2(K),
     *                 YCO2(K),YCO(K),WCOMB1(K),WMASS1(K),WDIFF1(K),
     *                 W1(K),WCOMB2(K),WMASS2(K),WDIFF2(K),W2(K),
     *                 WO2(K),WCO2(K),WCO(K)
1100  CONTINUE
      WRITE(6,1010)
1010  FORMAT(/3X,'K',5X,'XI',5X,'THES',6X,'THEG',6X,'COMC',8X,'YO2',
     *       10X,'YCO2',10X,'YCO',8X,'WCOMB1',8X,'WMASS1',8X,
     *       'WDIFF1',9X,'W1',11X,'WO2',9X,'WCO2',9X,'WCO',/)
1020  FORMAT(I4,F8.4,3F10.6,14E13.5)
      RETURN
      END
```

```
C ************************** SUBROUTINE
C CHECK TEMPERATURE DEPENDENT PROPERTIES
      SUBROUTINE CHECK
      INCLUDE 'CFP.FOR'
      INCLUDE 'CFD.FOR'
C WRITE PROPERTIES ON DPA.OUT FILE
      WRITE(8,1010)
C      DO 1000 K=1,NMAX,5
      DO 1000 K=1,NMAX,10
         ROG(K)=TROG(K)*ROGIN
         WRITE(8,1020) K,XI(K),CPG(K),VIG(K),VKG(K),ROG(K),
     *                 DO2(K),DN2(K),DCO2(K),VNUG(K)
1000  CONTINUE
      WRITE(8,1010)
1010  FORMAT(/3X,'K',5X,'XI ',6X,'CPG',9X,'VIG',9X,'VKG',9X,'ROG',
     *       9X,'DO2',9X,'DN2',8X,'DCO2',8X,'VNUG',/)
1020  FORMAT(I4,F8.4,8E12.4)
      RETURN
      END
```

```
C ************************** SUBROUTINE
C TRIDIAGONAL MATRIX ALGORITHM
      SUBROUTINE TRIDIA(NN,A,B,C,F,T)
      INCLUDE 'CFP.FOR'
      REAL*8 A(NMAX),B(NMAX),C(NMAX),F(NMAX),T(NMAX)
C ELIMINATION
      DO 5 I=2,NN
      D=A(I)/B(I-1)
      B(I)=B(I)-C(I-1)*D
      F(I)=F(I)-F(I-1)*D
5     CONTINUE
C BACK SUBSTITUTION
      T(NN)=F(NN)/B(NN)
      DO 6 I=1,NN-1
      J=NN-I
      T(J)=(F(J)-C(J)*T(J+1))/B(J)
6     CONTINUE
      RETURN
      END
```

```
C ************************** SUBROUTINE
C FIND THE MAXIMUM DIFFERENCE
      SUBROUTINE DAX(X1,X2,DXMAX,KLMAX)
      INCLUDE 'CFP.FOR'
      REAL*8 X1(NMAX),X2(NMAX)
      DXMAX=0.0
      KLMAX=NMAX
      DO 10 K=1,NMAX
         IF(X1(K).LT.1.0D-6) GO TO 10
         DX=ABS((X1(K)-X2(K))/X1(K))
         IF(DX.GE.DXMAX) THEN
            DXMAX=DX
            KLMAX=K
         ENDIF
10    CONTINUE
      RETURN
      END
```

CF.DAT for Standard Run

```
5       0.913      0.087     3.40D7       4.5D8      2.0        0.3
173.4   0.0280465  300.0     300.0        0.015      0.6096     0.6096
1.0     0.25       0.5       2.193D12     1.674D8
```